NOVEL PERSPECTIVES IN CANCER CHEMOPREVENTION VIA NRF2 PATHWAY: FROM PHARMACOGENOMICS TO PHARMACOEPIGENETICS

by

TIEN-YUAN WU

A Dissertation submitted to the

Graduate School-New Brunswick

Rutgers, The State University of New Jersey

In partial fulfillment of the requirements

For the degree of

Doctor of Philosophy

Graduate Program in Pharmaceutical Science

Written under the direction of

Professor Ah-Ng Tony Kong, Ph.D.

And approved by

_____

_____

_____

_____

New Brunswick, New Jersey

OCTOBER, 2012

ABSTRACT OF THE DISSERTATION

Novel Perspectives in Cancer Chemoprevention via Nrf2 pathway: from Pharmacogenomics to Pharmacoepigenetics

By TIEN-YUAN WU

Dissertation Director: Professor Ah-Ng Tony Kong

The cancer chemoprevention is the strategy of blocking or slowing the onset of premalignant tumors and decreases the incidence of cancer with relatively nontoxic chemical substance. More importantly, Nrf2 and Nrf2-antioxidant response element (ARE) pathway plays a critical role in the cancer chemoprevention. Studies of the induction of Nrf2 and subsequent phase II detoxifying/antioxidant drug metabolism enzymes expression by phytochemicals *in vivo* or *in vitro* are considered as a major topic. This thesis will focus on the factors important in the regulation of Nrf2 and phase II xenobiotic metabolizing enzymes which are generally considered as antioxidant and detoxifying enzymes in cancer chemoprevention. Accumulating evidence from epidemiological studies indicates that chronic inflammation and oxidative stress play

critical roles in neoplastic development. Our results show that tea *Chrysanthemun zawadskii* (CZ) and licorice *Glycyrrhiza uralensis* (LE) extracts exhibited potent anti-inflammatory activities by suppressing the mRNA and protein expression levels of pro-inflammatory biomarkers and the NF-κB luciferase activity. Both extracts also showed strong inhibitory effects against NF-κB-mediated inflammatory as well as strong activation of the Nrf2-ARE-antioxidative stress signaling pathways. Indole-3-carbinol (I3C) and its acid condensation product, 3,3'-diindolylmethane (DIM) were examined the chemopreventive effect and the molecular mechanism, particularly the anti-oxidative stress pathway regulated by Nrf2, in transgenic adenocarcinoma of mouse prostate (TRAMP) mice and TRAMP C1 cells. I3C and DIM significantly suppressed the incidence of palpable tumor ($p<0.05$) and reduced the genitourinary weight ($p<0.05$) and induced Nrf2 and related genes expression in TRAMP mice. DIM can also epigenetically modify the CpG methylation status of Nrf2 *in vivo* and *in vitro*, and enhanced expression of Nrf2 and Nrf2-mediated genes. Using dietary phytochemicals to modulate the genomic as well as epigenomic is thought to be plausible in cancer chemoprevention in the future.

PREFACE

This thesis is submitted for the Degree of Doctor of Philosophy in Pharmaceutical Sciences at Rutgers, The State University of New Jersey. It serves as the documentation of my research work carried out between September 2007 and August 2012 under the supervision of Dr. Ah-Ng Tony Kong at Department of Pharmaceutics. To the best of my knowledge, this work is original, except where suitable references are made to previous work.

This dissertation consists of six chapters. Chapter 1 gives a general introduction to the mechanisms involved in the cancer chemopreventive effects of dietary phytochemicals via Nrf2 pathway and the significance of the proposed research work. The following five chapters contain papers that are published or accepted by or intended to submit for international journals. Chapter 2 investigated the effects of the anti-inflammatory, anti-oxidative stress activities and differential regulation of Nrf2-mediated genes *in vitro* and *in vivo* by comparing the global gene expression profiles between Nrf2 wild type and Nrf2 knockout C57BL/6J mice elicited by tea *Chrysanthemun zawadskii* (CZ) and licorice *Glycyrrhiza uralensis* (LE) extracts. Chapter 3 was to elucidate the *in vivo* and *in vitro* mechanisms of the chemopreventive efficacy of indole-3-carbinol (I3C) using transgenic adenocarcinoma of mouse prostate (TRAMP) mice and TRAMP C1 cells. The expression of Nrf2 and its downstream genes, cell-cycle and apoptosis genes protein levels were investigated. Chapter 4 identified the potential epigenetic mechanism of the Nrf2 and its downstream genes using a cancer chemopreventive agent, 3,3'-diindolylmethane (DIM), as a DNA demethylation agent in TRAMP mice and in

TRAMP C1 cells. Chapter 5 further studied the pharmacokinetics and pharmacodynamics correlation of DIM in rats. These chapters cover various aspects of cancer chemoprevention, such as *in vitro* and *in vivo* mechanisms, pharmacology, pharmacokinetic characteristics and pharmacodynamics of cancer chemopreventive agents.

Tien-Yuan Wu

August 2012

ACKNOWLEDGEMENT

As I stand at the threshold of my doctoral degree, I recall the numerous people who have helped and supported me during my graduate studies at Rutgers. First of all, I would like to express my sincere gratitude to my dear advisor **Dr. Ah-Ng Tony Kong** for his endless support, inspiring advice and providing me the opportunity to study at Rutgers. I wouldn't have been able to achieve so much without his excellent guidance and mentoring during the past five years. I am also indebted to the other committee members **Dr. Suzie Chen, Dr. Nanjoo Suh, and Dr. Ioannis P. Androulakis** for their valuable comments, advice and time spent on this dissertation. All members and alumni of Dr. Kong's lab are thanked for their support and assistance. All of the projects have been carried out with their help and collaboration. Especially, I want to present my appreciation to my instructors and friends **Dr. Tin Oo Khor, Dr. Siwang Yu** and **Dr. Constance L. Saw** for their support and feedback on my research, and to the lab alumni and friends Drs. Wen Lin, Ka-Lung Cheung, Hu Wang, Esq. Rachel T. Wu and other members in Dr. Kong's lab and Graduate Program in Pharmaceutical Sciences. It's also my pleasure to acknowledge the administrative support from Ms. Hui Pung, Ms. Marianne Shen and Ms. Sharana Taylor in the Department of Pharmaceutics. All animals are thanked to be Bodhisattva devoting to the studies in this dissertation.

I also want to acknowledge the financial support from Department of Pharmaceutics and Department of Pharmacy Practice and Administration, Ernest Mario School of Pharmacy during the last four years of my graduate studies. More importantly, my research work was sponsored by the institutional funds to Dr. Ah-Ng Tony Kong.

As an international student, I am so lucky to have a lot of family friends in New Jersey and the other parts of United States. I would like to appreciate all my friends who give me enormous supports in my life and my mind and provide their words of encouragement and cheers. As a volunteer, I volunteer to work for compassion relief missions in the Tzu Chi Foundation. A lot of volunteers in TZU CHI Family, whether in Taiwan or in the U.S.A., support me in my life, my spirit, my mind and my soul during the past five years of my graduate studies.

Last but not the least, I would like to thank my dear parents supporting me everything, my three sisters and three brothers-in-low taking care of my parents, my nieces and nephews always giving me a lot of happy. My grandmother, who passed away in 2001, always encouraged me to study for devoting myself to human beings.

DEDICATION

My grandmother, Shu-Chai Huang-Wu

My dear father, Chien-Nan Wu

My dear mother, Ying-Luan Huang

My oldest sister, Fang-Chien Wu

My older sister, Pin-Yi Wu

My older sister, Huang-Yi Wu

AND

ALL HUMAN BEINGS

TABLE OF CONTENTS

LIST OF TABLES

LIST OF FIGURES

CHAPTER 1 Introduction of the Role of Dietary Phytochemicals in Cancer Chemoprevention[1,2,3]

1.1 Introduction

Chemoprevention was a term first coined in 1976 by Dr. Michael B. Sporn. The cancer chemoprevention is the strategy of blocking or slowing the onset of premalignant tumors and decrease the incidence of cancer with relatively nontoxic chemical substance (Figure 1-1) (1). Most of the substances use in cancer chemoprevention are natural phytochemicals derived from food (2). There is increasing evidence that human cancers can be prevented not only by reducing or avoiding exposure to carcinogens but also by consumption of dietary phytochemicals which are abundant in vegetables, fruits, spices, flavoring agents, and herbal supplements, for example, curcumin (derived from turmeric), capsaicin (from chili and peppers), epigallocatechin-3-gallate (EGCG from green tea), PEITC, indole-3-carbinol, 3,3'-diindolylmethane and sulforaphane (from cruciferous vegetables). There are several different cellular and molecular mechanisms that appear

---

[1] Part of this chapter has been submitted to an international journal.

[2] **Key Words**: Phase II drug metabolizing (DM) genes/enzymes, Nrf2, chemoprevention, gene polymorphism, pharmacogenomics, epigenetics, pharmacoepigenomics

[3] **Abbreviations**: ABC, ATP-binding cassette; ADME, absorption, distribution, metabolism, and elimination; ARE, antioxidant response element; DBM, dibenzoyl methane; DM(E), drug metabolizing (enzyme); EGCG, epigallacatechin-3-gallate; GCLC, glutamate-cysteine ligase catalytic subunit; GST, glutathione S-transferase; HCC, hepatocellular carcinoma; HDAC, histone deacetylase; ITC, isothiocyanate; LPS, lipoplysacharride; MDR, multidrug resistance; MLL, myeloid lymphoid leukemia; NAT, N-acetyltransferase; NF-κB, nuclear factor kappa-light-chain-enhancer of activated B cells; NQO, NAD(P)H quinine oxidoreductase; Nrf2, nuclear factor (erythroid-derived 2)-like 2; PEITC, phenyl isothiocyanate; SFN, sulforaphane; SNP, single nucleotide polymorphism; SULT, sulfotransferase; TRAMP, transgenic adenocarcinoma of mouse prostate; UGT, UDP-glucuronosyltransferase.

the blocking and suppressing effects of chemopreventive compounds, and many of them appear to possess both blocking and suppressing effects. Therefore, the anti-carcinogenic function of these compounds might be attributed to a combination of their cytoprotective effect on normal cells and their cytotoxic effect on pre-neoplastic and/or neoplastic cells (Table 1-1 & Figure 1-2) (3).

It is believed that one of the underlying mechanisms behind the chemopreventive activities of phytochemicals is induction of detoxifying enzymes. Two major groups of biotransformation enzymes induced by phytochemicals to metabolize xenobiotics and carcinogens are phase I and phase II drug metabolizing enzymes (DMEs) (4, 5). Phase I DMEs introduce or expose functional group in the substrates through oxidation, reduction and hydrolysis reactions. One major group of phase I DMEs is the superfamily of cytochrome P450 enzymes. Phase II DM enzymes primarily catalyze conjugation reactions to facilitate the excretion and elimination of their substrates, which can be cytotoxic agents or carcinogens (6). The phase II DMEs include sulfotransferases (SULT), UDP-glucuronosyltransferases (UGT), NAD(P)H quinone oxidoreductase (NQO), glutathione S-transferases (GST), and *N*-acetyltransferases (NAT). Compared to the phase I DMEs, the phase II DMEs are more prone to have protective effects against carcinogens and to prevent carcinogenesis. Reactive metabolites are detoxified by phase II DMEs via conjugation leading to increase hydrophilicity and thus facilitate the excretion into the bile or urine (6, 7).

The protective effects of phase II DMEs can be induced through the exposure of xenobiotics. One major class of the inducers of phase II DMEs are the electrophiles

capable of enhancing the binding of a transcription factor, nuclear factor (erythroid-derived 2)-like 2 (Nrf2), to the antioxidant response element (ARE) in the promoter region of many phase II DME genes. in the action of cell protection and cancer chemoprevention. For this reason, Nrf2 plays an important role to mediate the genes expression of many phase II DMEs (8). Besides this transcriptional mechanism, the epigenetic regulations of phase II DMEs have also emerged as another important mechanism (9-11).

In contrast to the essential functions of phase I and II DMEs in the metabolism of xenobiotics, the phase III membrane transporters play a critical role in absorption, distribution, metabolism and elimination (ADME) of xenobiotics in the body. They are mainly the members of ATP-binding cassette (ABC) transporter superfamily, which includes 48 ABC genes in the human genome. The regulation of phase III transporters is also through both transcriptional and epigenetic mechanisms. For example, the multidrug resistance gene (MDR1) was the first identified as a gene that related to drug-resistant cancer cells which can effectively pump out the cancer therapeutic drugs, leading to the resistance. The overexpression of P-glycoprotein, the protein product of MDR1 gene, in cancer cells has been attributed to the hypomethylation of MDR1 gene and chromatin modifications, which control the state of MDR1 expression (12, 13). New information on the methylation status of MDR1 promoter has provided better understanding on mechanism behind the progression of breast and colon cancers (13, 14). Furthermore, ABCG2 gene has been identified as another important efflux transporter contributing to the drug resistance in cancer cells. Hypermethylation of CpG islands occurs in the

promoter region of ABCG2 gene, leading to epigenetically silencing on human leukemia, breast, and renal carcinoma. During chemotherapy, drug-induced demethylated effects could repress the ABCG2 gene and increase the transporters on the cancer cells. This is another important issue for the drug development in the future (15-17). Overall, the epigenomics of transporters can directly affect the pharmacokinetics and pharmacodynamics of xenobitics and therefore are highly relevance to adverse drug events (18).

Another factor which can affect the expression as well as the activity of encoded DMEs is genetic polymorphisms, such as single nucleotide polymorphisms (SNPs), microsatellite and minisatellite sequences, which are the variations in DNA. Approximately 10 million SNPs are estimated to occur commonly in our human genome, affecting biological pathways involving in drug metabolism, DNA biosynthesis and repair, cell cycle control, apoptosis (19, 20). Through the application of genome-wide association studies, the Environmental Genome Project (EPG), initiated by the National Institute of Environmental Health Sciences, has characterized commonly occurring in candidate genes involved in xenobiotic metabolism, including phase II DMEs (19). Over one hundred of SNPs in P450 subfamily genes have been identified and linked to phenotypes and functional changes (19). Another prominent example of genetic polymorphism is the SNPs of the human MDR1 gene, which have been characterized as an important factor determining the pharmacokinetic properties of several cancer therapeutic agents (21, 22).

Modulation of the phase II DME genes by phytochemicals can enhance elimination of reactive species and is beneficial in chemoprevention. In this chapter, we would like to focus on phase II DMEs and the signaling pathways induced by phytochemicals. The inductions of the phase II DME enzymes by phytochemicals have been found in our laboratory. We will also discuss the recent epigenomics studies in regulation of phase II DM enzymes and cancer chemoprevention.

1.2 Genetic polymorphisms of phase II DME and cancer chemoprevention

Genetic polymorphisms of phase II DME genes determine their different effects in detoxification and prevention of diseases. The relationships between polymorphistic GST, UGT, NQO and cancer chemoprevention are discussed as follows (Table **1-2**).

1.2.1 Glutathione S-transferases (GST). GSTs conjugate glutathione to electrophilic molecules and oxidative metabolites. There are six subclasses of GSTs including alpha (A), kappa (K), mu (M), omega (O), pi (P), theta (T) and zeta (Z) (20). GSTT1 plays a critical role in phase II biotransformation of many drugs and industrial chemicals and GSTM1 is relevant in the deactivation of carcinogens. Moreover, both GSTT1 and GSTM1 play an important role in the deactivation of reactive oxygen species involved in inflammation, aging and degenerative diseases (23). Recent studies have shown that induction of GSTs by phytochemicals reduce the risk of colorectal and breast cancers (5, 24). Lee *et al*. reported that cruciferous vegetables with large amount of isothiocyanates, may reduce the risk of breast cancer via modulation of GSTP1 (24). In our laboratory, we demonstrate that GSTM1 was induced in the mice colon, upon stimulation by PEITC or DBM and was associated with the lower colorectal cancer incidence AOM/DSS model

(25). However, it has not been demonstrated that enhanced expression of GSTs in human colorectal contributes to the prevention of the colorectal cancer (5).

The occurence of polymorphism in GST genes, such as the null, low activity or altered inducible variants, varies significantly in different ethnic groups (20). Epidemiological studies reported that certain GST null variants correlate with high incidence rates of hepatocellular carcinoma (HCC). For example, individuals with GSTT1 deficiency or GSTM1 deficiency have a higher risk of HCC, and the dual deletion of GSTM1 and GSTT1 further significantly increases the risk of HCC (26). In addition, the genetic polymorphism of GSTP1 in smoking population has been found to be important in determining the risk of esophageal squamous cell carcinoma in the Iranian population (27). Besides cancer risk, inflammatory diseases such as asthma are also linked tothe genetic polymorphism of GSTs (28).

1.2.2 NAD(P)H: quinone oxidoreductase 1 (NQO1). NQO1 detoxifies reactive quinones to hydroquinones and therefore avoids DNA and protein damages (20, 29). Over 93 SNPs have been identified in the NQO1 gene, but only a few of them have been studied in detail and implicated in the risk of cancers (29, 30). Three well known NQO1 alleles are the wild type (NQO1*1), C609T (NQO1*2) variant, and C465T (NQO1*3) variant. NQO1 polymorphisms are correlated with its enzyme activity. The enzyme activity of NQO1*1/*1 is higher NQO1*1/*2, and the enzyme activity of NQO1*2/*2 is undetected (20, 29). Epidemiology studies reported that NQO1*2 variant allele has no strong association with childhood acute lymphoblastic leukemia, but may be associated with myeloid/lymphoid (MLL) gene positive childhood leukemia. However, exposure to

environmental quinones may increase cancer risks when the NQO1 polymorphisms are present (29).

1.2.3 UDP-glucuronosyltransferases (UGT). UGTs are key metabolic enzymes catalyzing the glucuronidation of lipophilic xenobiotics and endobiotics to hydrophilic compounds, which enhance their elimination and prevent the accumulation of toxic lipophilic compounds (20, 31). UGTs consist of two major classes, UGT1 and UGT2, with more than 30 isoforms. The abnormal dinucleotide-repeat sequences of UGT1A1 promoters were found to reduce glucuronidation (20). The UGT1A1*28 allele, one of the promoter polymorphisms within seven TA repeats, dramatically reduces the capacity for glucuronidation, causes inherited unconjugated hyperbilirubinemia and increasing the life-threatening toxicity of iriontecan, a chemotherapeutic drug, in clinic (20, 32, 33).

1.3 Regulation of phase II DM enzymes through Nrf2 signaling pathway by dietary phytochemicals

Nrf2 is the pivotal transcription factor in the regulation of antioxidant response, and is essential in the cellular defense against oxidative stress and carcinogenicity. Nrf2 is expressed in the liver, intestine, kidney and lungs tissue (34). Under normal conditions, Nrf2 is mainly associated with Keap1, an actin-binding protein. The formation of Nrf2-Keap1 complex prevents Nrf2 from migrating into the nucleus and promotes the proteasomal degradation of Nrf2. Typically, the half-life of Nrf2 in mammalian cells is less than an hour. It has been shown that chemical-induced oxidative stress, such as the treatment of H_2O_2, results in conformational changes in Nrf2-Keap1 complex through the oxidation of thiol groups, causing the dissociation of Nrf2 from Keap 1. Thereafter, Nrf2

translocate into the nucleus to bind with ARE, leading to the induction of phase II DMEs. This process has been exemplified by the treatment of sulforaphane, a chemopreventive agent, which delays the degradation of Nrf2, increases its stability, and enhances the expression of Nrf2-targeted genes (8).

Because many phytochemicals elicited their chemopreventive effects through Nrf2-mediatedup-regulation of phase II DMEs Nrf2 is a very important target to prevent carcinogenesis (2, 34). Nrf2-null mouse model has been extensively used to investigate the function of Nrf2 and Nrf2-dependent cancer preventive effects (35, 36). The expression levels of GSTa1, GSTa2, GSTm1, GSTm2, GSTm3, GSTm4 and GSTm6 in Nrf2-null mice, as well as UGT and NQO1 genes, are much lower than that of wild-type mice (36), suggesting these phase II DMEs are Nrf2-dependent (Figure 1-3) (37-41). Nrf2 deficiency makes Nrf2-null mice highly susceptible to cancer development, due to the lack of the protective functions of antioxidant and detoxifying system. Nrf2 deficiency also makes the Nrf2-null mice irresponsive to the treatments of chemopreventive phytochemicals and agents. For example, butylated hydroxyanisole (BHA) induces many detoxifying genes, such as Gstm1, Gstm3, Ugt8a, Ugt2b35, Nqo1, and glutamate-cysteine ligase, catalytic subunit (Gclc), were induced in the liver and small intestine of wild-type mice, but not in Nrf2-null mice (39). Similar results were also obtained from the treatments of curcumin, licorice extracts, and chrysanthemum extracts on these two mouse lines, in which curcumin induces the expression of Gsta2, Gsta3, Gsta4, Gstm1, Gstm3, Ugt2b5 genes in the small intestine of wild-type mice while licorice extracts and chrysanthemum extracts induce Gstm3, Ugt2b5, Nqo1 in the liver of

wild-type mice but not in the liver of Nrf2-null mice (40, 42). All these inducing effects of curcumin, licorice extracts and chrysanthemum extracts were not observed in the Nrf2-null mice. Furthermore, phase II DME genes, such as Ugt2b1, Gstm3, Gclc, and Sult1d1, were induced by soy isoflavones in the prostate of wild-type mice rather than in the Nrf2-nullmice (38). Dietary phytochemicals induce phase II DM genes via Nrf2 signaling pathway not only in the liver and small intestine but also in the prostate tissue. Taken together, Nrf2 through regulation of phase II DM genes expression is critical for dietary phytochemicals to exert their cancer chemopreventive effects.

1.4 Pharmacodynamics of anti-oxidant effect of dietary phytochemicals as cancer chemopreventive agents

Dietary phytochemicals elicit its chemopreventive effect through induction of Nrf2 signaling leading to elimination of carcinogen electrophiles, reactive oxygen species, and xenobiotic metabolites (1, 8, 43-45).

Phytochemicals have been investigated for cancer chemoprevention and cancer chemotherapy for decades. Isothiocyanates (ITCs), a group of compounds including sulforaphane (SFN), phenyl isothiocyanate (PEITC) from cruciferous vegetables, are one of the most widely investigated dietary phytochemicals. Other phytochemicals include epigallocatechin-3-gallate (EGCG) from green tea, curcumin from turmeric, and dibenzoylmethane (DBM) from licorice (25, 46-50). Through modulation of Nrf2 and phase II DM enzymes, these compounds decrease the “cellular stress” (47). Our laboratory has demonstrated the molecular mechanisms of SFN, PEITC, curcumin, DBM,

EGCG, and tocopherols using *in vitro* cell culture method and chemopreventive efficacy of these compounds were also tested *in vivo* (25, 46, 48, 50-56).

Reduction of oxidative stress is one of the most important strategies in cancer chemoprevention. It has been reported that SFN upregulates the expression of GSTM, GSTA, and NQO1 as well as GSTP enzymes, which were modulated by activating Nrf2 binding to the GSTP enhancer I (57). Danilov *et al*. reported that SFN protected the rat cortical astrocytes from cell death by exposure to oxygen and glucose deprivation. Moreover, mRNA, protein level and enzyme activity of NQO1 were increased by SFN in the astrocytes (58). In addition, SFN induced HO-1 in human intestinal Int 407 cells to attenuate oxidative stress and protect cells from injury (59). Our laboratory reported that SFN inhibited the skin tumorigenesis in C57BL/6J mice through induction of Nrf2 and relative phase II DM enzymes (60). Curcumin, one of the most popular spices in Indian food, have been shown to be a strong inducer of GSTP1 and Nrf2/ARE signaling pathway in HepG2 cell (61). *In vivo* studies reported that curcumin attenuated the oxidative stress of liver injury and neuronal injury through increasing phase II DM enzymes expression in rats (62, 63). Interestingly, our laboratory found that γ-tocopherol enriched mixed tocopherol, PEITC, and curcumin restored the Nrf2, phase II DM enzymes and antioxidant enzymes such as Ugt1a1and Gstm1 in Transgenic Adenocarcinoma of the Mouse Prostate (TRAMP) model (48, 64).

1.5 Pharmacodynamics of anti-inflammatory effect of dietary phytochemicals as cancer chemopreventive agents

Chronic inflammation has been identified as one of the critical mechanisms in tumorigenesis of many different cancers. Inflammatory responses are usually initiated by the generation of oxidative stress and promoted by a cascade of cytokine release and signaling (44). Therefore, the phytochemicals capable of reducing oxidative stress through activating Nrf2/ARE signaling pathway and inducing phase II DMEs under the inflammatory environment may attenuate the risk of neoplastic transformation. In addition, phytochemicals can also exhibit anti-inflammatory effect through the inhibition of nuclear factor kappa-light-chain-enhancer of activated B cells (NF-κB) pathway. Our laboratory found that PEITC, SFN and other ITCs inhibited lipoplysacharride (LPS) induced NF-κB luciferase activity in HT-29 cells transfected with NF-κB-luciferase-reporter (HT-29-N9) (65). Inhibition of NF-κB activities was found in the curcumin treated human prostate PC-3 and human colon HT-29 cells (65, 66). Furthermore, we also reported that Nrf2 gene deficient mice were more susceptible to dextran sulfate sodium (DSS)-induced colitis and colorectal carcinogenesis. Nrf2-null mice exposed to DSS had decreased phase II DMEs expression and increased expression of pro-inflammatory cytokines and biomarkers. These findings suggested that Nrf2 is important in the regulation of the expression of phase II DMEs against oxidative stress as well as the inhibition of pro-inflammatory signaling pathways (35).

1.6 Epigenomics of regulation of phase II DM enzymes and Nrf2 signaling pathway

As the results of structure modifications in chromatin, epigenetic events have been deemed as important factors in wide variety of biological processes (10, 11, 67). Epigenetic modifications of chromatin include DNA methylation, covalent and non-covalent modifications of histone, nucleosome and non-coding RNAs, such as microRNA remodeling (67). Many epigenetic events occur during cancer initiation and progression (67). For example, DNA methylation in the promoter regions leads to the changes of genes expression of oncogenes or tumor suppressor genes (68), and the hypermethylation may play a critical role in human cancer due to its effects on silencing tumor suppressor genes (Figure 1-4) (11, 67). Moreover, the loss of histone acetylation through overexpression of histone deacetylases (HDACs) occurs frequently in various types of cancers. Abnormal formation of fusion proteins through chromosomal translocations of genes happens in several types of cancers such as leukemia (9, 11, 67). Epigenetic regulation of phase II DM enzymes has been reported in human cancers. In human colon cancer cells such as HT-29 and HCT-116 it has been shown that between CpG-1 and -4 of the proximal UGT1A1 promoter region was methylated leading to a reduction in the expression of UGT1A1 gene (31, 69). Our laboratory found that the promoter region of murine Nrf2 gene was methylated at CpG sites in TRAMP prostate tumor and TRAMP C1 cells leading to the silencing of Nrf2 gene (70).

Different from genetic polymorphism, epigenetic changes are reversible. This reversible feature of epigenetic changes in cancer has led to the development of a new

therapeutic option, epigenetic therapy (67). For example, methylated DNA sequences in cancer cell lines can be recovered and rescued using demethylating agents (11). Based on this mechanism, FDA has approved 5-aza-CR (azacitidine) and 5-aza-CdR (decitabine), two demethylating agents, for treating myelodysplastic syndrome and myeloid leukemia (11, 67). Mavis *et al*. showed that were demethylated by a combination of 5-aza-CdR and HDAC inhibitor, trichostatin (TSA), has been shown to reduce the hypermethylation in the promoter of GST genes in TRAMP prostate cancer cells and restore the Nrf2 and NQO1 expression (70). Ongoing studies are investigating whether phytochemical chemopreventive agents, including curcumin, EGCG, SFN, and PEITC, elicit their tumor suppression effects through specific epigenetic mechanism such as DNA demethylation and histone modifications (10, 71-73).

1.7 Summary

Phase II DMEs play a very important role in maintaining antioxidant system, performing detoxifying functions, and preventing carcinogenesis. The expression and activities of phase II DMEs are significantly affected by genetic polymorphism, epigenetic profile and transcriptional regulation. Nrf2 and Nrf2-mediated phase II DME gene expression are important targets of dietary chemopreventive compounds. Recent data also suggested that the regulatory effects of dietary phytochemicals on phase II DME genes expression may be contributed by their epigenetic effects on DNA methylation or histone acetylation. Future study will shed more insights on these issues and provide guidance for developing personalized approach in phytochemical-based cancer chemoprevention.

Table 1-1 Mechanisms of dietary cancer chemopreventive agents (3)

Function	Compound	Source
Blocking Agent		
Enhance carcinogen detoxification	Curcumin	Turmeric
	Sulforaphane	Cruciferous vegetable
	Indole-3-carbinol & 3,3-diindolelylmethane	Cruciferous vegetable
Inhibit carcinogen activation	isothiocyanates	Cruciferous vegetable
Scavenge free radicals	Vitamin E	Vegetable oil
Suppressing Agent		
Cell cycle arrest and/or apoptosis	Curcumin	Turmeric
	Sulforaphane	Cruciferous vegetable
	Resveratrol	Grape skin
	Epigallacatechin-3-gallate	Green Tea

Table 1-2 Phase II DM Gene polymorphisms associated with human disease and cancer

Phase II DM genes and Subunit		Associated disease		Reference
GST	GSTP (π)	GSTP1 null: esophageal squamous cell carcinoma in smoking population GSTP1Ile105: asthma		(27, 28)
	GSTM (μ)	GSTM1 null: HCC; bladder cancer; asthma	GSTM1 and GSTT1 dual deletion: lung cancer; aero-digestive tract cancer	(23, 26, 28)
	GSTT (θ)	GSTT1 null: HCC; atophy		(23, 26)
NQO1	NQO1*2	NQO1*2 variant allele: Childhood leukemia with MLL-gene positive		(29)
UGT	UGT1	UGT1A1*28 allele: unconjugated hyperbilirubinemia in Caucasian UGT1A1 gene promoter: abnormal dinucleotide-repeat occurs as reduced glucuronidation		(20)

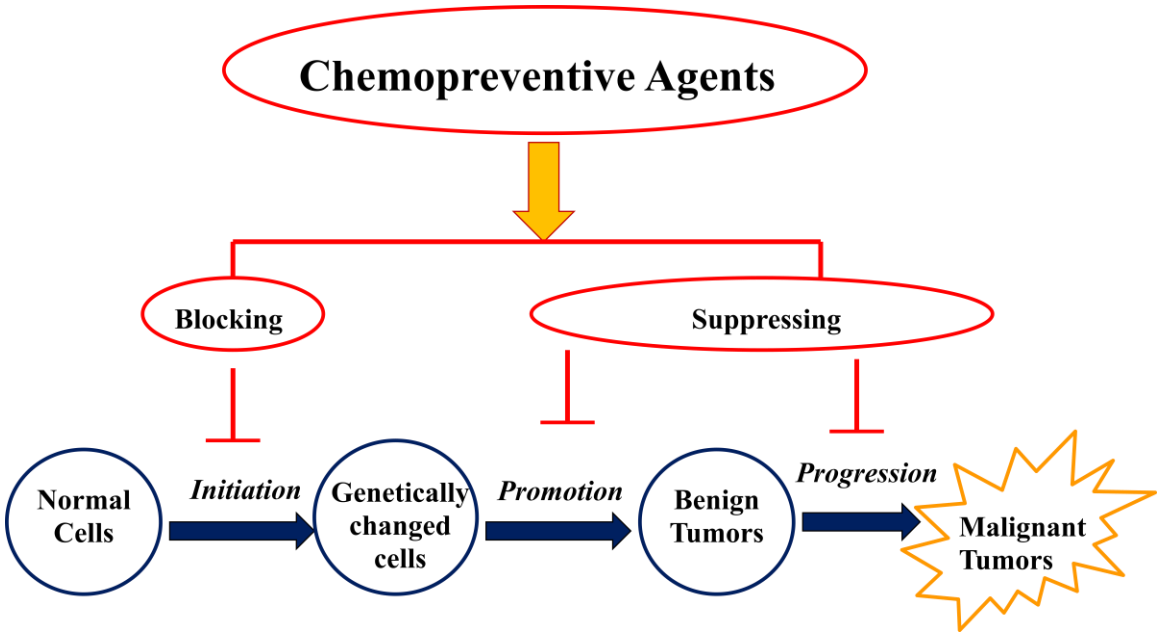

Figure 1-1 Function of cancer chemopreventive agents

Cancer chemopreventive agents are blocking or slowing the onset of premalignant tumors and decrease the incidence of cancer.

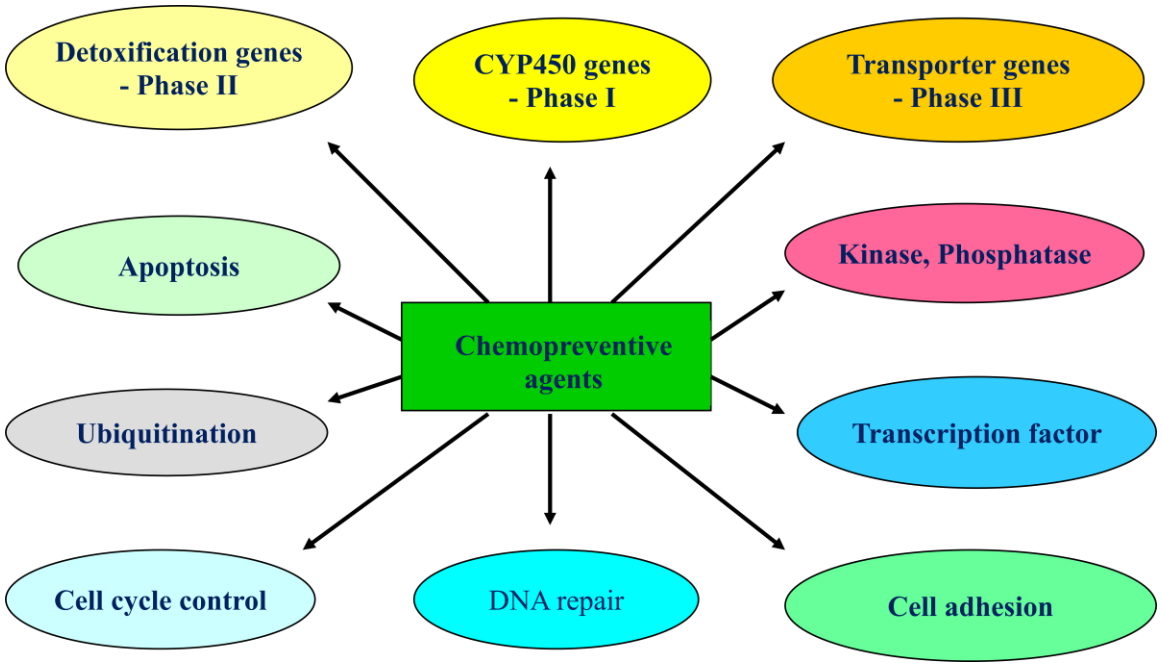

Figure 1-2 Potential mechanisms of cancer chemopreventive agents

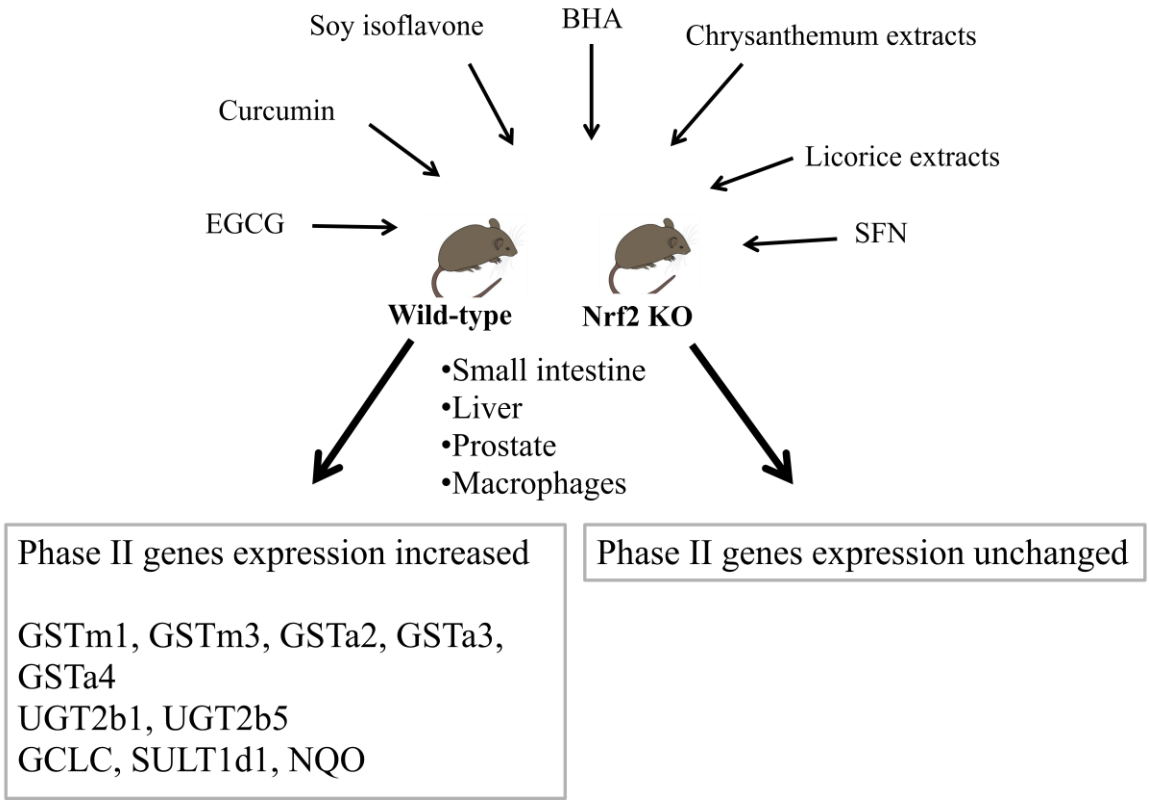

Figure 1-3 Pharmacogenomic profile of dietary phytochemicals in Nrf2 deficient mice (Nrf2 -/-) and wild-type mice (Nrf2 +/+).

Mice were treated with Curcumin, EGCG, Soy isoflavone, BHA, SFN, Licorice extracts, Chrysanthemum extracts and total RNA were isolated from small intestines, livers, prostates, macrophages. (39, 40, 42)

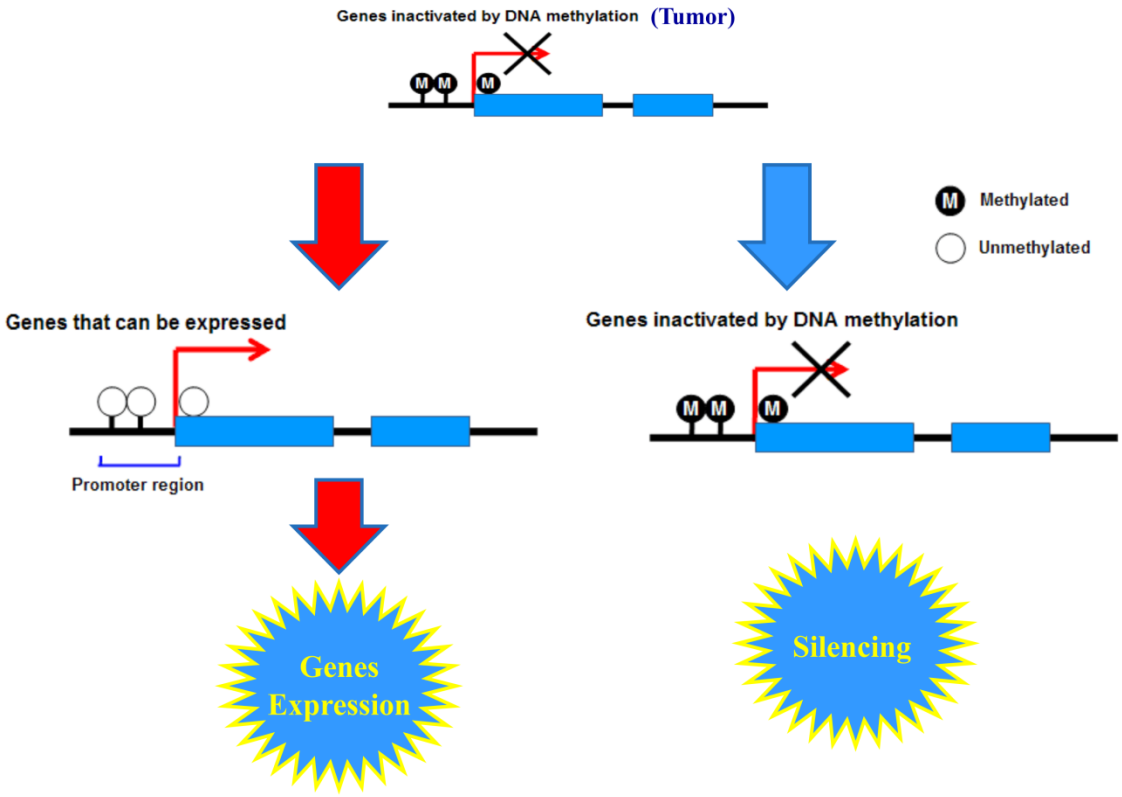

Figure 1-4 DNA methylation in the promoter regions

DNA hypermethylation in the promoter regions leads to the changes of genes expression of oncogenes or tumor suppressor genes.

CHAPTER 2 Role of Nrf2-mediated Genes regulated by herbals in Anti-inflammatory/Anti-oxidative Stress Activities [4,5,6]

2.1 Introduction

Normal inflammation in general is a process involving interactions between pro-inflammatory and anti-inflammatory signaling pathways. Inflammation occurs when the tissue is injured or infected by external challenges (74). In this context, generally acute inflammation is self-limiting and recovered by itself (74). However, chronic inflammation could increase the risk of developing diseases such as cancer in the inflamed tissues (75).

Nuclear factor (erythroid-derived 2)-like 2 (Nrf2) plays an important role to mediate phase II detoxifying/ antioxidant enzymes expression. Under normal conditions, Nrf2 appears to be associated with actin-binding Keap 1 that forms Nrf2-Keap1 complex preventing Nrf2 from entering into the nuclear and promoting its proteasomal degradation. Typically, the half-life of Nrf2 in un-stimulated mammalian cells is 15-45 min. Upon treatments of the cells with oxidants such as H_2O_2, oxidative stress or cancer chemopreventive compounds, conformational changes occur due to oxidation of thiol

[4] Part of this chapter has been published as **Wu**, *et al*, AAPS J. 2011 Mar;13(1):1-13

[5] **Keywords**: Licorice, Chrysanthemum, anti-inflammatory, anti-oxidative, Nrf2, phase II enzymes

[6] **Abbreviations**: AOX1, aldehyde oxidase 1; ARE, antioxidant response element; CUR, curcumin; CZ, Chrysanthemum zawadskii extracts; ELISA, Enzyme-linked immunosorbent assay; FKBP5, FK506 binding protein 5; GST, glutathione S-transferases; LE, Glycyrrhiza uralensis extracts; NF-κB, nuclear factor kappa-light-chain-enhancer of activated B cells; NQO, NAD(P)H dehydrogenase (quinone); Nrf2, nuclear factor (erythroid-derived 2)-like 2; PTPLAD1, protein tyrosine phosphatase-like A domain containing 1; qPCR, quantitative real-time PCR; SCARB1, scavenger receptor class B, member 1; SLC35A2, solute carrier family 35 (UDP-galactose transporter), member A2; UGT, UDP-glucuronosyl transferase; USP, ubiquitin specific peptidase

sensitive amino acids present in the Nrf2-Keap 1 complex and would drive the dissociation of Nrf2 from Keap 1, thereby allowing the translocation of Nrf2 into the nucleus, Nrf2 binds to the antioxidant response element (ARE) of ARE-target genes and leads to enhanced phase II detoxifying/ antioxidant enzymes expression (76, 77).

In Eastern Asia, the use of plants including roots and fruits as herbal medicines is common. There are numerous dietary supplements used for the treatment of stomach ulcers, bronchitis, and sore throat, as well as infections caused by viruses, such as hepatitis but have not been approved by Food and Drug Administration (FDA). Licorice and tea chrysanthemum are two popular herbal medicines used to treat various inflammatory diseases. Licorice (*Glycyrrhiza*) species have been used in Europe as herbal medicines for centuries as well. Licorice root is used for the treatment of gastric or duodenal ulcers, hepatitis, sore throats, coughs, bronchitis, arthritis, allergies, and cardiovascular disease (74, 78). Licorice, including glycyrrhizin, isoliquiritigenin, liquiritigenin, licochalcone A and B, and β-glycyhrritinic acid (79-81), have been shown to possess anti-inflammatory activities and glycyrrhizin can inhibit reactive oxygen species (ROS) [National Center for Complementary and Alternative Medicines (NCCAM; http://nccam.nih.gov/health/licoriceroot/)]. Licorice has also been shown to inhibit the expression of COX-2 and other pro-inflammatory proteins (78, 82, 83). There are currently (as of 07/15/2012) twenty on-going, completed or terminated clinical trials on “licorice or licorice-related” dietary supplement listed on Clinicaltrials.gov (http://www.clinicaltrial.gov). Chrysanthemum which includes five germacrane-type sesquiterpenes, kikkanols D, D monoacetate, E, F, and F monoacetate, were isolated from

the ethyl acetate-soluble portion and two flavanone glycosides, (2S)- and (2R)-eriodictyol 7-O-beta-D-glucopyranosiduronic acids, and a phenylbutanoid glycoside, (2S, 3S)-1-phenyl-2,3-butanediol 3-O-beta-D-glucopyranoside, isolated from the flowers of *Chrysanthemum*, has been used to treat vertigo, hypertension, bacterial and viral infectious diseases (84-87). Botanical chrysanthemum tea or extract are available as dietary supplements and promoted as health enhancing products. Extract of chrysanthemum has been shown to possess strong anti-oxidative stress, anti-inflammatory effects and previous studies revealed that different extraction methods yielding different soluble fraction of extracts would possessed different effects of anti-inflammation and immuno-modulation (84, 88). A completed clinical trial of chrysanthemum extract as dietary supplement to lower serum LDL cholesterol and raising HDL cholesterol is listed on Clinicaltrials.gov (http://www.clinicaltrial.gov).

Despite these diverse potential health beneficial and pharmacological effects of licorice and chrysanthemum, the molecular and the signaling mechanisms leading to these biological effects are still unclear. We theorized that the non-polar fractions of licorice and chrysanthemum may possess anti-inflammatory and anti-oxidative stress properties that could be further developed for diseases prevention including cancer chemoprevention. In this study, we aim to investigate the transcription regulation of licorice and chrysanthemum extracts on the transcriptional factor Nrf2 signaling pathway that controls the expression of many anti-oxidative stress and phase II drug metabolizing (DM)/detoxifying enzymes, which are typically elicited by many chemopreventive compounds (8, 19, 44). Therefore, in the current study, we utilized the Nrf2 deficient

mice (Nrf2-/-; KO) and Nrf2 wild-type (Nrf2+/+; WT) mice to examine whether the *in vivo* phase II DM/detoxifying/anti-oxidative/ properties elicited by the extracts would be mediated by Nrf2.

2.2 Materials and methods

2.2.1 Plant extracts

Whole plants of *Chrysanthemum zawadskii* (CZ) Herbich var**.** *latilobum* (Maxim.) Kitamura and licorice roots, derived from *Glycyrrhiza uralensis* (LE) Fisch. were purchased from a local drug store (Dea Guang Medical, Chunchon, South Korea) and identified by Emeritus Professor Hyung Jun Ji (Seoul National University, Seoul, Korea). Dried and ground *C. zawadskii* (5 kg) (CZ) and roots of *G. uralensis* (5 kg) (LE) were dip-extracted with hexane: ethanol (70 L) at a ratio 9:1 (v/v) at room temperature for 24 hours. The slurry was then filtered through filter paper and the residue was re-extracted twice. The combined extracts were filtered, and the filtrates were concentrated under reduced pressure at 40℃ to yield the hexane/ethanol extract of CZ (412 g, 0.82% yield) and LE (455 g, 0.91% yield).

2.2.2 Cell culture and treatment

The murine RAW 264.7 macrophage cells, a well-established model system for many inflammatory studies as well as the luciferase reporter assay of nuclear factor kappa-light chain enhancer of activated B cells (NF-κB) stabilized in human colon cancer cells HT-29 (HT-29-N9) were used to investigate the anti-inflammatory effects of licorice and chrysanthemum extracts (65). Similarly, the Nrf2-mediated ARE luciferase

assay stabilized in human hepatoma HepG2 cell (HepG2-C8) was used to investigate the potential of the extracts in activating the Nrf2/ARE signaling pathway (89). Mouse macrophage cell line RAW 264.7, was obtained from American Type Culture Collection. HepG2-C8 and HT-29-N9 cells were generated in our laboratory as described previously (52, 90-92). All cells were cultured in Dulbecco's Modified Eagle's Medium (Invitrogen Corp., Carlsbad, CA, U.S.A.) supplemented with 10% (V/V) FBS (Lifeblood Medical, Inc), penicillin 100 U/ml, and streptomycin 100 μg/ml. Cells were maintained in a humidified incubator with 5% CO_2 at 37^{o}C. The cells were treated with LPS (1 μg/ml, Sigma, St. Louis, MO, U.S.A.) alone or pretreated 1 hour with LE 25 μg/ml, CZ 25 μg/ml, or curcumin (CUR) 10 μg/ml (as positive control) dissolved in DMSO before they were challenged with LPS (65, 92)

2.2.3 Nitrite assay

The culture medium of the cells treated with different compounds was mixed with a Griess reagent in an equal volume of 0.1% (1 mg/ml) N-(1-naphthyl)ethylenediamine dihydrochloride in deionized water and 1.0% (10 mg/ml) sulfanilic acid in 5% phosphoric acid solution. The mixed sample was incubated at 37°C for 30 min. Absorbance at 548 nm was measured and concentrations were calculated using a sodium nitrite standard curve.

2.2.4 RNA isolation and reverse transcription polymerase chain reaction (RT-PCR) analysis

The RAW 264.7 cells were cultured in 6-well plates and were challenged by LPS 1μg/ml with or without pretreatment with LE, CZ, or CUR for 8 h at the 37°C incubator.

Total RNA was isolated by TRIZOL® according to the manufacturer's protocol (Invitrogen Corp., Carlsbad, CA, U.S.A.). First- strand cDNA was synthesized from 5 μg of total RNA using SuperScript III First-strand Reverse Transcriptase (Invitrogen Corp. Carlsbad, CA, U.S.A.) and oligo dT primers according to the manufacturer's instructions. After reverse transcription, the PCR reactions were performed by using 1 μL of reverse transcription product, 1 μL of primer mixture (final concentration, 10 μmol/L), and 8 μL of Platinum® *Taq* DNA Polymerase kit (Invitrogen Corp. Carlsbad, CA, U.S.A.), and preformed with initial denaturation at 94°C for 2 min, 25 cycles of amplification, and extension at 72°C for 10 min. PCR products were fractionated on 1.5% agarose gel. The primers used in this experiment are shown in Table 2-1.

2.2.5 Western blotting

The RAW 264.7 cells were challenged by LPS 1 μg/ml with or without pretreatment with LE, CZ, or CUR. After 24 h, the cells were washed with ice-cold phosphate buffer saline (PBS) (pH 7.4), and scraped into microcentrifuge tubes and pelleted. Cells were resuspended and lysed in RIPA buffer (Sigma, St. Louis, MO). 20 μg protein per lane was loaded onto 4-15% SDS-PAGE (Bio-Rad Laboratories, Hercules, CA). After separation by SDS-PAGE, the protein was transferred onto nitrocellulose membrane (Millipore Corp., Billerica, MA, U.S.A.), and then was blocked in 5% bovine serum albumin (BSA) (Fisher Scientific, Fair Law, NJ, U.S.A.) in tris buffer saline tween-20 (TBST) solution for 1 h. Membranes were probed by respective antibodies including β-actin, COX2, $cPLA_2$, and iNOS (1:1000; Santa Cruz Biotechnology, Santa Cruz, CA) overnight at 4℃. Blots were washed with TBST solution 15 min for 4 times and

incubated with respective secondary antibodies for 1 hr. After washing 15 min for 4 times with TBST solution, the immunoreactive bands were determined by adding SuperSignal West Femto mix (1:1 mix of stable peroxide buffer and luminol/enhancer solution, Thermo Scientific, Rockford, IL) to detect immunoreactive bands which were then visualized and quantified by BioRad ChemiDoc XRS system (Hercules, CA).

2.2.6 Enzyme-linked immunosorbent assay (ELISA)

The RAW 264.7 cells were cultured in 96-well plate with 200 µl medium. IL-6 and IL-1β ELISA assay kits were purchased from Invitrogen Corporation, Carlsbad, CA, U.S.A. The assays were performed according to the manufacturer's instructions. For the ELISA assay, 50 µl of incubation buffer was first added to all the wells. After adding incubation buffer, 50 µl standard diluent buffers and 50 µl of standards, controls, or samples were added to each well in a stepwise fashion.

2.2.7 Luciferase reporter assay

The NF-κB- and ARE-luciferase activities were measured using a luciferase reporter assay system according to the manufacturer's instructions (Promega, Madison, WI, USA). Briefly, after treatments, the cells were washed with ice-cold PBS and harvested in reporter lysis buffer. After centrifugation, 10 µl of the supernatants were mixed with 50 µl of luciferase assay substrate and measured for luciferase activity by using a Sirus Luminometer (Berthold Detection Systems GmbH D-75173 Pforzheim, Germany). The luciferase activity was normalized against known protein concentrations and expressed as fold induction of luciferase activity over the control cells, which were treated with 0.1%

DMSO. The protein level was determined by Bio-Rad protein assay according to the manufacturer's instructions as we have described previously (35, 91).

2.2.8 Quantitative real-time PCR assays (qPCR)

The HepG2-C8 cells were cultured in 6-well plates and were treated with respective extracts for 8 h at 37°C and the total RNA collected respectively. The primers for qPCR are listed in Table 2-2 (Integrated DNA Technologies, Coralville, IA, U.S.A.). The PCR reactions were carried out using 1 μl cDNA product, 50 nM of each primer, and Power SYBR Green master mix (Applied Biosystems, Foster City, CA, U.S.A.) in 10 μl reactions. The reactions were performed using an ABI Prism 7900HT sequence detection system amplified specificity was verified by first-derivative melting curve analysis using the ABI software (SDS2.3, Applied Biosystems, Foster City, CA, U.S.A.). Relative quantification of each gene expression profile was calculated using a ΔΔCt method and presented as relative quantitative value (RQ value) = $2^{-\Delta\Delta Ct}$ (RQ manager, Applied Biosystems, Foster City, CA, U.S.A.) (38, 93).

2.2.9 Animals and in vivo study

The second generation (F2) Nrf2 (-/-) mice (C57BL/SV129) and the C57BL/6J wild-type mice (The Jackson Laboratory, Bar Harbor, ME) were used for the *in vivo* study to investigate if the induction of phase II detoxifying/ antioxidant enzymes by the extracts was Nrf2-dependent (50). Five animals were used in each group of Nrf2 (-/-) mice (Nrf2 KO) and wild type mice (Nrf2 WT). The mice were treated with vehicle (as a negative control; cremophor: tween 80: ethyl alcohol: deionized water= 2:1:1:6), LE 150 mg/kg, LE 300 mg/kg, CZ 150 mg/kg, and CZ 300 mg/kg by oral gavage in a final

volume of 100-110 µl (88). After 12 h, livers were collected for the RNA extraction, and total RNA were used for PCR, qPCR, and microarray analyses (Figure 2-8). Housing and care of the animals were in accordance with the guidelines established by the University's Animal Research Committee consistent with the NIH Guidelines for the Care and Use of Laboratory Animals.

2.2.10 Microarray gene expression analysis

Affymetrix MOE_430 microarrays (containing 45,101 probes) were used to probe the global gene expression profile of pooled RNA from Nrf2 WT or KO mice after oral administration of CZ and LE of 150 mg/kg. These microarrays were conducted as published previously (38). The ".CEL" files containing intensity values were created from the scanned image by using Microarray Suite 5 (Affymetrix). The .CEL files and the .CDF file (information on the location and identity of different probe cells) were then analyzed using the d-Chip analysis software to identify genes that were differentially expressed in Nrf2-associated pathways in the liver samples of both treated and untreated controls (94-96). Normalization against the median using default settings in d-Chip (median chip) was used and the expression values of each probe of all arrays (median intensities range 110-280) were calculated using default d-Chip model-based algorithms with perfect match only for fluorescence intensities. A transformed normalized data was generated and saved in an Excel file, which was later being imported into the Ingenuity Pathway Analysis Program (www.ingenuity.com, IPA 8.0) for further data characterization (94, 97). Over 2,000 highly differentially expressed genes were filtered using cut-off intensity at 1,750 and a subset of Nrf2-mediated oxidative stress response

genes was performed using the canonical pathway analysis function. Comparative analysis was performed between treated groups for CZ and LE with their respective counterparts' control.

2.2.11 Statistical analysis

Values were presented as means ± standard error of mean (SEM). Statistical analysis of the data was performed by Student's *t* test. P values lower than 0.05 were considered significant. Nonparametric statistical Mann-Whitney U test of the qPCR results for the *in vivo* animal study was performed using SPSS software (version 17, U.S.A.) (98, 99).

2.3 Results

2.3.1 Inhibition of mRNA and protein levels of pro-inflammatory markers by LE and CZ extracts

To demonstrate the anti-inflammatory effects of LE and CZ extracts, the mRNA expression levels of pro-inflammatory makers, COX-2, IL-1β, IL-6, and iNOS in LPS-stimulated RAW 264.7 cells were found to be strongly suppressed by LE and CZ (Figure 2-1.) Similarly, the LE and CZ extracts also demonstrated strong inhibitory effect on the protein expression levels of COX-2, $cPLA_2$ and iNOS (Figure 2-2.)

2.3.2 LE and CZ extracts inhibit IL-6 and IL-1β

To investigate the suppression effect of pro-inflammatory proteins levels by LE and CZ, the expression of IL-1β and IL-6 was analyzed by using enzyme-linked immunosorbent assay (ELISA). LE significantly inhibited the expression level of LPS-

induced IL-1β ($p<0.05$) and IL-6 ($p<0.001$), whereas, CZ significantly inhibited only the expression level of LPS-induced IL-6 ($p<0.001$) (Figure 2-3).

2.3.3 Inhibitory effect of LE and CZ extracts on LPS-induced nitrate oxide (NO) production

Nitric Oxide (NO) is a molecular mediator of many physiological processes, including vasodilation, inflammation, thrombosis, immunity and neurotransmission (100). The inhibitory effect of extracts on the production of nitric oxide, which could be due to inflammatory reaction, was determined by the Griess reaction to measure the level of nitrite, an indicator of NO synthesis. The extracts, CZ (25 μg/ml) and LE (25 μg/ml), significantly inhibited LPS-induced NO production ($p<0.001$) by 44% and 48%, respectively (Figure 2-4).

2.3.4 Effect of LE and CZ extracts on NF-κB luciferase activity in HT-29-N9 cells

NF-κB pathway can trigger the expression of pro-inflammatory proteins. To investigate the effect of inhibition of NF-κB by LE and CZ, HT-29-N9 cells were stimulated by LPS with or without pretreatment of LE and CZ. Both LE and CZ significantly suppressed the LPS-induced NF-κB luciferase activity ($p<0.05$). LE had a slightly stronger inhibitory effect on NF-κB luciferase activity inhibition in comparison to CZ ($p<0.001$) (Figure 2-5).

2.3.5 Effect of LE and CZ extracts on ARE luciferase activity and expression of Nrf2 and its trans-activated target genes in HepG2 C8 cells

To investigate whether LE and CZ extracts could induce the Nrf2-mediated ARE luciferase activity as well as the transcriptional regulation of Nrf2 target genes, ARE luciferase assay and qPCR analysis were performed. LE and CZ extracts significantly induced the ARE luciferase activity in HepG2C8 cells, by four ($p<0.001$) and three ($p<0.01$) folds, respectively, as compared to the control group (Figure 2-6). Interestingly, LE and CZ significantly induced the endogenous Nrf2-target gene, NAD(P)H dehydrogenase (quinone) 1 (NQO-1), by 3.57 and 2.92 folds, respectively. The expression of phase II UDP-glucuronosyl transferase 1A1 (UGT1A1) was also induced by LE and CZ by 2.50 and 1.51 folds, respectively (Figure 2-7).

2.3.6 Effect of LE and CZ extracts on the expression of Nrf2 and its trans-activated target genes in the liver of Nrf2 WT C57BL/6J mice and Nrf2 deficient (KO) mice

To investigate if the phase II detoxifying/anti-oxidant genes activation by the extracts was mediated through Nrf2 signaling pathway, the expression level of these genes in the liver of Nrf2 KO and WT mice treated with the extracts were measured using qPCR. Figure 7 shows that NQO-1 and UGT1A1 mRNA were substantially induced in the Nrf2 WT mice as compared to the Nrf2 KO. While LE extracts could induce the expression of NQO-1 and UGT1A1 genes in both Nrf2 KO and WT mice, the induction of NQO-1 by CZ extracts was only observed in the Nrf2 WT mice. In contrast, the induction of UGT1A1 gene in Nrf2 KO mice by CZ was only observed at the higher dose level. As expected, Nrf2 mRNA was only expressed in the Nrf2 WT mice and induced by

CZ and LE, but not expressed nor induced by CZ and LE in the Nrf2 KO mice (Figure 2-9).

2.3.7 Microarray analysis of LE and CZ induced Nrf2-dependent genes in the liver of Nrf2 WT mice and Nrf2 KO mice

Using Affymetrix MOE_430 microarrays (containing 45,101 probes) the gene expression profiles of CZ and LE treated Nrf2 WT and KO mice were compared. In general, CZ treatment has a stronger effect on the expression of Nrf2-target genes as compared to LE (data not shown); therefore, we focused on reporting the CZ data. Genes that were induced by CZ only in the WT mice but not in the Nrf2 KO mice were considered as CZ-induced Nrf2-dependent genes. The canonical pathway of Nrf2-mediated oxidative stress response by CZ is presented in Figure 8. Similar trends were also observed for LE treatment but to a lesser extent (data not shown). Among the Nrf2-dependent phase II detoxification and antioxidant genes that were found to be induced by CZ were aldehyde oxidase 1(AOX1), FK506 binding protein 5 (FKBP5), different isoforms of glutathione S-transferases (GST), protein tyrosine phosphatase-like A domain containing 1 (PTPLAD1), ubiquitin specific peptidase 14 (USP14) (tRNA-guanine transglycosylase) and phase III transporter genes, solute carrier family 35 (UDP-galactose transporter), member A2 (SLC35A2), and scavenger receptor class B, member 1 (SCARB1).

Figure 2-11 shows that Nrf2 gene expression was induced by both LE and CZ treatments in the WT but not Nrf2 KO mice. AOX-1 was induced in WT mice to a higher

level than in Nrf2 KO mice by both LE and CZ. GSTmu3 and NQO-1 genes were induced in WT mice by both CZ and LE treatments.

2.3.8 Validation of microarray data by quantitative real-time PCR (qPCR)

To validate the results of the microarray, qPCR, was performed to quantify the expression level of seven selected genes (Table 2-4). The values of each gene were normalized by the value of β-actin. Nonparametric Mann-Whitney U test was used to compare the differences between groups (Figures 2-12). The qPCR data was in agreement with the trends observed in microarray such as Nrf2 (Figure 2-12 Top), AOX1, GSTμ3, and NQO-1 (Figure 2-12 Bottom).

2.4 Discussion

Licorice and Chrysanthemum have been used traditionally for many years as preventive and/or therapeutic agents for inflammatory related diseases in Eastern Asia and Europe (78, 83, 84). However, the precise cellular and molecular mechanisms remain unclear. Therefore we investigated the non-polar fractions of licorice (LE) and chrysanthemum (CZ) on the expression of anti-inflammatory and anti-oxidative stress genes as well as Nrf2-mediated signaling pathways using *in vitro* (cell culture) and *in vivo* (Nrf2 KO and WT mice) approaches.

In agreement with previously published studies (74, 82, 83), our data show that the LE and CZ extracts possess strong anti-inflammatory properties (Figures 2-1 to 2-4). LE and CZ inhibited the NF-κB luciferase activity (Figure 2-5), which implies that LE and CZ can attenuate the NF-κB signaling pathway. It has been reported that NF-κB pathway

can trigger the expression of iNOS, COX-2, IL-6 via IKK and p38 (74, 92). Therefore, the inhibition of NF-κB pathway by LE and CZ could potentially mediate the suppression effects of LE and CZ on the pro-inflammatory markers such as COX-2, IL-6, iNOS, and IL-1β (Figures 1 and 2). In addition, our results also demonstrate that NO production was suppressed by LE and CZ (Figure 2-4). The trend of NO suppression correlated well with iNOS mRNA and protein expression levels since NO is downstream of iNOS, and this result suggests that LE and CZ extracts suppressed the transcription and protein expression of iNOS.

The crosstalk between the Nrf2 and NF-κB mediated inflammatory signaling pathways is thought to be a potential mechanism (35, 50). We have previously shown that the Nrf2 signaling pathway plays an important role in the down-regulation and defense of acute inflammation as well as induction of detoxifying and anti- oxidation (35, 52). NF-κB which could mediate inflammatory signaling pathway is a redox-sensitive transcription factor regulated by intracellular redox status (101). Therefore, the potential of LE and CZ extracts in the induction of Nrf2 signaling pathway was investigated as we have performed previously (8, 90, 91, 102-106). Our results showed that ARE was significantly induced by LE ($p<0.001$) and CZ extracts ($p<0.01$) (Figure 2-6). Our result on ARE luciferase assay were in agreement with previous findings that licorice and chrysanthemum possess strong antioxidant and free radical inhibitory effects (78, 107). Furthermore, LE and CZ extracts were found to induce the mRNA transcription of Nrf2 and its downstream target genes such as NQO-1 and UGT1A1 (Figure 2-7). This data

suggest that LE and CZ can transcriptionally activate Nrf2 and induced phase II detoxifying and antioxidant genes.

To investigate if the effect of LE and CZ is Nrf2-dependent, WT and Nrf2 KO mice were gavaged with LE and CZ. NQO-1 was not induced in the Nrf2 KO mice but in the WT mice treated with CZ. Similarly, CZ induced UGT1A1 in the WT but not Nrf2 KO mice (Figure 2-9). NQO-1 was induced more in the WT than in the Nrf2 KO mice when treated with both CZ and LE. Our data also demonstrate that the induction of Nrf2 target genes such as AOX1, GSTμ3, UGT1A1, UGT 2B5 and NQO-1 by LE and CZ extracts are Nrf2 dependent (Figures 2-9, 2-10, 2-11, 2-12). The microarray data also revealed that these detoxifying and antioxidant genes are highly Nrf2-dependent. Although AOX1 gene was also expressed in Nrf2 KO mice in microarray, the expression intensities were lower than the Nrf2 WT mice. These genes were induced by LE and CZ extracts in the liver of WT but not Nrf2 KO mice (Figure 2-10a and 2-10b). As compared to the *in vitro* cell culture study (Figure 2-7), the *in vivo* data show a much higher degree of induction of Nrf2-mediated genes by CZ and LE. The reasons for these discrepancies are not clear, but could possibly due to the present of the active metabolites of CZ and LE *in vivo* (78, 84), such as β-glycyhrritinic acid, licochalcone, and isoliquiritigenin from licorice or luteolin, luteolin-7-glucoside and acacetin-7-rhamnoglucoside from chrysanthemum extracts (88). Such active metabolites, together with the parent compounds, could collectively induce greater expression of the Nrf2-mediated genes especially in the WT mice *in vivo*.

2.5 Summary

In summary, our study shows that Nrf2 signaling pathway plays a very important role not only in the up-regulation of anti-oxidative and detoxifying enzymes but also down-regulation of inflammatory pathways. Our current findings show that the licorice (LE) and chrysanthemum (CZ) extracts exert strong anti-inflammatory, anti-oxidative stress and detoxification properties. It is believed that chronic inflammation is related to 20% of human cancers. Thus, the anti-inflammatory and anti-oxidative stress abilities of LE and CZ can be potentially utilized for cancer chemoprevention in human.

Table 2-1 PCR Primers of pro-inflammatory and Nrf2 related genes

Gene	Forward	Reverse
GAPDH	5'-TGC TCG AGA TGT CAT GAA GG-3'	5'-TTG CGC TCA TCG TAG GCT TT-3'
IL-1β	5'-GAG TGT GGA TCC CAA GCA AT-3'	5'-CTC AGT GCA GGC TAT GAC CA-3'
IL-6	5'-AGT TGC CTT CTT GGG ACT GA-3'	5'-GCC ACT CCT TCT GTG ACT CC-3'
TNF-α	5'-ACG GCA TGG ATC TCA AAG AC-3'	5'-GGT CAC TGT CCC AGC TT-3'
iNOS	5'-GTG GTG ACA AGC ACA TTT GG-3'	5'-GGC TGG ACT TTT CAC TCT GC-3'
COX-2	5'-TCC TCC TGG AAC ATG GAC TC-3'	5'-TGA TGG TGG CTG TTT TGG TA-3'
Nrf-2	5'-AGC AGG ACA TGG AGC AAG TT-3'	5'-TTC TTT TTC CAG CGA GGA GA-3'
UGT1A1	5'-GTG GCC CAG TAC CTG ACT GT-3'	5'-CGA TGG TCT AGT TCC GGT GT-3'
NQO-1	5'-CAG ATC CTG GAA GGA TGG AA-3'	5'-AAG TTA GTC CCT CGG CCA TT-3'

Table 2-2 Human Primers for Quantitative Real-Time PCR

Gene	Forward	Reverse
GAPDH	5'-TCG ACA GTC AGC CGC ATC TTC TTT-3'	5' ACC AAA TCC GTT GAC TCC GAC CTT-3'
UGT1A1	5'-TAA GTG GCT ACC CCA AAA CG-3'	5'-TCT TGG ATT TGT GGG CTT TC-3'
NQO-1	5'-CTG GAG TGT GCC CAA TGC TA-3'	5'-CAT GAA TGT CAT TCT CTG GCC A-3'
Nrf-2	5'-TGC TTT ATA GCG TGC AAA CCT CGC-3'	5'-ATC CAT GTC CCT TGA CAG CAC AGA-3'

Table 2-3 Confirmation of Genotype of the Nrf2 in Animals

Gene	Primers
3'-primer	5'-GGA ATG GAA AAT AGC TCC TGC C-3'
5'-primer	5'-GCC TGA GAG CTG TAG GCC C-3'
lacZ primer	5'-GGG TTT TCC CAG TCA CGA C-3'

Table 2-4 Murine Primers for Quantitative Real-Time PCR

Gene	Forward	Reverse
β-actin	5'-CGT TCA ATA CCC CAG CCA TG-3'	5'-GAC CCC GTC ACC AGA GTC C-3'
AOX1	5'-TGC ACT GGT CTC TCA TGG TGG AAT-3'	5'-AGT CCA TTG AGA TCT GCC ACC ACA-3'
FKBP5	5'-AGC GAG CAA CTG AGA AGA CTG GAT-3'	5'-ACC CGA GAA CAT CAT GGT CGA AGT-3'
GSTm3	5'-ACT GTG GCT CCC GGT TCT CT-3'	5'-AAA TAA AGG CTG CAT GGG CTT-3'
NQO1	5'-AGC CCA GAT ATT GTG GCC G-3'	5'-CCT TTC AGA ATG GCT GGC AC-3'
Nrf2	5'-AGC AGG ACA TGG AGC AAG TT-3'	5'-TTC TTT TTC CAG CGA GGA GA-3'
UGT2b5	5'-CAA TGG TGT CTA CGA GGC GAT-3'	5'-CTC CTT TGG CCA CCA TAT GG-3'
USP14	5'-AAT GCA GAA GAC ATC TGG AGG CCA-3'	5'-TCC CAT ACA GCA TTT CCT GTG GGT-3'

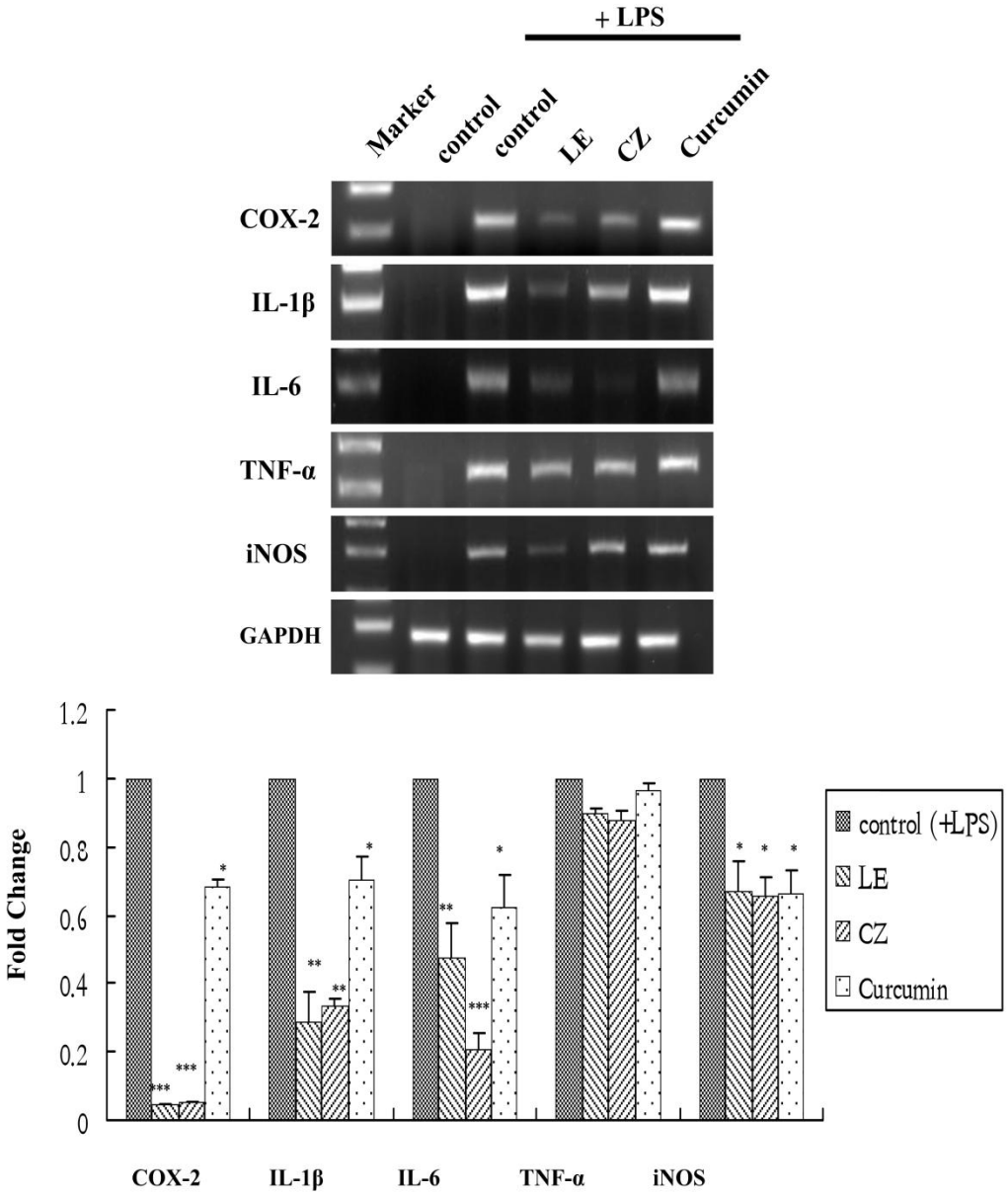

Figure 2-1 Effect of LE and CZ extracts on the mRNA expression of pro-inflammatory biomarkers in LPS stimulated RAW 264.7 cells.

LE 25 μg/ml; CZ 25 μg/ml; Curcumin 10 μM. The gene bands were quantified by densitometry and normalized by GAPDH, ratio. (*** compare with LPS-induced, $p<0.001$; ** compare with LPS-induced, $p<0.01$; * compare with LPS-induced, $p<0.05$)

(Wu, *et al*, AAPS J. 2011 Mar;13(1):1-13.)

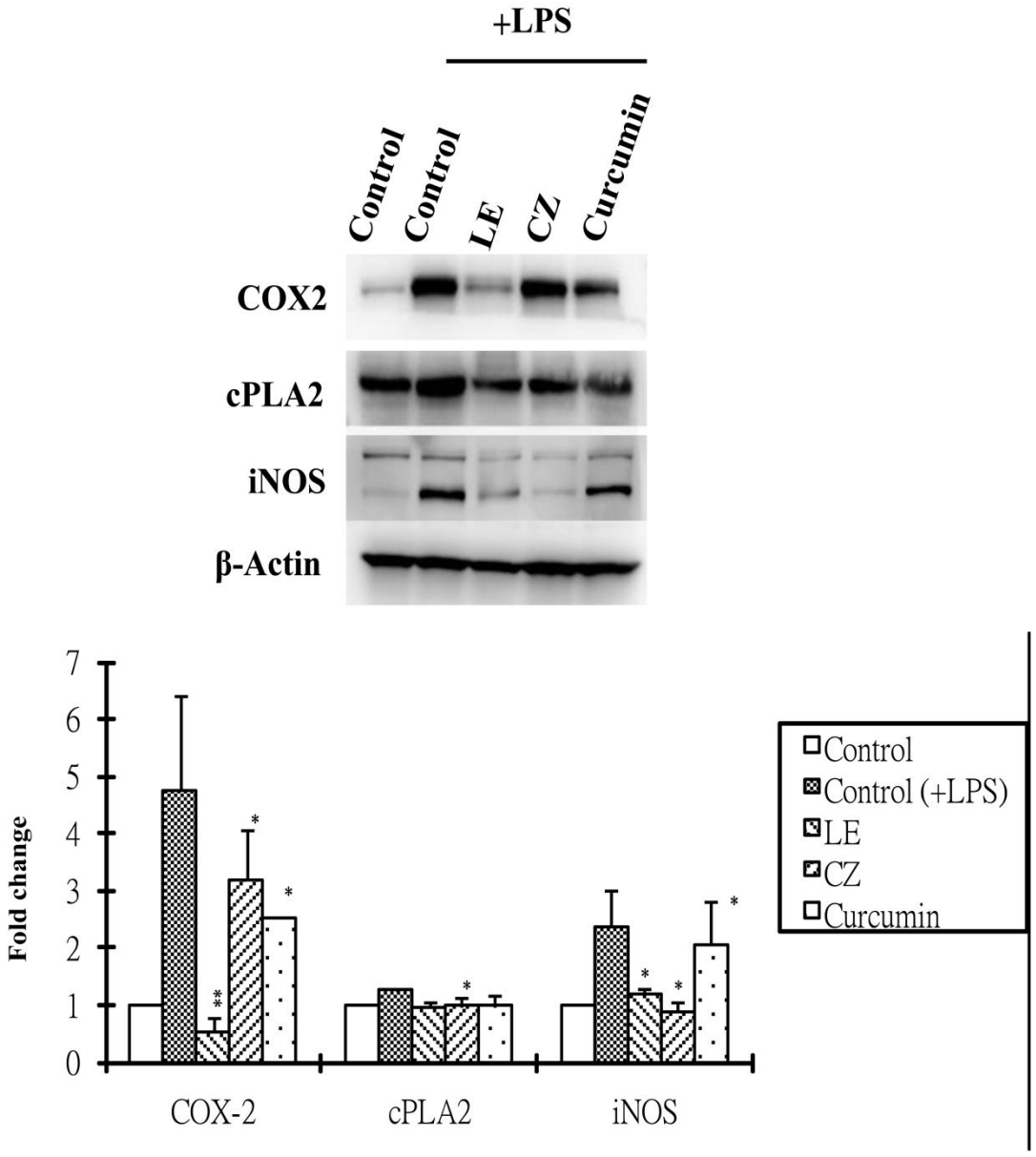

Figure 2-2 Effect of LE and CZ extracts on the protein expression of pro-inflammatory biomarkers (protein) in LPS-stimulated RAW 264.7 cells. (Western Blots)

LE 25 μg/ml; CZ 25 μg/ml; Curcumin 10 μM. Pro-inflammatory proteins analyzed performed by western blotting, the protein bands were quantified by densitometry and normalized by β-actin (data representative of 3 separate experiments) ratio is shown here.

(Wu, *et al*, AAPS J. 2011 Mar;13(1):1-13.)

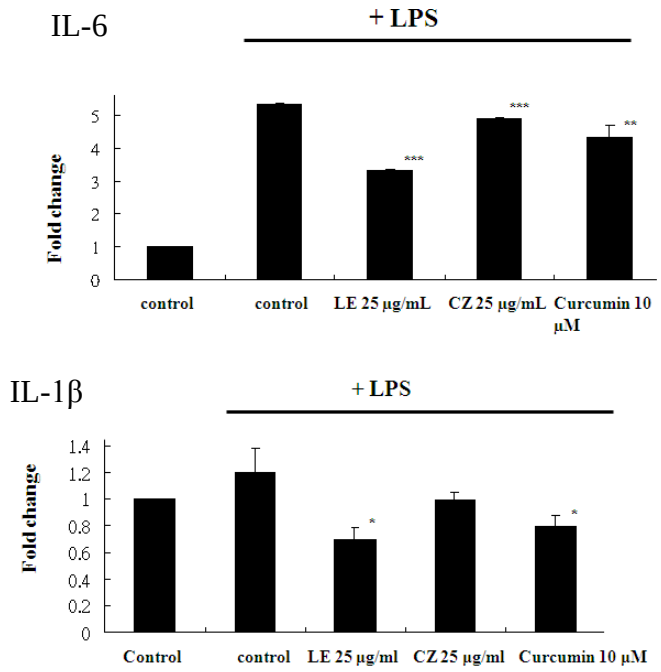

Figure 2-3 Effect of LE and CZ extracts on the protein expression of pro-inflammatory biomarkers (protein) in LPS-stimulated RAW 264.7 cells. (ELISA)

LE 25 µg/ml; CZ 25 µg/ml; Curcumin 10 µM. Expression of IL-6 performed by ELISA (n=3) (Top). Expression of IL-1β performed by ELISA (Bottom). (*** compare with LPS-induced, $p<0.001$; ** compare with LPS-induced, $p<0.01$; * compare with LPS-induced, $p<0.05$)

(Wu, *et al*, AAPS J. 2011 Mar;13(1):1-13.)

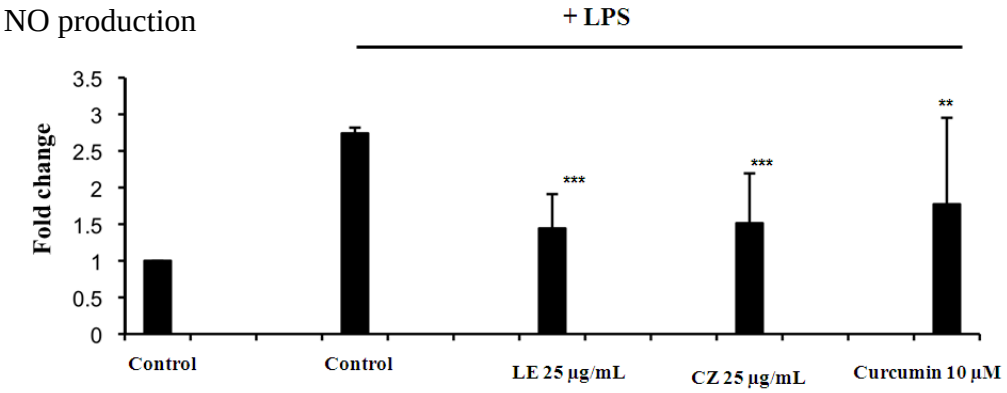

Figure 2-4 Effect of LE and CZ extracts on production of NO in LPS-stimulated RAW 264.7 cells

(* compare with LPS-induced, p<0.001; ** compare with LPS-induced, p<0.01)**

(Wu, *et al*, AAPS J. 2011 Mar;13(1):1-13.)

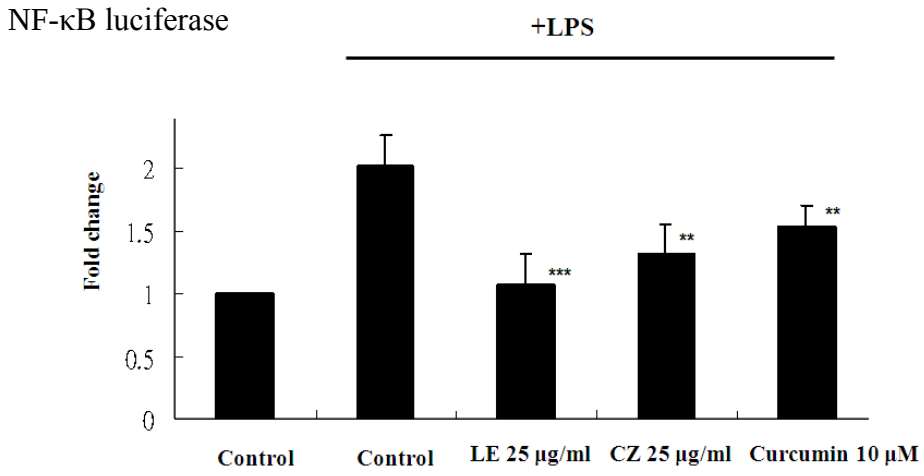

Figure 2-5 Effect of LE and CZ extracts on NF-κB luciferase activity in HT-29 cells. (*** compare with LPS-induced, $p<0.001$; **compare with LPS-induced, $p<0.01$)

(Wu, *et al*, AAPS J. 2011 Mar;13(1):1-13.)

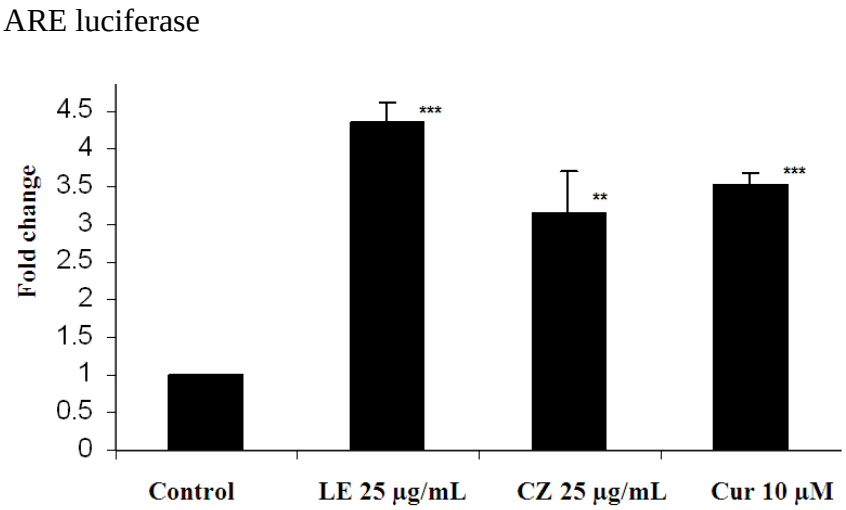

Figure 2-6 Effect of LE and CZ extracts on ARE luciferase activity in HepG2 C8 cells. (*** compare with control, $p<0.001$; ** compare with control, $p<0.01$)

(Wu, *et al*, AAPS J. 2011 Mar;13(1):1-13.)

mRNA expression

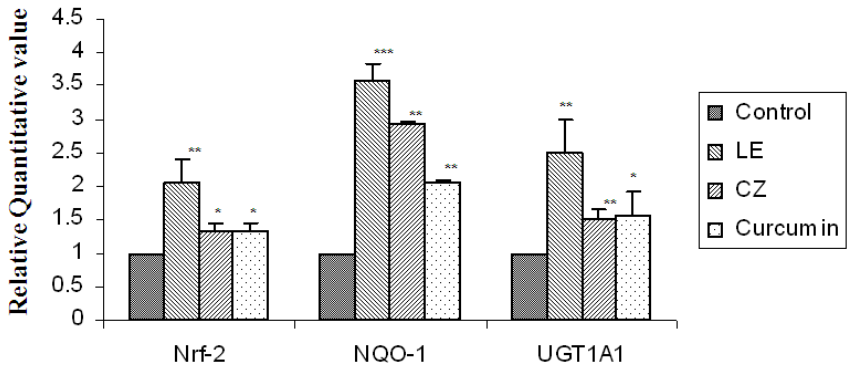

Figure 2-7 Induction of effects of LE and CZ extracts on the mRNA expression of Nrf2 and Phase II genes in HepG2 C8 cell.

LE 25 μg/ml; CZ 25 μg/ml; Curcumin 10 μM. Quantitative real-time PCR results were normalized by β-actin, ratios. Normalized RQ mRNA expression values for Nrf2, NQO1, and UGT1A1 were shown as bar charts.(*** compare with control, $p<0.001$; ** compare with control, $p<0.01$; * compare with control, $p<0.05$)

(Wu, *et al*, AAPS J. 2011 Mar;13(1):1-13.)

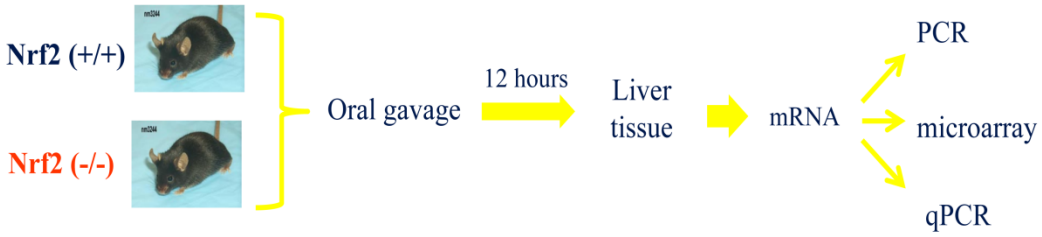

Figure 2-8 *In vivo* study schemes

The second generation (F2) Nrf2 (-/-) mice (C57BL/SV129) and the C57BL/6J wild-type mice were used for the *in vivo* study to investigate if the induction of phase II detoxifying/ antioxidating enzymes by the extracts was Nrf2-dependent. The mice were treated with vehicle (as a negative control; cremophor: tween 80: ethyl alcohol: deionized water= 2:1:1:6), LE 150 mg/kg, LE 300 mg/kg, CZ 150 mg/kg, and CZ 300 mg/kg by oral gavage in a final volume of 100-110 μL.

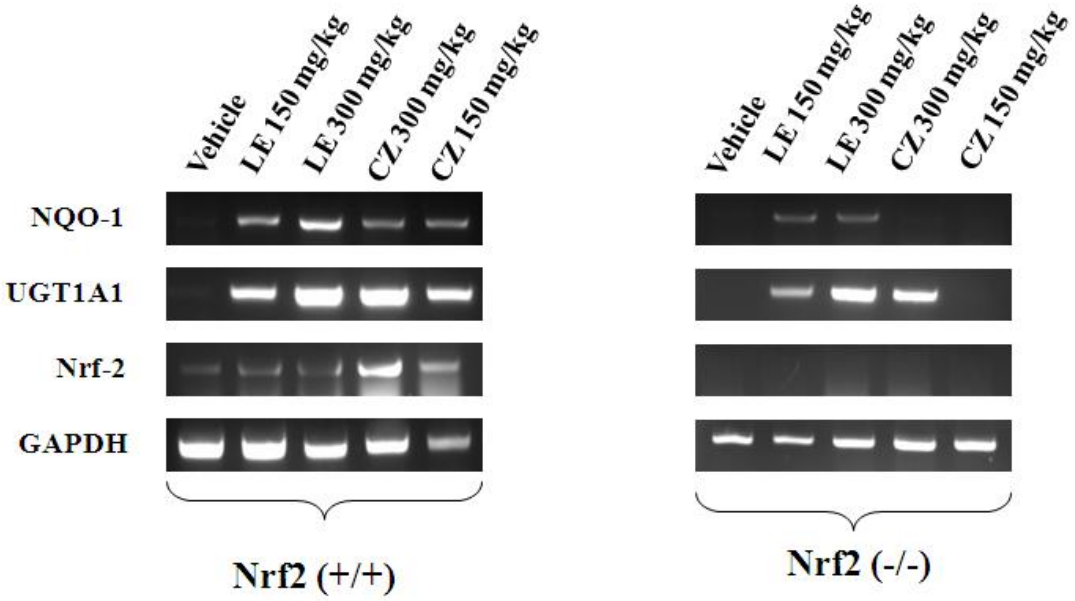

Figure 2-9 Effect of LE and CZ extracts on the mRNA expression in the mice

The mRNA expression of Nrf2 and its transactivated target genes such as phase II detoxifying/antioxidant genes in the liver of C57BL/6J mice and Nrf2 (-/-) mice.

(Wu, *et al*, AAPS J. 2011 Mar;13(1):1-13.)

a.

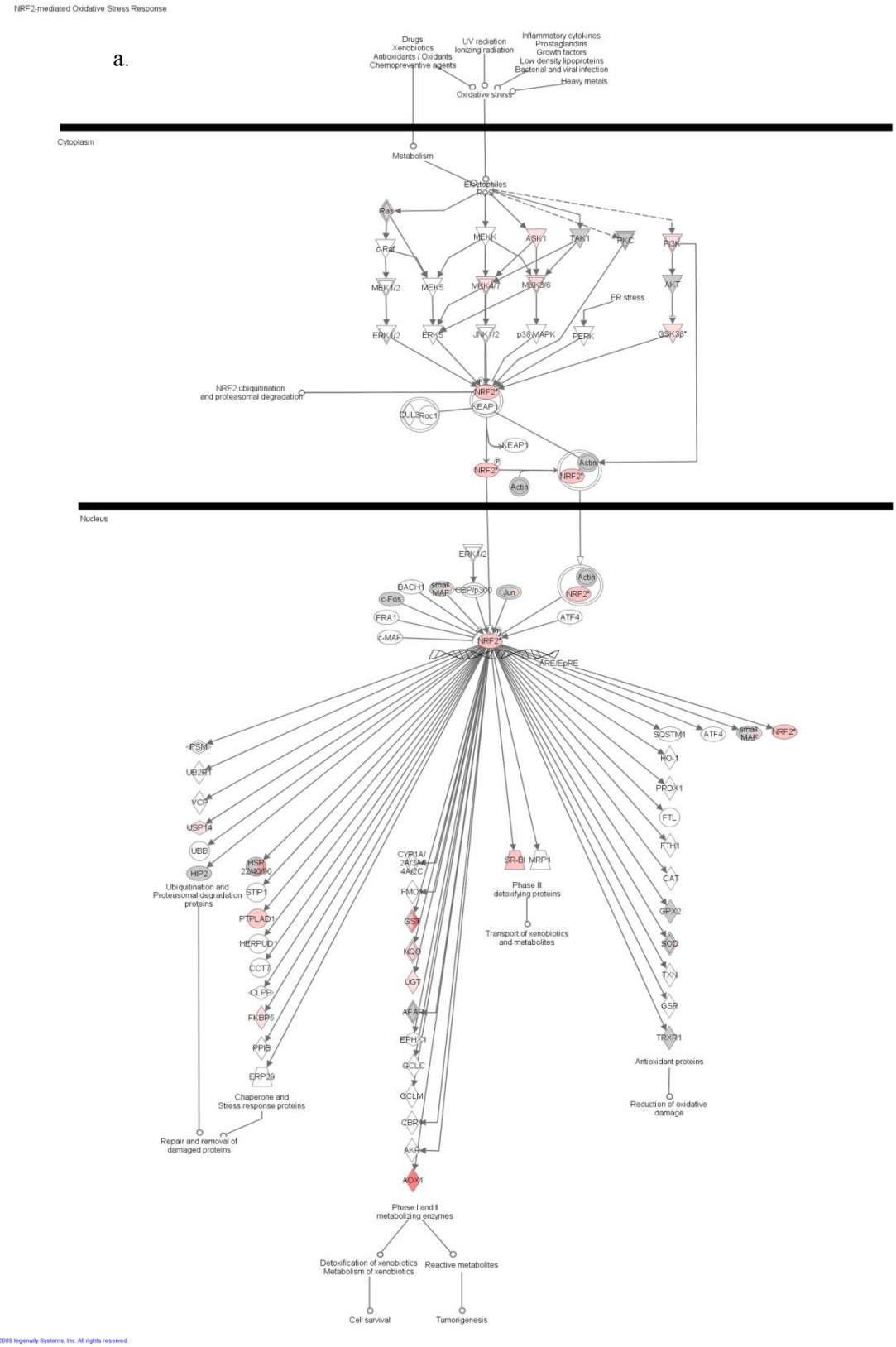
NRF2-mediated Oxidative Stress Response
Drugs
Xenobiotics
Antioxidants / Oxidants
Chemopreventive agents
UV radiation
Ionizing radiation
Inflammatory cytokines
Prostaglandins
Growth factors
Low density lipoproteins
Bacterial and viral infection
Heavy metals
Oxidative stress
Cytoplasm
Metabolism
Electrophiles
ROS
Ras
c-Raf
MEKK
ASK1
TAK1
PKC
PI3K
AKT
MEK1/2
MEK5
MKK4/7
MKK3/6
ER stress
ERK1/2
ERK5
JNK1/2
p38 MAPK
PERK
GSK3β*
NRF2 ubiquitination
and proteasomal degradation
NRF2*
KEAP1
CUL3Roc1
Actin
Nucleus
ERK1/2
BACH1
small MAF
CBP/p300
Jun
c-Fos
FRA1
c-MAF
ATF4
ARE/EpRE
PSMB
UBE2H
VCP
USP14
UBB
HIP2
Ubiquitination and
Proteasomal degradation
proteins
HSP 22/40/60
STIP1
PTPLAD1
HERPUD1
CCT7
CLPP
FKBP5
PPIB
ERP29
Chaperone and
Stress response proteins
Repair and removal of
damaged proteins
CYP1A/ 2A/3A/ 4A/2C
FMO1
GSR
NQO
UGT
AFAR1
EPHX1
GCLC
GCLM
CBR1
AKR1
AOX1
SR-BI
MRP1
Phase II
detoxifying proteins
Transport of xenobiotics
and metabolites
SQSTM1
HO-1
PRDX1
FTL
FTH1
CAT
GPX2
SOD
TXN
GSR
TRXR1
Antioxidant proteins
Reduction of oxidative
damage
Phase I and II
metabolizing enzymes
Detoxification of xenobiotics
Metabolism of xenobiotics
Reactive metabolites
Cell survival
Tumorigenesis
000-2009 Ingenuity Systems, Inc. All rights reserved.

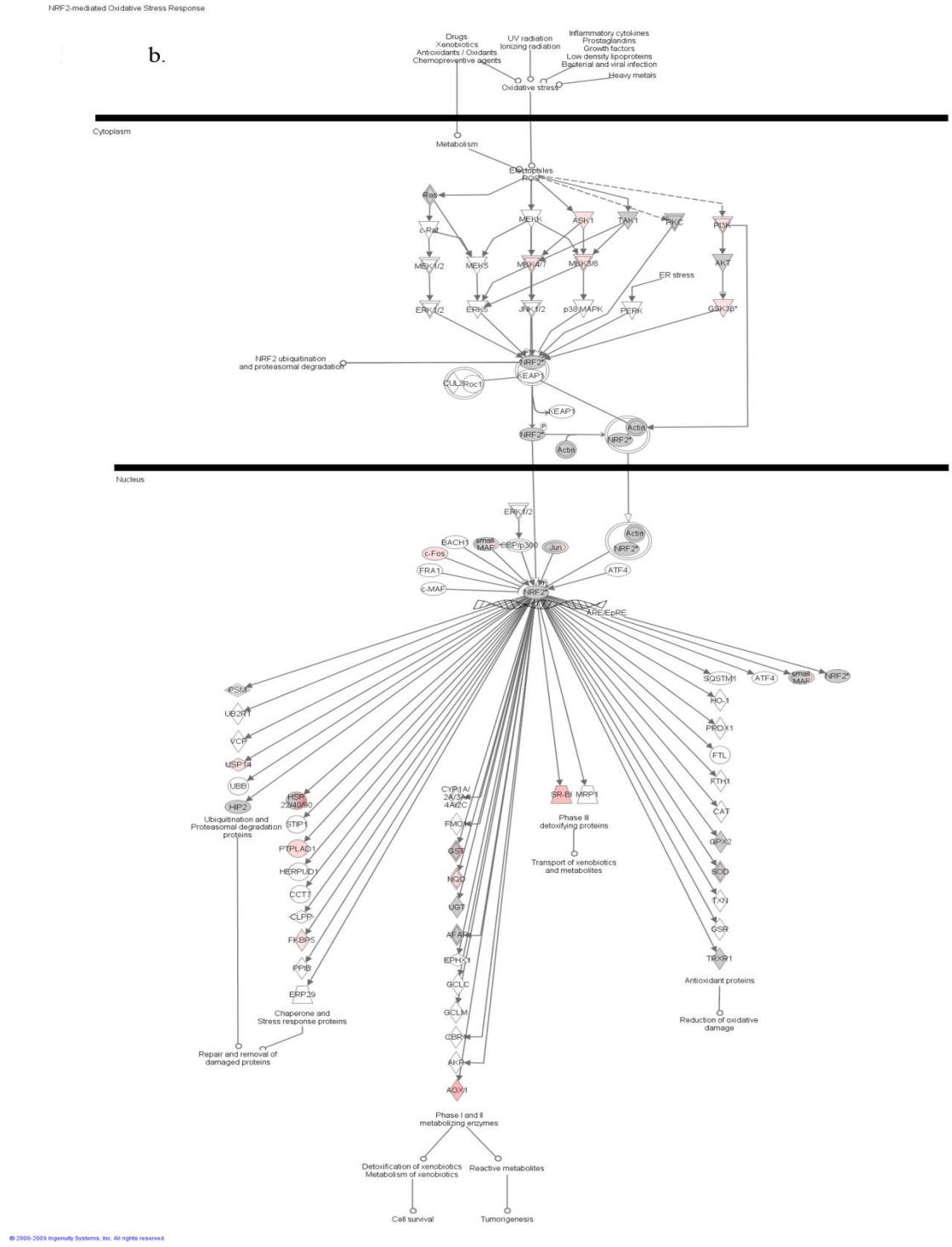

Figure 2-10 (a) Nrf2 pathway induced by CZ treatment in Nrf2 (+/+) mice; (b) Nrf2 pathway induced by CZ treatment in Nrf2 (-/-) mice.

(Wu, et al, AAPS J. 2011 Mar;13(1):1-13.)

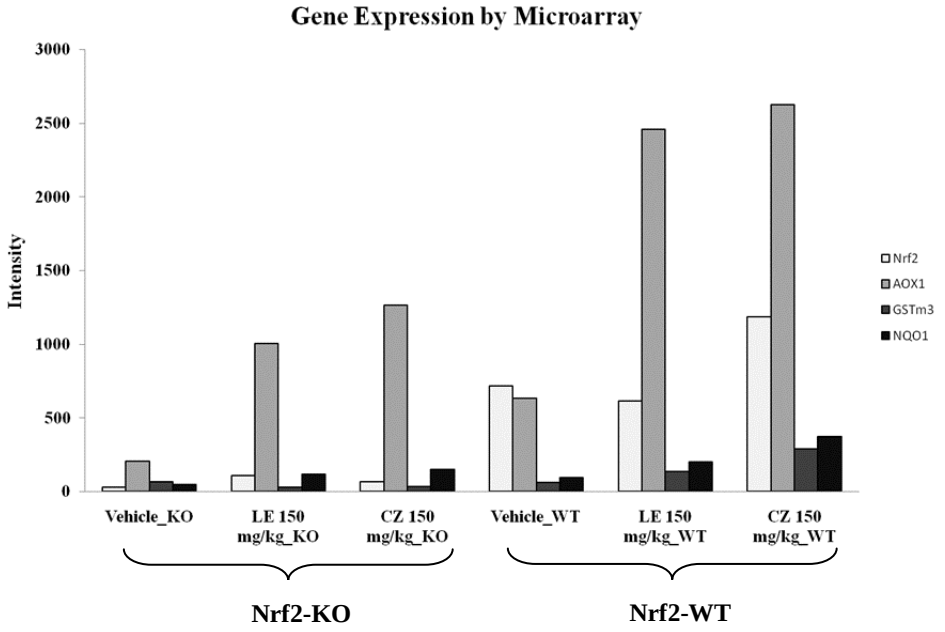

Figure 2-11 Microarray assay for LE- and CZ-induced Nrf2-dependent genes in the liver of C57BL/6J mice and Nrf2 deficient mice.

The figure shows the intensity of Nrf2, AOX1, GSTμ3, and NQO1 genes expression in the six groups of mice, respectively.

(Wu, *et al*, AAPS J. 2011 Mar;13(1):1-13.)

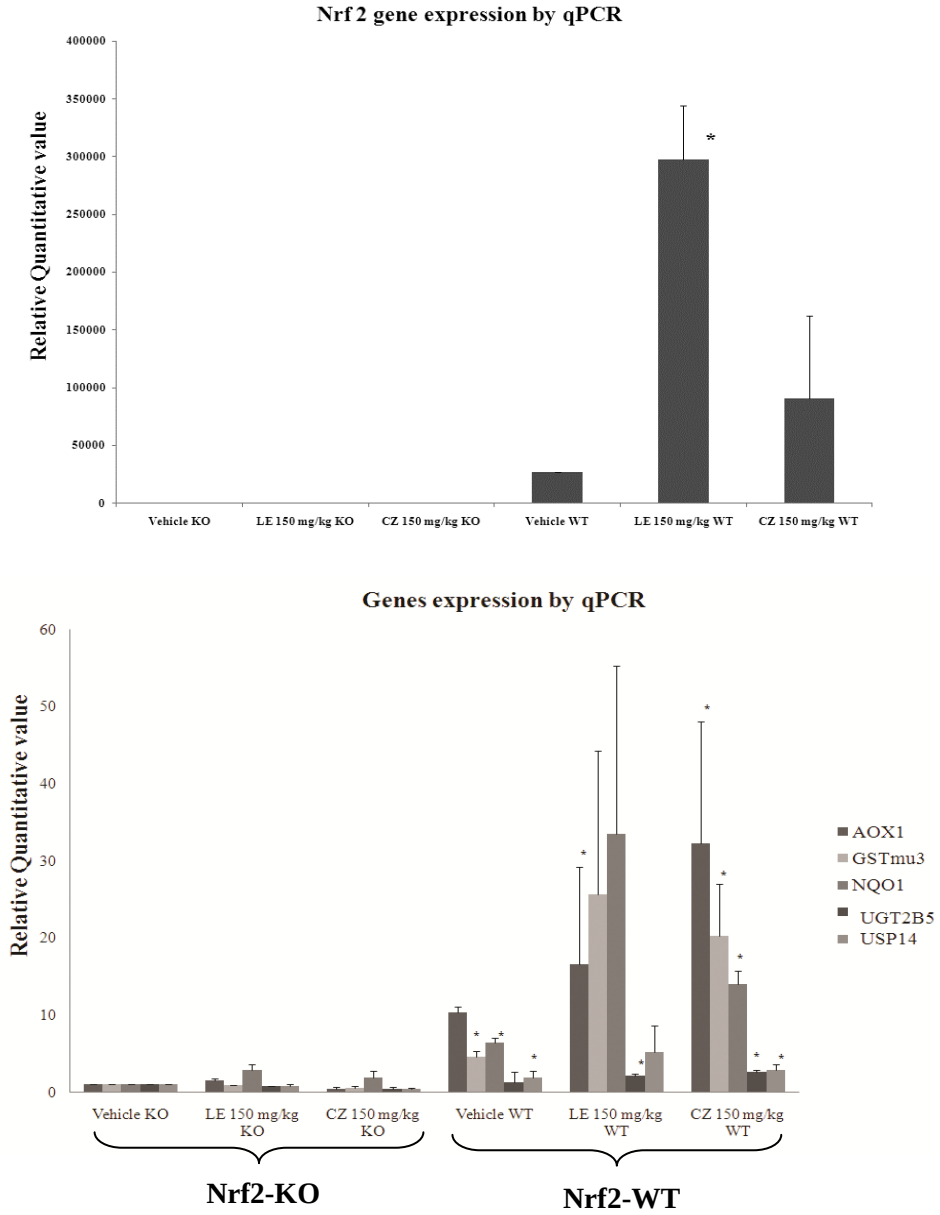

Figure 2-12 Microarray verification of genes induced by LE- and CZ- induced Nrf2 dependent genes by qPCR results were normalized by β-actin, ratios.

Normalized RQ values of each mouse was compared with Nrf2 KO mouse with vehicle treatment for Nrf2 (Top), and AOX1, FKBP5, GSTμ3, NQO1, UGT2b5, and USP14 (Bottom) were shown, respectively. Genes were normalized to β-actin expression (* compare with Vehicle KO, $p<0.05$)

(Wu, *et al*, AAPS J. 2011 Mar;13(1):1-13.)

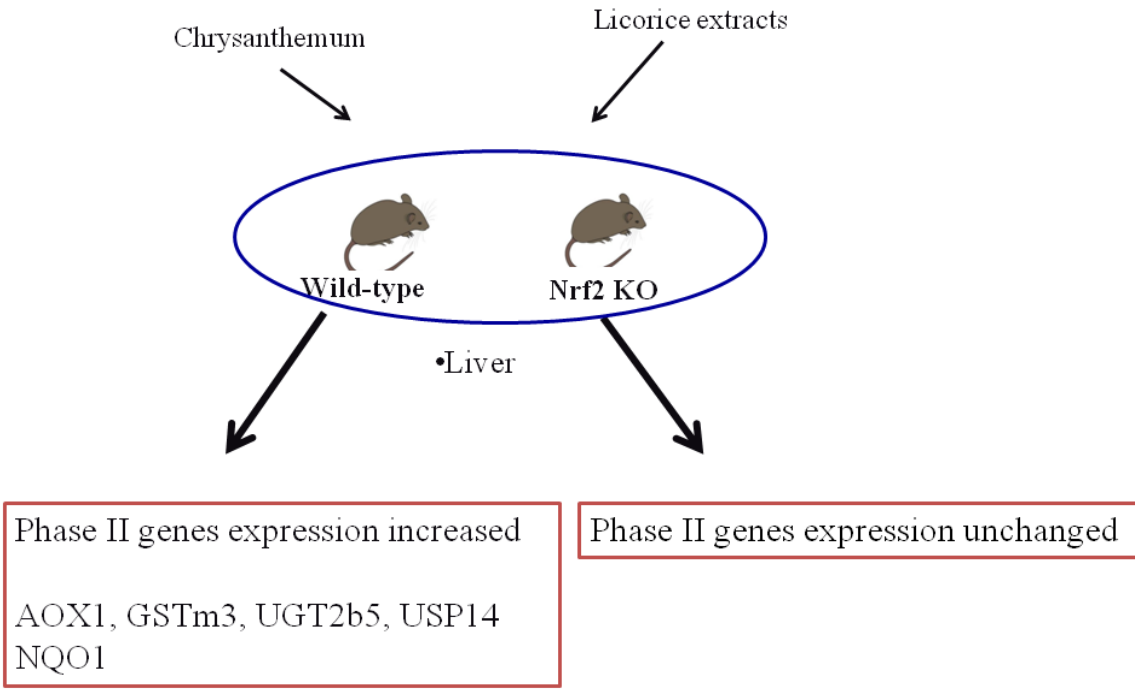

Figure 2-13 Summary of genes induced by LE- and CZ- induced Nrf2 dependent genes in Nrf2(-/-) and wild type mice

Compared with Nrf2 KO mice, phase II detoxifying/antioxidant genes including AOX1, FKBP5, GSTμ3, NQO1, UGT2b5, and USP14 expression were increased. Genes were normalized to β-actin expression

(Summarized from Wu, *et al*, AAPS J. 2011 Mar;13(1):1-13)

CHAPTER 3 Indole-3-carbinol and 3,3'-diindolylmethane in the Inhibition of Prostate Cancer in Transgenic Adenocarcinoma of Mouse Prostate (TRAMP) mice [7,8,9]

3.1 Introduction

Prostate Cancer (PCa) is the most frequently diagnosed form of cancer and the second leading cancer related death among men in the U.S.A. One in six American men will be diagnosed in their lifetime with PCa (NCI; http://www.cancer.gov/cancertopics/types/prostate). According to the American Cancer Society, there will be 217,730 estimated new cases diagnosed with PCa and 32,050 male will die of PCa in the USA in 2010 (108). The development and formation of prostate carcinoma in men is usually a very long process involving a cascade of genetic/epigenetic changes. Progression of prostate carcinoma from prostate intra-epithelial neoplasia (PIN) (109), known as pre-neoplastic lesions, to androgen-independent invasive carcinoma usually takes several decades to occur (110). The long latency from PIN to metastatic and invasive disease provides an excellent opportunity for cancer chemoprevention.

---

[7] Work described in this chapter has been published as **Wu** *et al*; Molecular Carcinogenesis. 2012 Oct; 51(10):761-70.

[8] **Key Words**: Indole-3-carbinol; Nrf2, phase II detoxifying/ antioxidant enzymes; prostate cancer; TRAMP mice

[9] **Abbreviations**: ARE, antioxidant response element; BSA, bovine serum alnumin; DIM, 3,3'-diindolylmethane; FBS, fetal bovine serum; GCLC, glutamate cysteine ligase catalytic; GUT, genitourinary apparatus; HO-1, heme oxygenase-1; I3C, indole-3-carbinol; IHC, immunohistochemistry; NQO-1, NAD(P)H quinine oxidoreductase 1; Nrf2, nuclear factor (erythroid-derived 2)-like 2; PARP, poly (ADP-ribose) polymerase; PCa, prostate cancer; PIN, prostate intra-epithelial neoplasia; qPCR, quantitative real-time polymerase chain reaction; SD, standard deviation; TBST, tris buffer saline tween-20; TRAMP, transgenic adenocarcinoma of mouse prostate

Presently, metastatic PCa is not curable and median survival duration is 1-3 years. Epidemiologic studies show that dietary and environmental factors play an important role in prostate carcinogenesis (111). Men in Asia appear to have a much lower incidence of PCa than men in North America. The differences of the PCa incidence between different ethnic groups are believed to be partly due to the different lifestyle and environmental factors (112). Higher vegetable, fruits and lower fat and proteins consumption and life-style difference appear to be associated with a reduction of the risk of PCa.

Indole-3-caribinol (I3C, structure shows in Figure 3-1), a common phytochemical found abundantly in cruciferous vegetables such as broccoli, bok choy, cauliflower, cabbage and cress, has been reported to be a potent anti-cancer and cancer chemoprevention agent. Preclinical studies show that I3C inhibited tumorigenesis in breast, prostate, liver, lung, cervix, gastrointestinal tract and colorectal in different animal models (113-119). Among the anti-carcinogenic properties of I3C include cell cycle regulation, DNA repairing, suppression of NF-κB-Akt signaling, suppression of cyclin-dependent kinase activities and endoplasmic reticulum stress, induction of apoptotic pathway, caspase activation, and BRCA gene expression (119-121). I3C can suppress inflammatory mediators including TNF-α, iNOS, and IL-10 in lipopolysaccharide stimulated RAW 264.7 (122). Both I3C and its condensation by-product, 3,3'-diindolylmethane (DIM, structure shows in Figure 3-1), supplementation have been investigated in clinical trials for human papillomavirus related diseases such as cervical cancer and respiratory pappillomatosis as well as breast cancer and vulvar intraepithelial neoplasia (123). There is also an ongoing clinical trial using I3C in treating PCa patients

with PSA recurrence after surgery (clinicaltrial.gov). In addition, another study demonstrated that I3C and DIM protected human breast and prostate cancer cells against cell killing by oxidative stress induced by hydrogen peroxide (H_2O_2). In the same study, both I3C and DIM were found to induce NAD(P)H quinine oxidoreductase 1 (NQO-1) luciferase response (124).

Long-term oxidative stress has been implicated in the development and progression of PCa based on epidemiological, experimental, preclinical and clinical studies (123, 125-127). Nuclear factor (erythroid-derived 2)-like 2 (Nrf2) appears to play an important role in mediating transcription regulation of the antioxidant response element (ARE) presents in the promoter of many phase II drug metabolizing/detoxifying/antioxidant enzymes expression (128). Under unstimulated normal conditions, Nrf2 is associated with actin-binding Keap 1 forming the Nrf2-Keap1 complex, sequestering Nrf2 in the cytoplasm, and preventing Nrf2 for entering into the nuclear and promoting its proteasomal degradation. Typically, the half-life of Nrf2 in mammalian cells is 15-45 min. It has been shown that treatments with oxidants such as H_2O_2-mediated oxidative stress resulting in protein conformational changes due to potential oxidation of thiol groups present on the Nrf2-Keap 1 complex resulting in dissociation of Nrf2 from Keap 1, Nrf2 then translocates into the nucleus, binds to the ARE and leads to enhanced phase II detoxifying/ antioxidant enzymes expression. Similarly, treatment with chemopreventive agents found to attenuate the degradation of Nrf2, increases Nrf2 stability and enhances the expression of Nrf2 targeted genes (128). Interestingly, a recent report shows that in clinical PCa there is a progressive loss of

expression of Nrf2 and its downstream target genes such as NQO-1 (127). Furthermore, recently our laboratory reports that as PCa tumor progresses in Transgenic Adenocarcinoma of Mouse Prostate (TRAMP) mice there is a progressive loss of Nrf2 and NQO-1 expression in prostate tumors through epigenetic methylation of CpG islands of the promoters of Nrf2 (126). TRAMP model appears to be an ideal model of which the prostate tissue progresses into the different stages of tumors and exhibiting histological and molecular features to human PCa. In the present study, we hypothesized that I3C would up-regulate/re-activate Nrf2 and its target genes as a potential novel mechanism to counteract oxidative stress, and contributing to the overall PCa prevention. Therefore, in this study, we investigated the *in vitro* Nrf2-ARE-mediated anti-oxidative stress signaling mechanism and the *in vivo* efficacy in conjunction with the *in vivo* molecular mechanism of I3C as a chemopreventive agent in inhibiting prostate tumorigenesis in TRAMP mice.

3.2 Materials and methods

3.2.1 Cell culture

HepG2-C8 cells, stably expression ARE-luciferase reporter gene established in our lab (42, 52, 89-91), and TRAMP C1 cells, originally derived from TRAMP prostate tumor (129), were cultured in Dulbecco's Modified Eagle's Medium (Invitrogen Corp., Carlsbad, CA, U.S.A.) supplemented with 10% (V/V) fetal bovine serum (FBS) (Invitrogen Corp., Carlsbad, CA, U.S.A.), penicillin 100 U/ml, and streptomycin 100 μg/ml (Invitrogen Corp., Carlsbad, CA, U.S.A.). Cells were maintained in a humidified incubator with 5% CO_2 at 37^{o}C.

3.2.2 Luciferase report assay

HepG2-C8 cells were cultured in 6-well plates, and then treated with different concentrations of I3C or DIM (Sigma-Aldrich, St. Louis, MO, U.S.A.) in 1% FBS DMEM medium for 24 hr. The cells were washed with ice-cold PBS and harvested in reporter lysis buffer to analyze the ARE-luciferase reporter activities (Promega, Madison, WI, USA) as we have performed previously (42, 91). Following frozen in -80℃ for 3 hr and centrifugation, 10 μl of the supernatants were mixed with 50 μl of luciferase assay subtract and measured for luciferase activity using a Sirus Luminometer (Berthold Detection Systems GmbH D-75173 Pforzheim, Germany). The luciferase activity was normalized against known protein concentrations and expressed as fold induction of luciferase activity over the control cells, which were treated with 0.1% DMSO. The protein level was determined by Bio-Rad protein assay according to the manufacturer's instructions. Three independent experiments were carried out; the data were shown as mean ±SD.

3.2.3 Quantitative real-time PCR assays (qPCR)

The TRAMP C1 cells were cultured in 6-well plate overnight, and were treated with different concentrations of I3C for 8 h at 37°C and Total RNA were collected and reversed transcribed. The primers, Nrf2, Nrf2 target genes, NQO-1, hemeoxgenase-1 (HO-1), glutamate cysteine ligase catalytic (GCLC) and control β-actin, of qPCR are listed in Table 3-1 (Integrated DNA Technologies, Coralville, IA, U.S.A.). The qPCR reactions were carried out 1 μl cDNA product, 50 nM of each primer, and Power SYBR Green master mix (Applied Biosystems, Foster City, CA, U.S.A.) in 10 μl reactions. The

reactions were performed using an ABI Prism 7900HT sequence detection system, specificity of amplification was verified by first-derivative melting curve analysis using the ABI software (SDS2.3, Applied Biosystems, Foster City, CA, U.S.A.). Relative quantification of gene expression profile was calculated using a ΔΔCt method (RQ manager, Applied Biosystems, Foster City, CA, U.S.A.) as we have performed previously (38, 93). Three independent experiments were carried out showing similar results. The results are presented as mean ±SD.

3.2.4 Animals

Female hemizygous C57BL/TGN TRAMP mice, line PB Tag 8247NG, and male C57BL/6 mice were purchased from The Jackson Laboratory (Bar Harbor, ME, U.S.A.). The animals were bred on the same genetic background and maintained in the Laboratory Animal Service facility at Rutgers University. Housing and care of the animals was performed in accordance with the guidelines established by the University's Animal Research Committee consistent with the NIH Guidelines for the Care and Use of Laboratory Animals. Transgenic males for the studies were obtained as [TRAMP x C57BL/6] F1 or [TRAMP x C57BL/6] F2 offspring. Identity of transgenic mice was established by PCR-based DNA genotyping using the primers suggested by The Jackson Laboratory (Table 3-2). Throughout the experiment the animals were housed in a temperature-controlled room (68-72°F) with a 12 hr light dark cycle, at a relative humidity of 45% to 55%.

3.2.5 Diet and study design

I3C was obtained from Sigma Inc. (St. Louis, MO, U.S.A.). AIN-76A diets containing 1% I3C were prepared by Research Diets Inc. (New Brunswick, NJ, U.S.A.) and stored at -20℃. The dose was chosen based on previous studies (130, 131), where I3C was fed in mice with 20 mg/ kg and no toxicity was observed. In our present study, 1% I3C was well-tolerated for these TRAMP mice. The control TRAMP males (*n*=19) received AIN-76A diets throughout the experiment while the treated TRAMP males received 1% I3C diet from 8 weeks of age (*n*=8) as group 1 (G1) and from 12 weeks of age (*n*=8) as group 2 (G2). Fresh diets were added to the cages twice a week. In this study, TRAMP males were weighed weekly and general health was monitored on a regular basis. All mice were sacrificed at the age of 24 weeks by cervical dislocation and the genitourinary apparatus (GUT) consisting of seminal vesicles, prostate, and bladder were isolated for further analyses (Figure 3-2).

3.2.6 Histopathology

The dorso-lateral prostate (*n*=5) was excised and fixed in 10% formalin for 24 hr and then transferred to 70% ethanol for 24 hr. After dehydration processing and embedding with paraffin, tissue sections (4 μM) were cut from paraffin embedded prostate tissue and mounted on slides. The sections were stained with Hematoxylin and Eosin (H&E) to observe any neoplastic changes. Sections were evaluated by histopathologist in a blinded fashion to classify prostatic intra-epithelial neoplasia (PIN) lesion as we have reported previously (48, 64, 126). Lesions were classified as PIN I, PIN II, PIN III, and PIN IV as described by Park *et al* as well as we have reported previously

(48, 64, 126, 132) . For classification ease, PIN I and PIN II were combined as low grade PIN (LG-PIN) while PIN III and PIN IV were combined as high grade PIN (HG-PIN) as we have done previously.

3.2.7 Immunohistochemistry (IHC) staining for apoptotic assay

Sections (4 μM) were cut from the paraffin embedded prostate tissue and mounted on glass slides. The slides were de-parafinized in xylene and antigen unmasking was performed by applying proteinase K digestion directly on the slides for 15 min. Endogenous peroxidase was blocked by incubating in 3% H_2O_2 for 5 min, and ApopTag Plus Peroxidase *In Situ* Apoptosis Detection Kit (Millipore, Temecula, CA, U.S.A.) was used to detect apoptotic cells. Vectastain ABC kit (Vector Laboratories, Inc., Burlingame, CA, U.S.A.) was used to detect apoptotic cells by applying enzyme conjugated avidin, peroxidase substrate, and 3,3'-diaminobenzidine (DAB) to develop color for visualization.

3.2.8 Assessment of IHC staining

Quantitative of IHC staining was done using the Aperio ScanScope® GL system according to the manufacture's protocol (Aperio Technologies Inc., Vista, CA, U.S.A.). This is a single-slide scanning system for digital pathological analysis of IHC of tumor samples to analyze our IHC-stained slides for the various cell cycle and apoptotic markers. The Aperio ImageScope software (v 10.1.3.2028) allowed the unbiased quantification and quantitative analysis of the IHC staining of biomarkers of prostate tumor samples obtained from untreated control versus the treated TRAMP mice.

3.2.9 Western blot

The dorso-lateral prostate tissues collected from treated and control groups were pooled and homogenized with RIPA buffer (Sigma, St. Louis, MO, U.S.A.) and 10 μg/ml protease inhibitor cocktail (EMD Chemicals, Gibbstown, NJ, U.S.A.). Protein (20 μg) was loaded onto 4-15% SDS-PAGE (Bio-Rad Laboratories, Hercules, CA, U.S.A.). After separation by SDS-PAGE, the protein was transferred onto nitrocellulose membrane (Millipore Corp., Billerica, MA, U.S.A.), and then was blocked in 5% bovine serum albumin (BSA) (Fisher Scientific, Fair Law, NJ, U.S.A.) in tris buffer saline tween-20 (TBST) solution for 1 h. Membranes were probed using the different mono- or polyclonal-antibodies (1:1000) overnight at 4℃. Blots were washed with TBST solution for 15 min 4 times and incubated with the respective secondary antibodies for 1 hr. After washing 15 min 4 times with TBST solution, the immunoreactive bands were determined by adding SuperSignal West Femto mix (1:1 mix of stable peroxide buffer and luminol/enhancer solution (Thermo Scientific, Rockford, IL, U.S.A.) to detect immunoreactive bands. The bands were visualized and quantified by BioRad ChemiDoc XRS system (Hercules, CA, U.S.A.). The primary antibodies used were β-actin, Nrf2, NQO-1, p21, cyclin D1 (Santa Cruz Biotechnology, Santa Cruz, CA, U.S.A.), cleaved caspase-3, cleaved caspase-7, cleaved poly (ADP-ribose) polymerase (PARP) and PARP (Cell Signaling Technology, Danvers, MA, U.S.A.). The secondary antibodies used were goat polyclonal IgG for β-actin, Nrf2, NQO-1 and rabbit polyclonal IgG for p21, cyclin D1, cleaved caspase-3, cleaved caspase-7, cleaved PARP and PARP were purchased from Santa Cruz Biotechnology, Santa Cruz, CA, U.S.A.

3.2.10 Statistical analysis

Results were presented as means ± standard deviation (SD). Data were analyzed using SPSS software (version 17, IL, U.S.A.), and nonparametric statistical test Mann-Whitney U (98, 99) was performed for *in vivo* animal study. Box-plots presentation were used: the upper boundary of the box represents the 75^{th} percentile while the lower boundary of the box represents 25^{th} percentile of the data distribution, the horizontal line within each box represents the median value and the error bars represent the 95% confidence intervals. The student's *t*-test was used to determine the statistical differences for the *in vitro* study.

3.3 Results

3.3.1 I3C and DIM activated ARE luciferase activity in HepG2C8 cells

HepG2C8 cells were treated with I3C to test the ability of I3C in inducing Nrf2-mediated ARE luciferase activity. I3C induced ARE luciferase activities, significantly, ranging from 1.5 folds to 5 folds with concentrations of 50 μM, 75 μM, and 100 μM (Figure 3-3). DIM also induced ARE luciferase activities, significantly, with concentrations of 1, 5, 12.5, and 25 μM (Figure 3-4).

3.3.2 I3C induced Nrf2 and phase II detoxifying/ antioxidant genes expression in TRAMP C1 cells

To investigate whether I3C could induce Nrf2 and antioxidant genes expression in TRAMP C1 cells, qPCR was performed to quantify the mRNA expression of four Nrf2 mediated phase II detoxifying/ antioxidant genes, Nrf2, NQO-1, glutamate cysteine ligase

catalytic (GCLC), and heme oxygenase-1 (HO-1). As shown in the Figure 3-5, the induction of these four genes by I3C was highly dose-dependent. Compared with non-treated cells, GCLC and NQO-1 genes were induced significantly ($p<0.05$) by I3C 25 μM, 50 μM, and 75 μM. Nrf2 and HO-1 genes were induced significantly by I3C at 75 μM (Figure 3-5).

3.3.3 I3C supplemented diet and general health observations in TRAMP mice

The overall health of all the mice was observed throughout the study period and was found to be good. During the course of the study, all the mice were weighed and checked every week. No significant changes in the body weights were found throughout the study period. In addition, I3C treatment has no significant effect on the weights of the liver, spleen, and kidneys. There was no other sign of toxicity.

3.3.4 Effects of I3C supplemented diet on prostate tumorigenesis

There was a statistically significant decrease in the wet weight of GUT in the I3C treated group (G1) (p=0.021) as compared to the non-treated group (Figure 3-6). Effect of the wet GUT weight in the I3C treated group (G2) was not statistically significance different from the control group (p=0.071) indicating that the timing of I3C in the diet was contained in order to effectively preventing the PCa in TRAMP mice.

Upon necropsy, seven control untreated mice revealed hyperplasia and lesion of the prostate tissues or the seminal vesicles. The effect of I3C in reducing the incidence of palpable tumor and metastasis are summarized in Table 3-3. Although primary palpable prostate tumor was found in six control mice and five of them were associated with distinct lymph nodes metastases, no lung or liver metastasis was observed. Histological

analyses showed that the remaining control mice had either HG-PIN or carcinoma. I3C was found to significantly reduce the incidence of palpable tumor and lymph node metastasis ($p<0.05$) in TRAMP mice from both G1 and G2. Control mice ($n=13$) showed approximately 54% incidence of HG-PIN and 46% of carcinoma. In contrast, G1 demonstrated 40% incidence of HG-PIN and 40% LG-PIN and only 20% (one mouse) was diagnosed as carcinoma. In G2, the mice treated with I3C started from 12 weeks old showed 60% incidence of HG-PIN, 20% incidence of LG-PIN and 20% of carcinoma (Figure 3-7 & Table 3-3). Compared to the control mice, lower tumor incidence and decrease in PIN levels in the I3C treated mice suggesting that I3C possess the inhibitory effect in PCa tumor formation and progression. The I3C treatments did not affect the expression of SV-40 transgene (data not shown).

3.3.5 Effects of I3C supplemented diet induced apoptosis

The percentages of apoptotic cells in the dorso-lateral prostates of the TRAMP mice are shown in Figure 3-8. The percentage of apoptotic cells in the prostate tumor tissues of mice treated by I3C was significantly higher than the control mice ($p=0.002$ in G1 and $p=0.004$ in G2). Although the percentage of apoptotic cells in G1 was higher than in G2, this difference was not statistically significant.

3.3.6 I3C supplemented diet induced protein expressions of Nrf2 and NQO-1

I3C significantly induced Nrf2 in G1 and G2 TRAMP prostate tissue (Figure 3-9). Similarly the Nrf2-mediated downstream antioxidant enzyme NQO-1 was also significantly induced by I3C (Figure 3-9). There was not detectable Nrf2 or NQO-1 expression in the control prostate tumor samples (Figure 3-9).

3.3.7 Effects of I3C supplemented diet on the expression of proteins involved in the cell cycle regulation and apoptosis

In order to identify the molecular targets involved in the cell cycle regulation and apoptosis modulated by I3C using western blot (Figure 3-10). I3C induced the protein expressions of p21 in G1 and G2 TRAMP prostate tissue as compared to the untreated animals. Cleaved caspase-3 ($p<0.05$) and -7 ($p<0.05$) were also induced by the administration of I3C. However, cyclin D1 protein expression was suppressed by I3C treatment. In our figure, PARP cleavage shows lesser in treatment groups compared to control group. However, our western blotting results also show that PARP is lesser in treatment groups than control. After calculating the ratio of cleaved PARP/PARP, we find control (1.33±0.33), G1 (2.32±1.46) and G2 (2.27±1.54). The results present that our treatment decrease PARP expression and the ratio of cleaved PARP/PARP illustrate that treatment groups yield more cleaved PARP than control.

3.4 Discussion

I3C, a phytochemical, found abundantly in cruciferous vegetables has been studied as an anti-cancer agent for quite some time. I3C has been used in clinical trials for some diseases including vulvar intraepithelial neoplasia, respiratory papillomatosis, and breast cancer prevention (123). Previous published studies show that I3C can inhibit tumor formation by inhibiting cell proliferation, inducing apoptosis, regulating cell cycle, and suppressing aberrant inflammation *in vivo* or *in vitro* (112, 119, 121, 130).

Several previous studies discussed the anti-cancer effects of I3C in the prostate cancer cell lines and animal model which involved with the injection/implantation of

prostate cancer cells into animals (112, 130). In our current study, we used TRAMP as an animal model to investigate the PCa chemoprevention efficacy of I3C. TRAMP model develops LG-PIN by approximately 6-8 weeks of age, and HG-PIN by approximately 12-18 weeks of age spontaneously. By 24-28 weeks of age, the TRAMP prostate progresses to poorly differentiated carcinoma, and finally metastasize to lymph nodes, liver, and lungs by 28-30 weeks of age (64). Our present results demonstrated that by 24 weeks of age, six out of nineteen (31.6%) TRAMP mice without treatment developed palpable tumors with lymph nodes metastasis. On the other hand, none of the I3C treated groups (G1 or G2) developed any presence of palpable tumors or metastasis and there was significant difference in the incidence of palpable tumors and lymph node metastasis between the treated groups and untreated group (Figure 3-7). In addition, I3C has a strong inhibitory effect on the tumor burden, the GUT weights (carcinoma versus normal prostate) as shown in the Figure 3-6. In the control group, there were several severe carcinoma cases that the seminal vesicles and bladder were not distinguishable from the prostate tumor. I3C slowed down and retarded the growth of tumor formation and metastasis, resulting in significantly lower GUT weights, especially when the mice were treated starting from 8 weeks of age (G1).

Histological analysis of the prostatic sections of the control animals displayed high level of epithelial proliferation and neoplasia (Figure 3-7). In contrast, the sections from animals fed with I3C supplemented diet displayed low level of epithelial proliferation (Figure 3-7).

Nrf2, which is a redox sensitive transcription factor, plays an important role in ARE-mediated gene expression of phase II drug metabolizing/ antioxidant enzymes. Previous study from our laboratory revealed that prostate tumor progression including during PIN development and tumor formation in TRAMP is associated with the reduction in the expression of anti-oxidative and phase II detoxifying or drug metabolizing enzymes (126). Surprisingly, when we studied the chemopreventive effect of gamma (γ)-tocopherol-enriched mixed tocopherol (gTmT) in TRAMP mice, we found that Nrf2 was re-expressed by gTmT as compared to untreated control animals (126). In the present study, we found that I3C is a potent inducer of antioxidant enzymes such as NQO-1, HO-1, GCLC, and a transcription activator of Nrf2 in the TRAMP C1 cells (Figure 3-5). Utilizing the specific Nrf2-ARE-mediated transcriptional activation luciferase assay also demonstrated that I3C induced ARE activity in the HepG2-C8 cells significantly, suggesting that I3C could indeed activate Nrf2-ARE signaling pathway (Figure 3-3). *In vivo* results also showed that administration of I3C increased the expression of Nrf2 and Nrf2 target gene NQO-1 in TRAMP prostate tissues. Therefore, all these results suggest that I3C possesses the ability to induce the phase II detoxifying/ antioxidant enzymes to protect the murine prostate tissues against oxidative stress via Nrf2-signaling pathway. This is consistent with previous report showing that I3C could induce the Nrf2 protein expression in HepG2-C8 cells (52).

Several previous studies suggested that I3C could induce apoptotic cell death as well as cell-cycle arrest in human breast cancer cells, human PCa cells, and TRAMP C2 cells (112, 121, 130, 133, 134). Akt signaling pathway is one of the important signal

transduction pathways playing a critical role in cell survival and apoptosis. Our results showed that I3C induced apoptosis in the G1 and G2 TRAMP prostate tissues (Figure 3-8 and 3-10). In addition, Akt pathway appears to be suppressed by I3C, coupled with high expression of cleaved caspase-3 and -7 (Figure 3-10). In agreement with other *in vitro* cell culture studies of I3C in human cancer cells (112, 134), our current finding also shows that p21 is significantly induced and cyclin D1 is suppressed by I3C treated G1 and G2 TRAMP prostate tissues *in vivo*. Therefore, it appears that I3C inhibits tumor growth in TRAMP prostate tissues possibly by suppressing tumor cell proliferation via cell-cycle arrest and apoptosis signaling pathways, contributing to its overall PCa chemoprevention efficacy. During the preparation of this manuscript, a study from Cho et al. reported that DIM inhibited PCa in TRAMP mice via induction of apoptosis and inhibition of cell cycle progression (135). Although DIM is a major *in vivo* derivative of I3C, the effects of I3C itself have not been studied, and furthermore, the focus of our studies is different in that we are focusing on effect of I3C in modulating the Nrf2 anti-oxidative stress signaling pathway leading to its cancer chemopreventive effect. Our study clearly showed that I3C is as effective as DIM in preventing the development of prostate cancer in TRAMP mice. Hence, the potential clinical utility of both I3C and DIM would be potentially feasible.

3.5 Summary

I3C is an effective cancer chemopreventive agent against PCa in TRAMP mouse model. I3C appears to be a multi-targets cancer chemopreventive compound that is effective against PCa *in vivo*. Our *in vitro* cell culture results corroborate well with the *in*

vivo TRAMP mice results on Nrf2-mediated anti-oxidative stress response pathway especially this would play an important role at the early initiation stage of PCa carcinogenesis (47). Furthermore, cell cycle arrest and apoptotic signaling pathways would also contribute to the overall cancer chemoprevention, particularly at the later stages of tumorigenesis when tumor cells are formed and progressed (47). Taken together, our present results clearly demonstrate that I3C can pharmacodynamically up-regulate Nrf2-mediated signaling, anti-oxidative stress response, regulate cell cycle and induce apoptosis culminating in the overall cancer chemoprevention of PCa in TRAMP mice. This is the first report to show a detail study on the anti-oxidative activities of I3C via up-regulating the Nrf2 pathway *in vitro* and *in vivo* systems. Our findings may provide a novel Nrf2-mediated signaling pathway that is clinically relevant.

Table 3-1. Murine Primers for Quantitative Real-Time PCR

Gene	Forward	Reverse
β-actin	5'-CGT TCA ATA CCC CAG CCA TG-3'	5'-GAC CCC GTC ACC AGA GTC C-3'
NQO1	5'-AGC CCA GAT ATT GTG GCC G-3'	5'-CCT TTC AGA ATG GCT GGC AC-3'
Nrf2	5'-AGC AGG ACA TGG AGC AAG TT-3'	5'-TTC TTT TTC CAG CGA GGA GA-3'
HO-1	5'-CCC ACC AAG TTC AAA CAG CTC-3'	5'-AGG AAG GGG GTC TTA GCC TC-3'
GCLC	5'-CTC ATT CCG CTG TCC AGG T-3'	5'-CCT TTG CAG ATG TCT TTC CTG AA-3'

Table 3-2. Confirmation of genotype of the TRAMP mice

Gene	Primers
Tcrd Forward	5'- CAA ATG TTG CTT GTC TGG TG-3'
Tcrd Reverse	5'- GTC AGT CGA GTG CAC AGT TT-3'
SV1	5'- GGA CAA ACC ACA ACT ATG CAG TG-3'
SV5	5'- CAG AGC AGA ATT GTG GAG TGG-3'

Table 3-3. Indole-3-carbinol (I3C) inhibit palpable tumor and metastasis in TRAMP males

	Number of animals	Incidence of palpable tumor	Incidence of lymph nodes metastasis
Control	19	6/19 [a]	5/19 [b]
I3C_8wk (G1)	8	0/8[a, *]	0/8[b, †]
I3C_12wk (G2)	8	0/8[a, *]	0 /8[b, †]

[a] Numbers represent the presence of palpable tumor showed at the end of the experiment at 24 weeks of age. Fisher's exact test was used to compare the incidence of palpable tumor between the control and the 1% I3C diet treated mice sacrificed at 24 weeks of age. *p* values <0.05 were considered as significant, indicated by *.

[b] Numbers represent the presence of lymph nodes metastasis showed at the end of experiment when the mice were sacrificed. Fisher's exact test was used to compare the incidence of lymph node metastasis between the control and the I3C treated mice sacrificed at 24 weeks of age. *p* values <0.05 were considered as significant, indicated by †.

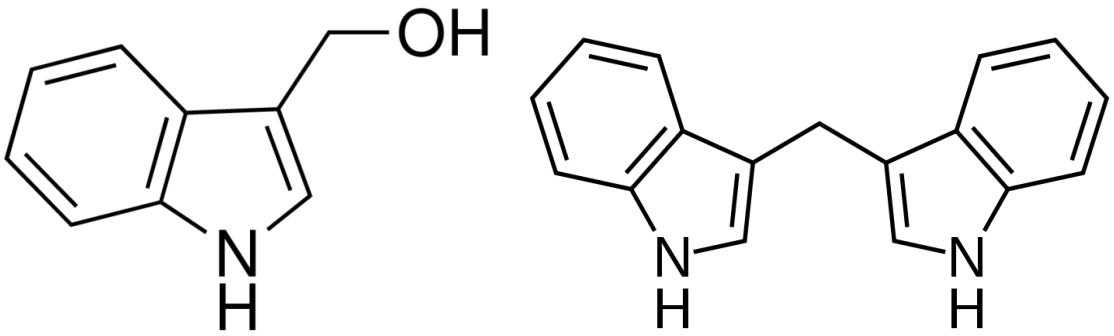

Figure 3-1 Chemical structure of Indole-3-carbinol (Left) and 3,3'-diindolylmethane (DIM) (Right)

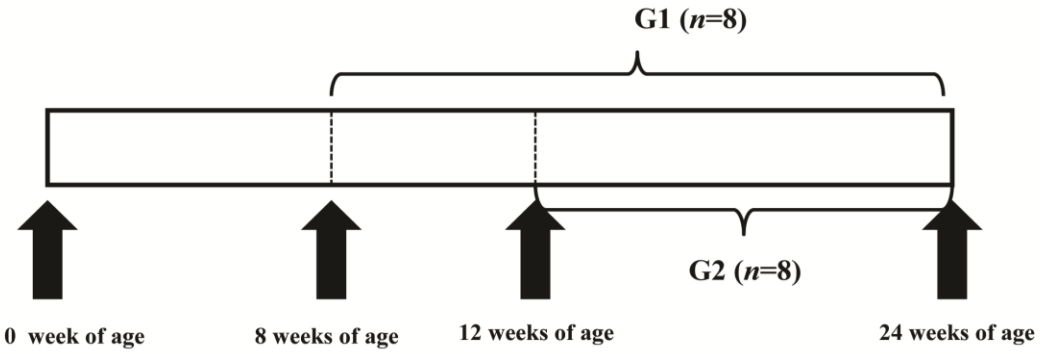

Figure 3-2 Time line, I3C supplemented diet in TRAMP mice.

G1=Eight weeks of age TRAMP males were put on AIN-76A diet supplemented with 1% I3C and were sacrificed at 24 weeks of age; G2= 12 weeks old TRAMP males were put on AIN-76A with 1% I3C and were sacrificed at 24 weeks of age.

(**Wu** *et al*; Molecular Carcinogenesis. 2012 Oct;51(10)

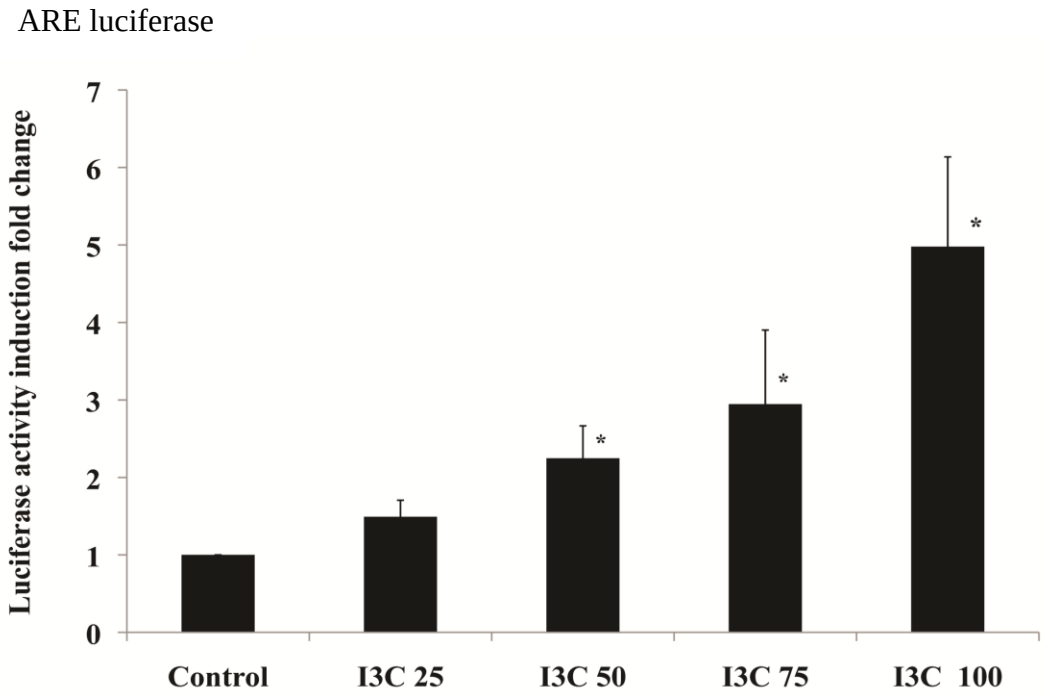

Figure 3-3 Effect of I3C on the activity of ARE-luciferase in HepG2 C8 cells

HepG2C8 cells treated with 25, 50, 75, 100 μM I3C, respectively. The control cells were treated with DMSO 0.1%. Data were presented as mean ±SD. ***** Significantly different from the control (p<0.05). (**Wu** *et al*; Molecular Carcinogenesis. 2012 Oct; 51(10))

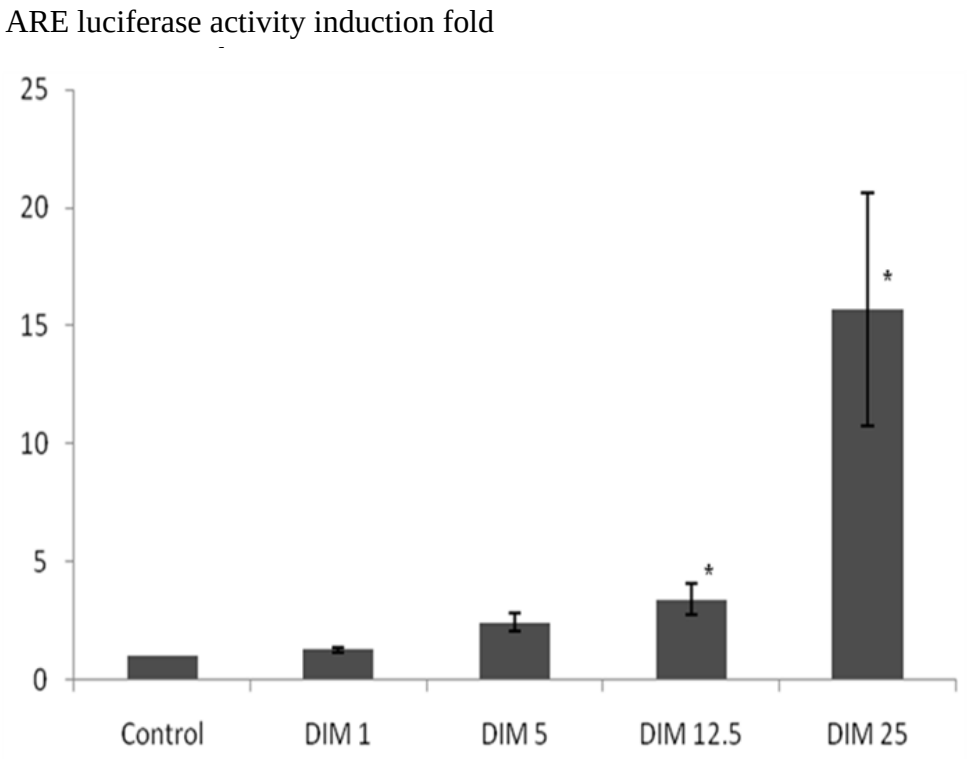

Figure 3-4 Effect of DIM on the activity of ARE-luciferase in HepG2 C8 cells

HepG2C8 cells treated with 1, 5, 12.5, 25 μM DIM, respectively. The control cells were treated with DMSO 0.1%. Data were presented as mean ±SD. ***** Significantly different from the control ($p<0.05$).

(**Wu** *et al*; Molecular Carcinogenesis. 2012 Oct; 51(10))

mRNA expression

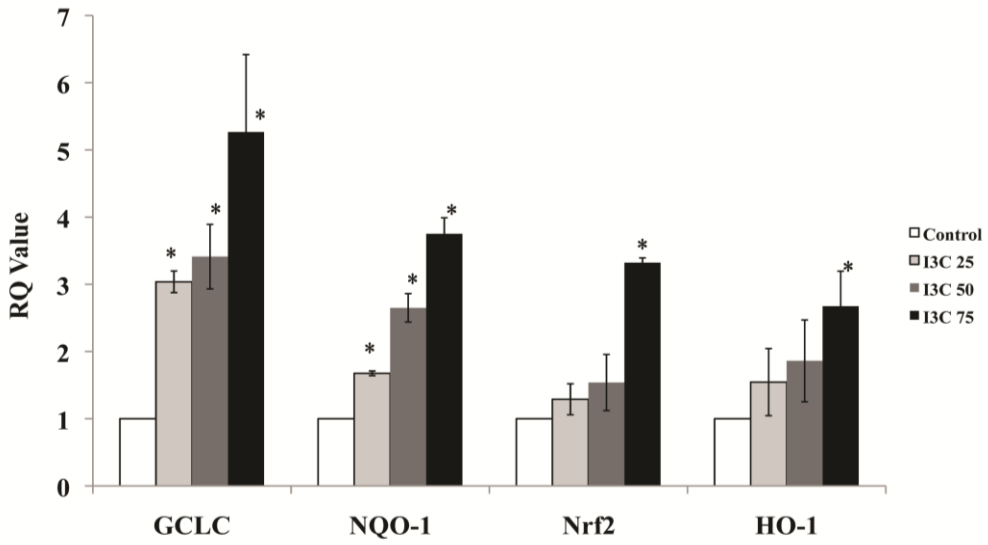

Figure 3-5 The qPCR data of the effect of I3C induced mRNA expression.

Expression of Nrf2 and Nrf2-mediated phase II detoxifying/ antioxidant genes in TRAMP C1 cells treated with 25, 50, 75 μM I3C, respectively. The control cells were treated with DMSO 0.1%. The data were shown as mean ±SD. ***** Significantly different from the control (p<0.05).

(**Wu** *et al*; Molecular Carcinogenesis. 2012 Oct; 51(10))

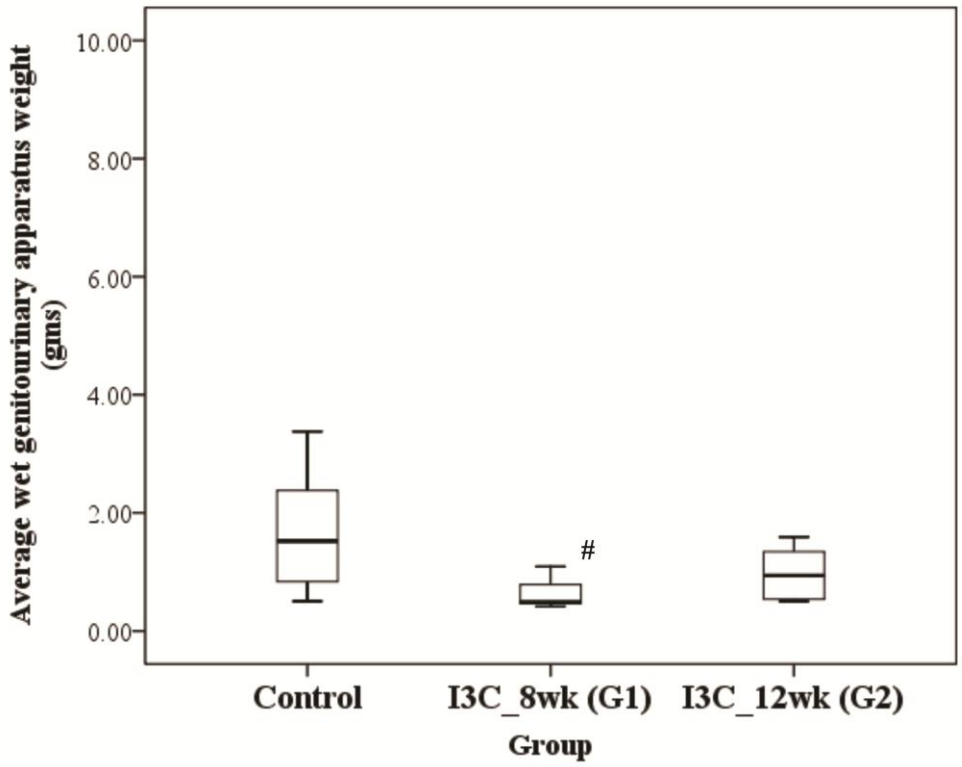

Figure 3-6 Effects of I3C supplemented diet on TRAMP males.

Effects of I3C on the genitourinary apparatus weights of animals treated from 8 weeks old and 12 weeks old. # Significantly different from the control (p<0.05) based on Mann-Whitney Test. (**Wu** *et al*; Molecular Carcinogenesis. 2012 Oct; 51(10))

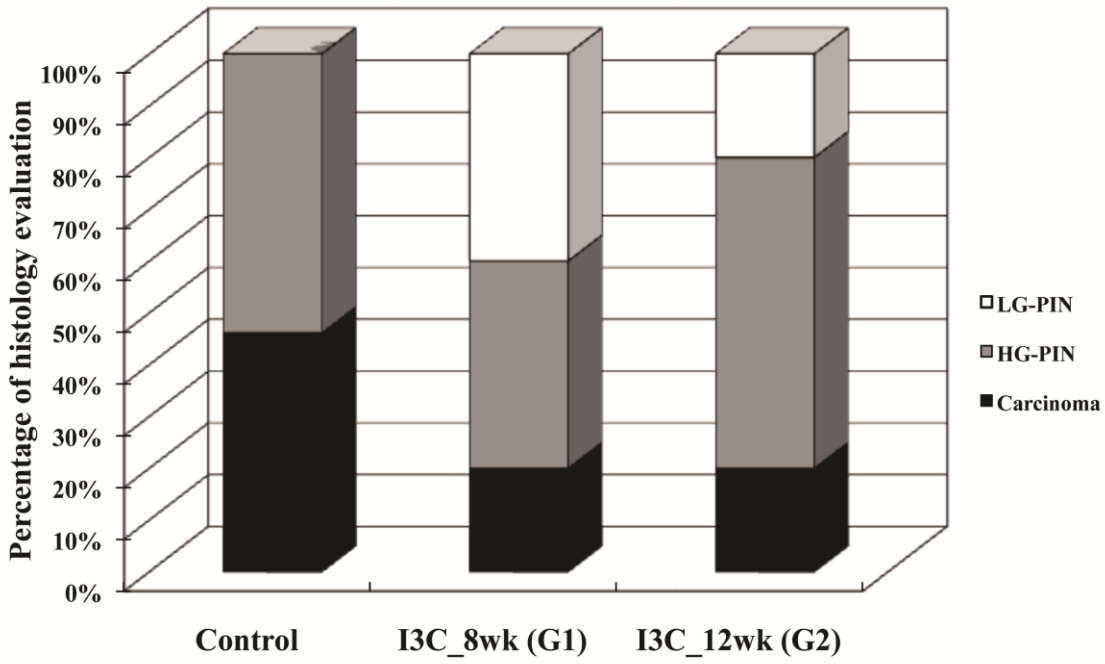

Figure 3-7 Histological evaluation of the incidence of PIN and carcinoma.

(Please refer to Table 3-3 for further detail.)

(**Wu** *et al*; Molecular Carcinogenesis. 2012 Oct; 51(10))

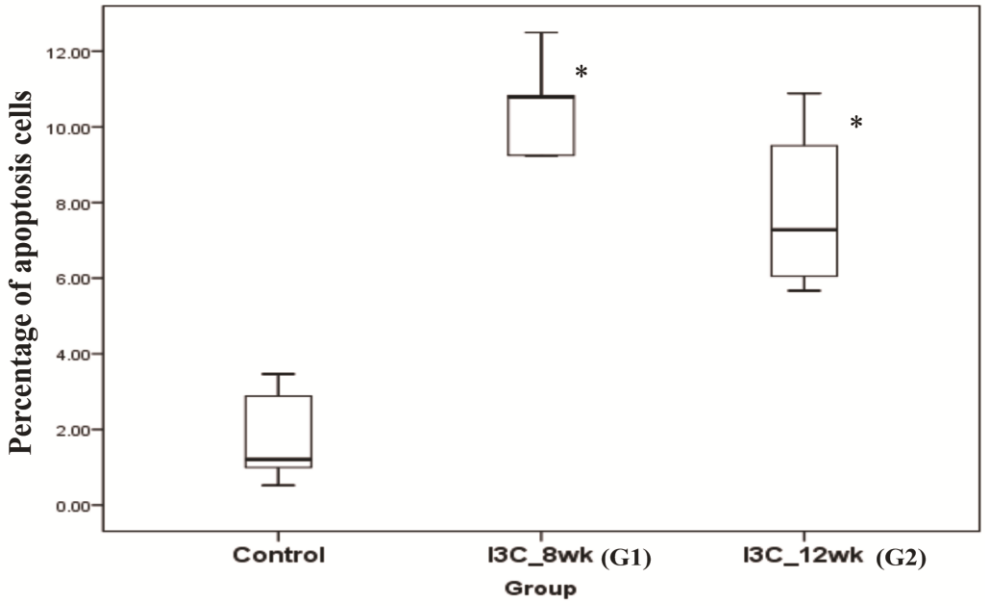

Figure 3-8 Immunohistochemical analysis on the apoptotic markers (TUNEL)

The effects of I3C supplemented diet on TRAMP males on the apoptotic markers. *****Significantly different from the control (p<0.05) was based on Mann-Whitney Test. (**Wu** *et al*; Molecular Carcinogenesis. 2012 Oct; 51(10))

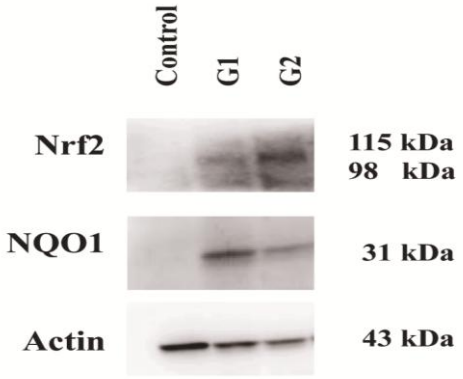

Figure 3-9 Western blot analysis of biomarkers for Nrf2 and Nrf2-regulated NQO-1

The TRAMP prostates or tumors treated with I3C and control diet. Nrf2 and NQO-1 were re-activated by I3C in G1 and G2 significantly different from the control. There was no expression of Nrf2 and NQO-1 found in the control animals.

(**Wu** *et al*; Molecular Carcinogenesis. 2012 Oct; 51(10))

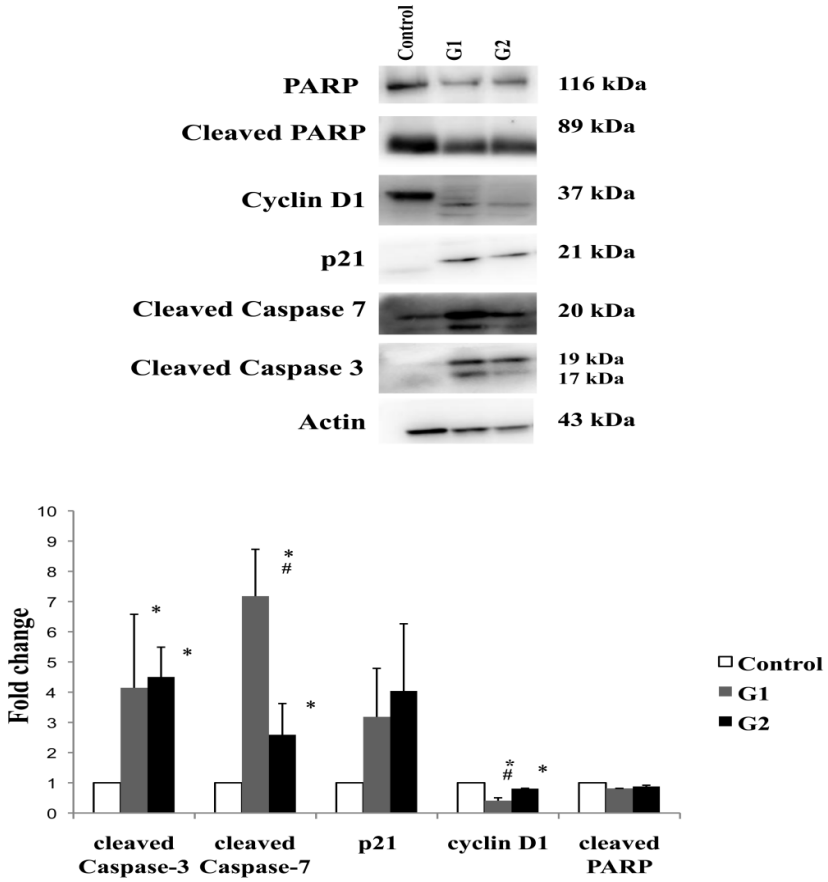

Figure 3-10 Western blot analysis of biomarkers for cell cycle regulation, and apoptosis. The TRAMP prostates or tumors treated with I3C and control diet. The graphs represent the relative expression of each biomarker normalized to actin. ***** Significantly different from the control (p<0.05) by Student's t-Test. # Significantly different between G1 and G2. The experiment was performed three times, similar findings were obtained. Selected representative western blot images are presented. Data represented is the mean ±SD. Compared to the control, the results of western blot analysis of p21 and cleaved caspase-3 and-7 were induced greatly, respectively. Cleaved PARP, cyclin D1 were suppressed significantly by I3C treatment. (**Wu** *et al*; Molecular Carcinogenesis. 2012 Oct; 51(10))

CHAPTER 4 Epigenetic modifications of Nrf2 CpG Island by 3,3'-diindolylmethane in TRAMP prostate tumors and in TRAMP C1 cells[10,11,12]

4.1 Introduction

Epigenetic modifications, including chromatin structure modification, DNA and histones covalent and non-covalent modification, nucleosome and small non-coding RNAs remodeling, are fundamental in controlling the normal development and maintenance of genes expression (10, 11, 67). Epigenetic alteration in general infers changes of gene expression, which is reversible and heritable, without altering the DNA sequence (136). Aberrant DNA methylation in the promoter regions of tumor suppressor genes plays a critical role in cancer development and progression (67). Hypermethylation of promoters of tumor suppressor genes such as ESR1 (estrogen receptor α) in colorectal and breast cancers, GSTP1 (glutathione S-transferase π1) in breast and prostate cancers, RARβ2 (retinoid acid receptor β2) in colorectal, breast and prostate cancers, DAPK1 (death-associated protein kinase 1) in breast and lung cancers, have been linked to cancer development and progression in human (137, 138).

---

[10] Work described in this chapter has been submitted to an international journal.

[11] **Key words**: 3,3'-diindolylmethane (DIM); epigenetic; Nrf2; methylation; prostate cancer

[12] **Abbreviations**: 5-MC, 5-methylcytosine; BGS, Bisulfite genomic sequencing; ChIP, Chromatin immune-precipation; DIM, 3,3'-diindolylmethane; DNMT, DNA methyltransferase; gTmT, γ-tocopherol-rich mixture of tocopherols; GU, genitourinary apparatus; HDAC, histone deacetylase; HG-PIN, high grade prostatic intra-epithelial neoplasia; I3C, indole-3-carbinol; IHC, immunohistochemical; IP, immunoprecipitation; LG-PIN, low grade prostatic intra-epithelial neoplasia; MeDIP, methylation DNA immunoprecipitation; Nrf2, nuclear factor (erythroid-derived 2)- like 2; PCa, prostate cancer; PCNA, proliferating cell nuclear antigen; SD, standard deviation; TRAMP, transgenic adenocarcinoma of mouse prostate

Prostate cancer (PCa) is the most commonly diagnosed male cancer (1/6 men in their lifetime) and the second leading cancer related death in men in the USA (NCI website). Prostate cancer has a very long latency period involving a cascade of epigenetic and genetic changes. Epidemiological, experimental, preclinical, and clinical studies have shown that long-term oxidative stress and chronic inflammatory status would drive the development and progression of PCa (125-127). Nuclear factor (erythroid-derived 2)-like 2 (NFE2L2 or Nrf2) plays a critical role in the anti-oxidative stress response including the coordinated regulation many detoxifying/antioxidant enzymes (128, 139). Recently, Frohlich et al. reported a progressive loss of expression of Nrf2 and its downstream target genes in clinical PCa patients (127). Previously, we have reported that PCa progresses in transgenic adenocarcinoma of mouse prostate (TRAMP) mice, there is a progressive loss of expression of Nrf2 and its downstream target anti-oxidative genes such as NQO1, HO-1, GSTm1, GCLC, and UGT1a1(64, 126, 140). Coincidentally, we also found that the promoter region of Nrf2 was hypermethylated in the CpG island in TRAMP prostate tumors and in TRAMPC1 cells (141) and enhanced Nrf2 CpG methylation as TRAMP prostate tumor progresses, associated with attenuated expression of Nrf2 and Nrf2-target genes (142). Interestingly, dietary feeding of TRAMP mice with γ-tocopherol-rich mixture of tocopherols (gTmT), which inhibited PCa, maintained Nrf2 expression in prostate tumors via epigenetic inhibition of CpG methylation (142).

Clinically, advanced and metastasized cancers in human are very tough to treat, resistant to radiation and chemotherapy because of too many epigenetics, genetics and loss of heterozygocity (LOH), among others (143). Hence it would be logical and

clinically feasible if one could utilize relatively non-toxic dietary phytochemicals and or medicinal drugs such as NSAIDs, to prevent, block or delay the progression of benign tumors from becoming advanced/metastasized cancers (43, 144). Increasing evidence suggests that during prostatic carcinogenesis, epigenetic changes arise earlier than genetic defects, linking the appearance of epigenetic alterations in some way to disease etiology (138). Many relatively non-toxic dietary phytochemicals such as polyphenols from green tea and isothiocyanates from plant food have been shown to inhibit cancer development via epigenetic mechanisms both *in vivo* and *in vitro* (72). Recently, we have found that curcumin, a potent anti-cancer agent in many cancer models including PCa, suppresses the expression of DNA methyltransferase (DNMT) and histone deacetylase (HDAC) in the human prostate LNCaP cells and reverses the DNA CpG hypermethylation of the promoter region of Nrf2 in TRAMP C1 cells and Neurog1 in LNCaP cells (145, 146). 3,3'-diindolylmethane (DIM) and its parent compound, Indole-3-carbinol (I3C), are found abundantly in cruciferous vegetables, and it is a potent anti-cancer and cancer chemopreventive agent in many in vivo and in vitro cancer models (112, 119, 147). Currently there are around ten clinical trials are being conducted in early stage of prostate, breast, and cervical cancer patients (www.clinicaltrial.gov). However, it is unclear whether DIM would inhibit tumorigenesis in TRAMP mice and secondly whether epigenetic mechanism might be involved.

In our current study, we first investigated the inhibitory efficacy of prostate tumorigenesis of DIM in TRAMP mice and secondly we examined the epigenetic modifications of the promoter of Nrf2, a well-accepted tumor suppressor gene mediating

cellular defense against oxidative stress and inflammation (128), in vivo in TRAMP prostate tumors and in vitro TRAMP C1 cells. The results show that DIM effectively inhibits the progression and development of prostate cancer in TRAMP mice and DIM demethylates and re-expresses Nrf2 and Nrf2-target genes in vivo and in vitro. This is the first report on the de-methylation ability of DIM both *in vivo* and *in vitro*, which may translate to human studies.

4.2 Materials and methods

4.2.1 Reagents and cell culture

The DIM used in the study contains approximately 98% of DIM purchased from Sigma-Aldrich (St. Louis, MO, USA). TRAMP C1 cells (provided by Dr. Barbara Foster, Department of Pharmacology and Therapeutics, Roswell Park Cancer Institute, Buffalo, NY), originally derived from TRAMP prostate tumor (129), were cultured in Dulbecco's Modified Eagle's Medium (Invitrogen Corp., Carlsbad, CA, U.S.A.) supplemented with 10% (V/V) fetal bovine serum (FBS) (Invitrogen Corp., Grand Island, NY, U.S.A.), penicillin 100 U/ml, and streptomycin 100 μg/ml (Invitrogen Corp., Grand Island, NY, U.S.A.). Cells were maintained in a humidified incubator with 5% CO_2 at 37^{o}C. Cells were seeded in 10 cm plates for 24 h and then treated along with 0.1% DMSO (control) or different concentration DIM in 1% FBS containing medium for 5 days. The medium was changed every 2 days (145).

4.2.2 Animals

Female hemizygous C57BL/TGN TRAMP mice, line PB Tag 8247NG, and male C57BL/6 mice were purchased from The Jackson Laboratory (Bar Harbor, ME, U.S.A.).

The animals were bred on the same genetic background and maintained in the Laboratory Animal Service facility at Rutgers University. Housing and care of the animals was performed in accordance with the guidelines established by the University's Animal Research Committee consistent with the NIH Guidelines for the Care and Use of Laboratory Animals. Transgenic males for the studies were obtained as [TRAMP x C57BL/6] F1 or [TRAMP x C57BL/6] F2 offspring. Identity of transgenic mice was established by PCR-based DNA genotyping using the primers suggested by The Jackson Laboratory (Table 4-1). Throughout the experiment the animals were housed in a temperature-controlled room (68-72℉) with a 12 h light dark cycle, at a relative humidity of 45% to 55%.

4.2.3 Diet and animal study design

DIM was obtained from Sigma-Aldrich (St. Louis, MO, U.S.A.). AIN-76A diets containing 1% DIM were prepared by Research Diets Inc. (New Brunswick, NJ, U.S.A.) and stored at -20℃. The dose was chosen based on previous studies (148, 149). In our present study, 1% DIM was well-tolerated for these TRAMP mice. The control TRAMP males (n=19) received AIN-76A diets throughout the experiment while the treated TRAMP males received 1% DIM diet from 8 weeks of age (n=9) as group 1 (D-G1) and from 12 weeks of age (n=8) as group 2 (D-G2). Fresh diets were added to the cages twice a week. In this study, TRAMP males were weighed weekly and general health was monitored on a regular basis. All mice were sacrificed at the age of 24 weeks by cervical dislocation and the genitourinary apparatus (GU) consisting of seminal vesicles, prostate, and bladder were isolated for further analyses (Figure 4-1) (140).

4.2.4 Histopathology

The dorso-lateral prostate (*n*=5) was excised and fixed in 10% formalin for 24 h and then transferred to 70% ethanol for 24 h. After dehydration processing and embedding with paraffin, tissue sections (4 μM) were cut from paraffin embedded prostate tissue and mounted on slides. The sections were stained with Hematoxylin and Eosin (H&E) to observe any neoplastic changes. Sections were evaluated by histopathologist in a blinded fashion to classify prostatic intra-epithelial neoplasia (PIN) lesion as we have reported previously (48, 64, 126, 140). Lesions were classified as PIN I, PIN II, PIN III, and PIN IV as described by Park *et al* as well as we have reported previously (48, 64, 126, 132) . For classification ease, PIN I and PIN II were combined as low grade PIN (LG-PIN) while PIN III and PIN IV were combined as high grade PIN (HG-PIN) as we have done previously.

4.2.5 Immunohistochemistry (IHC) staining assay

Sections (4 μm) were cut from the paraffin embedded prostate tissue and mounted on glass slides. The slides were de-parafinized in xylene and antigen unmasking was performed by applying proteinase K digestion directly on the slides for 15 min. Endogenous peroxidase was blocked by incubating in 3% H_2O_2 for 5 min, and ApopTag Plus Peroxidase *In Situ* Apoptosis Detection Kit (Millipore, Temecula, CA, U.S.A.) was used to detect apoptotic cells. For detection of proliferative cells, monoclonal mouse anti-proliferating cell nuclear antigen (PCNA) antibody (Clone PC10, 1:50, Dako North America, Carpinteria, CA, U.S.A.) was used (64). The staining was performed following as the manufacturer's protocols. Anti-5-methylcytosine (5-MC) mouse monoclone

antibody (Clone 162 33 D3, 1:50, EMD Chemicals, Philadelphia, PA, U.S.A.) was used to detect genome-wide methylated DNA. Vectastain ABC kit (Vector Laboratories, Inc., Burlingame, CA, U.S.A.) was used to detect apoptotic cells by applying enzyme conjugated avidin, peroxidase substrate, and 3,3'-diaminobenzidine (DAB) to develop color for visualization (140).

4.2.6 Assessment of IHC staining

Quantitative of IHC staining was done using the Aperio ScanScope® GL system according to the manufacture's protocol (Aperio Technologies Inc., Vista, CA, U.S.A.). This is a single-slide scanning system for digital pathological analysis of IHC of tumor samples to analyze our IHC-stained slides for the various cell cycle and apoptotic markers. The Aperio ImageScopoe software (v 10.1.3.2028) allowed the unbiased quantification and quantitative analysis of the IHC staining of biomarkers of prostate tumor samples obtained from untreated control versus the treated TRAMP mice.

4.2.7 Western blot

The TRAMP C1 cells or dorso-lateral prostate tissues collected from treated and control groups were pooled and homogenized with RIPA buffer (Cell Signaling Technology, Inc., Danvers, MA, U.S.A.) and 10 μg/ml protease inhibitor cocktail (EMD Chemicals, Philadelphia, PA, U.S.A.). Protein (20 μg) was loaded onto 4-15% SDS-PAGE (Bio-Rad Laboratories, Hercules, CA, U.S.A.). After separation by SDS-PAGE, the protein was transferred onto nitrocellulose membrane (Millipore Corp., Billerica, MA, U.S.A.), and then was blocked in 5% bovine serum albumin (BSA) (Fisher Scientific, Fair Law, NJ, U.S.A.) in tris buffer saline tween-20 (TBST) solution for 1 h.

Membranes were probed using the different mono- or polyclonal-antibodies (1:1000) overnight at 4℃. Blots were washed with TBST solution for 15 min 4 times and incubated with the respective secondary antibodies for 1 hr. After washing 15 min 4 times with TBST solution, the immunoreactive bands were determined by adding SuperSignal West Femto mix (1:1 mix of stable peroxide buffer and luminol/enhancer solution (Thermo Scientific, Rockford, IL, U.S.A.) to detect immunoreactive bands. The bands were visualized and quantified by BioRad ChemiDoc XRS system (Hercules, CA, U.S.A.). The primary antibodies used were β-actin, Nrf2, NQO1 (Santa Cruz Biotechnology, Santa Cruz, CA, U.S.A.), HDAC1, HDAC2, HDAC3, HDAC4, and HDAC8 (Cell Signaling Technology, Inc., Danvers, MA, U.S.A.) and DNMT1, DNMT3a, DNMT3b (Imgenex, San Diego, CA, U.S.A). The secondary antibodies used were goat polyclonal IgG for β-actin and NQO1, rabbit polyclonal IgG for Nrf2, HDAC1, HDAC2, HDAC3, HDAC4 and HDAC8, and mouse polyclonal IgG for DNMT1, DNMT3a, DNMT3b (Santa Cruz Biotechnology, Santa Cruz, CA, U.S.A.)

4.2.8 Quantitative real-time PCR assays (qPCR)

Total RNA extracted from DIM treated TRAMP C1 cells were collected and reversed transcribed. The primers, DNMT1, DNMT3a, DNMT3b, and control β-actin of qPCR are listed in Table 4-2 (Integrated DNA Technologies, Coralville, IA, U.S.A.). The qPCR reactions were carried out 1 μl cDNA product, 50 nM of each primer, and Power SYBR Green master mix (Applied Biosystems, Foster City, CA, U.S.A.) in 10 μl reactions. The reactions were performed using an ABI Prism 7900HT sequence detection system; specificity of amplification was verified by first-derivative melting curve analysis

using the ABI software (SDS 2.3, Applied Biosystems, Foster City, CA, U.S.A.). Relative quantification of gene expression profile was calculated using a ΔΔCt method (RQ manager, Applied Biosystems, Foster City, CA, U.S.A.) as we have performed previously (38, 93). Three independent experiments were carried out showing similar results. The results are presented as mean ±SD.

4.2.9 DNA extraction and bisulfite genomic sequencing (BGS)

Genomic DNA was isolated from the control or DIM treated TRAMP C1 cells and TRAMP dorso-lateral prostate tissues collected from control and DIM treated groups pooled and homogenized using the DNeasy tissue kit (Qiagen, Valencia, CA, U.S.A.) The genomic DNAs were extracted to subject to bisulfate conversion carried out using 750 ng of genomic DNA and applying to EZ DNA Methylation Gold Kits (Zymo Research Corp., Orange, CA, U.S.A.) following the manufacturer's instructions. The converted DNA was amplified by PCR using Platinum PCR SuperMix (Invitrogen, Grand Island, NY, U.S.A.) with a set of specific primers, forward: 5'- AGT TAT GAA GTA GTA GTA AAA A-3' and reverse: 5'- AAT ATA ATC TCA TAA AAC CCC AC-3', amplifying the first 5 CpGs located between -1266 and -1086 of the Nrf2 translation initiation site defined as +1. Gel extraction using Qiaquick^{TM} gel extraction kit (Qiagen, Valencia, CA, U.S.A.) were used to purify the PCR products, then cloned into pCR4 TOPO vector using a TOPO™ TA Cloning kit (Invitrogen, Grand Island, NY, U.S.A.). Plasmids DNA from at least 20 colonies per each treatment were prepared using QIAprep Spin Miniprep Kit (Qiagen, Valencia, CA, U.S.A.) and sequenced (Genwiz, Piscataway, NJ, U.S.A.) as we have previously reported (141, 145).

4.2.10 Methylation DNA Immunoprecipitation (MeDIP) Analysis

DNA (8 µg each) extracted from control and DIM treated TRAMP C1 cells were used for the MeDIP analysis modified from previous reports (150, 151). Briefly, the DNAs were adjusted to 150 µl using TE buffer, followed by sonication on ice-water using a Bioruptor sonicator (Diagnode Inc., Sparta, NJ, U.S.A.) and the size of sheared DNA fragment (around 300 to 500 bp) was checked. Inputs took from each sample around one tenth amount of fragmented DNAs; the remaining DNA were followed by denaturing 10 min, and immune-precipitation (IP) in 1x IP buffer (10 mM sodium phosphate pH 7.0, 140 mM NaCl, 0.25% Triton X-100) using anti-methylcytosine (anti-mecyt, purchased from Anaspec, Fremont, CA, U.S.A.) antibody, and negative control antibody (anti-cMyc, purchased from Santa Cruz, Santa Cruz, CA) for 2 hrs at 4℃, respectively. After the incubation, 30 µl magnetic beads (Cell signaling, Boston, MA) were added, and rotated at 4℃ for another 2hr; the pulled-down DNA-beads complex were washed four times using ice cold IP buffer and digested with protease K at 50 ℃ overnight, and followed by DNA purification using miniprep kit from Qiagen (Valencia, CA, U.S.A). The inputs and precipitated DNA were used as templates for PCR amplification of Nrf2 promoter region position from -1092 to -1190 in covering the first 5 CpGs as described previously. A forward primer 5’- GAG GTC ACC ACA ACA CGA AC-3’ and a reverse primer 5’- ATC TCA TAA GGC CCC ACC TC-3’ were used to amplify the Nrf2 fragment. PCR was performed using Platinum PCR superMix (Invitrogen, Grand Island, NY, U.S.A.) The PCR products were performed by agarose gel electrophoresis and visualized by ethidium bromide (EB) staining using a Gel Documentation 2000 system (Bio-Rad Laboratories, Hercules, CA, U.S.A).

4.2.11 Statistical analysis

Results were presented as means ± standard deviation (SD). Data were analyzed using SPSS software (version 17, IL, U.S.A.), and nonparametric statistical test Mann-Whitney U (98, 99) was performed for *in vivo* animal study. Box-plots presentation were used: the upper boundary of the box represents the 75^{th} percentile while the lower boundary of the box represents 25^{th} percentile of the data distribution, the horizontal line within each box represents the median value and the error bars represent the 95% confidence intervals. The student's *t*-test was used to determine the statistical differences for the *in vitro* study.

4.3 Results

4.3.1 Effect of DIM Supplement Diet and General Health Observations

The overall health of all mice was observed during the study period and found to be good. All mice were weighed and checked weekly during the course of this study. No significant change in the body weights of all the mice was found throughout the period. In addition, livers, kidneys, spleens on DIM treatment groups were collected and weighed when the animals were sacrificed and there was no significant effect on the weights. There was no specific sign of toxicity.

4.3.2 Effect of DIM supplemented Diet on Prostate Tumorigenesis

There were statistically significant different in the wet GUT weight between DIM treated groups (D-G1 and D-G2, $p<0.05$) and the non-treated control group (Figure 4-2). Seven control untreated mice were found to have hyperplasia and lesion of the prostate

tissues or the seminal vesicles and six mice were found to have primary palpable prostate tumors. The effect of DIM in decreasing the incidence of palpable tumor and metastasis are summarized in Table 4-3. Among the six untreated mice which were found to have primary palpable tumors, five were associated with distinct lymph nodes metastases, no lung or liver metastasis was observed. The remaining mice in the control group were found to have either HG-PIN or carcinoma by histological analysis. DIM significantly reduce incidence of palpable tumor in D-G2 ($p<0.05$) and lymph nodes metastasis in both D-G1 and D-G2 ($p<0.05$). Although there was a palpable tumor which was also diagnosed as carcinoma in histological analysis found in D-G1, mice treated with DIM starting from 8-week of age demonstrated 60% incidence of LG-PIN and 20% of HG-PIN. In contrast, mice treated with DIM starting from 12-week of age (D-G2) showed 80% of HG-PIN and 20% of LG-PIN but no carcinoma (Figure 4-3). Compared to control group, DIM treated mice have a lower tumor incidence and decrease in PIN levels suggesting that DIM possesses the inhibitory effect in suppressing PCa tumor formation and progression. No suppression effect of SV-40 transgene expression was found in this study (data not shown).

4.3.3 Effect of DIM in cell proliferation and apoptosis

PCNA is an auxiliary protein for DNA polymerase known to be cell cycle regulated (64). TRAMP males treated with DIM for 16 (D-G1) or 12 (D-G2) weeks resulted in significantly lower levels of PCNA ($p= 0.042, 0.030$, respectively) as observed by IHC analysis (Figure 4-4). The percentage of apoptotic cells in the dorso-lateral prostates of the TRAMP males fed with DIM supplemented diet for both D-G1 and D-G2 was

significantly higher than control group (p<0.001). Moreover, the percentage of apoptotic cells in D-G1 was significantly higher than in D-G2 (p=0.029) (Figure 4-5). The results indicate that the tumor inhibitory effect of DIM is partly correlated with increased apoptosis and suppressed proliferation of prostatic epithelial cells.

4.3.4 DIM supplement induced protein expressions of Nrf2 and NQO-1

DIM induced Nrf2 proteins expression in D-G1 and D-G2 in the dorso-lateral prostate tissues of the TRAMP mice. Moreover, NQO-1, a Nrf2-mediated downstream antioxidant enzyme, was also induced by DIM in both D-G1 and D-G2 (Figure 4-6). The Nrf2 or NQO-1 protein expression in the control prostate tumor samples was undetectable.

4.3.5 DIM supplement suppressed global CpG methylation staining by 5-MC in TRAMP prostate tissues

Aberrant CpG DNA methylation is acquired during carcinogenesis (152). 5-methylcytosine (5-MC) is generated when DNA methyltransferases (DNMT) add a methyl group to the 5-carbon atom of the DNA base cytosine (C). In mammalian cells, 5-MC is found predominantly within CpG dinucleotides (153). Aberrant hypermethylation of CpG islands of many tumor suppressor genes has been linked to the development of cancer (152). Furthermore, 5-MC has been proposed to be a critical clinical biomarker for the diagnosis of cancer and tumors formation (152). Figure 4-7 shows that DIM significantly decreased 5-MC IHC staining of the prostate tissue in both group D-G1 and D-G2 (p<0.001, respectively). In addition, the percentage of 5-MC in D-G1 was significantly lower than in D-G2 (p<0.05).

4.3.6 DIM demethylates the first 5 CpGs on the Nrf2 gene promoter of TRAMP prostate tissues

We have previously reported that the first 5 CpGs on the Nrf2 gene promoter region are hypermethylated in TRAMP prostate tumors and TRAMP C1 cells but not in normal prostate tissues (141). In the present study, BGS was performed to investigate the effect of DIM supplement on the methylation status of these 5 CpGs on the Nrf2 gene promoter region in TRAMP prostate tissues or tumors. In agreement with our previous study, the 5 CpGs were hypermethylated in control group (Figure 4-8, control, 98% methylation). In contrast to control group of Nrf2, in D-G1/ D-G2 was significantly reduced the methylation of the 5 CpGs (Figure 4-8, 37.6%, 54.4%, respectively, $p<0.001$). Moreover, compared with two treated groups, it was found that D-G1 has a significantly lower methylation level than D-G2 ($p=0.011$).

4.3.7 DIM decreased the hypermethylation of first 5 CpGs in the promoter region of Nrf2 gene and enhanced expression of Nrf2 and Nrf2-target genes in TRAMP C1 cells

To further confirm the *in vivo* results in TRAMP mice above, BGS was performed to test if DIM could reverse the methylation status of the first 5 CpGs in the promoter region of Nrf2 genes as observed in the TRAMP mice above. In agreement with the *in vivo* results, the first 5 CpGs were hypermethylated in TRAMP C1 cells (Figure 4-10, 96.8% methylated). Treatment of cells with 2.5 μM or 5 μM of DIM for 5 days, significantly decreased the methylation status of these 5 CpGs on the Nrf2 promoter

region in a dose-dependent manner (Figure 4-10, 73.7% and 55.8% methylation, respectively, Fisher's exact test, $p<0.001$).

MeDIP/ChIP analysis has been commonly used to enrich the methylated CpG DNA in an unbiased manner (150). Anti-mecyt antibody which binds specifically to the methylated cytosine (MC) was used to immunoprecipitate (IP) the genomic DNA harvested from control and DIM-treated TRAMP C1 cells. The IP DNA was purified and used for PCR to amplify the Nrf2 promoter region containing the first 5 CpGs. MeDIP results showed that DIM reduced the methylated DNA bound by anti-mecyt antibody to the first 5 CpGs of Nrf2 gene promoter (Figure 4-9).

4.3.8 DIM induced anti-oxidative stress genes Nrf2 and Nrf2-target genes and proteins expression in TRAMP C1 cells

DIM enhanced the mRNA expression of Nrf2 and Nrf2-targert genes NQO1 and GSTm1 in TRAMP C1 cells (Figure 4-11), which was originally derived from TRAMP prostate tumor (141). In agreement with the results of mRNA expressions, Nrf2 and Nrf2-target gene, NQO1, protein levels were significantly induced in TRAMP C1 cells treated with DIM (Figure 4-12). These results suggest that DIM is able to modify the epigenetic status of CpG methylation of Nrf2, and restores Nrf2 and Nrf2 target genes mRNA and proteins expression in TRAMP C1 cells in vitro, which substantiate the in vivo results in TRAMP prostate tissues.

4.3.9 DIM suppressed DNA methyltransferases (DNMTs) genes and proteins expression in TRAMP C1 cells

The *in vivo* results from the TRAMP mice and *in vitro* results from TRAMPC1 cells above clearly show that DIM supplementation in the diet and cell treatment reduced the methylation status on the Nrf2 gene promoter region and decreased global CpG methylation. To elucidate the potential molecular epigenetic mechanism by which DIM exerts its DNA hypomethylation effect, the effect of DM on DNMTs and HDACs expression was examined. Figure 4-13 shows the effect of DIM on the mRNA expression of DNMT1, DNMT3a, and DNMT3b quantitated by qPCR in TRAMP C1 cells. DIM significantly suppressed the mRNA expression of DNMT1 at both 5 μM and 10 μM concentrations ($p<0.05$) whereas DNMT3a was suppressed by DIM at 5 μM concentration more significantly ($p<0.05$). As the data shown in the gene expression of DNMT1, 3a and 3b (Figure 4-13), the western blotting results also show that DIM possesses the ability to suppress the proteins level of DNMT1, 3b as well as HDAC2 and HDAC3 in TRAMP C1 cells (Figure 4-14).

4.4 Discussion

DIM is a metabolically active product of I3C found abundantly in our dietary cruciferous vegetables. It has been shown in many *in vitro* and *in vivo* anti-cancer models that it is a potent of anti-cancer chemopreventive agent and currently there are more than ten clinical oncological trials in human prostate, breast and cervical cancers. DIM appears to elicit anti-inflammatory, anti-oxidative stress, cell-cycle regulation and induction of apoptosis resulting in its anti-cancer effect (124, 135, 140, 154-156). Accumulating

evidence suggest that aberrant DNA methylation in the promoter regions of tumor suppressor genes plays a critical role in cancer development and progression (67) and that several naturally occurring anti-cancer phytochemicals have been shown to possess the ability to prevent cancer via epigenetic modifications (145, 146, 157). However, no study has been reported so far on the potential epigenetic modifications of DIM and the anti-cancer efficacy of DIM in a transgenic prostate cancer mouse model such as TRAMP mice remains unknown.

Our present study shows that TRAMP mice fed with DIM-supplemented diet had lower percentage of palpable tumor and incidence of lymph node metastasis as compared to the control diet (5.8% v.s. 31.6% for palpable tumor in treated v.s. control and 0% v.s. 26.3% for lymph node metastasis in treated v.s. control) (Table 4-3). The GU weights were significantly lower in DIM treated groups as compared to the control (Figure 4-2). IHC analysis of the prostatic sections show DIM-fed mice had lower percentage of PCNA (cell proliferation marker) (Figure 4-4) and higher percentage of apoptotic cells (Figure 4-5), in agreement with previous reports (135, 156). These results show that DIM is an effective prostate cancer chemopreventive agent that blocks the development and progression of prostate cancer in TRAMP mice.

Nrf2 is a redox sensitive transcriptional factor and plays a very important role in the cellular defense against oxidative and inflammatory stresses (128). Our previous studies show that as prostatic tumor progresses in TRAMP mice, there is a decrease in the expression of Nrf2 and Nrf2 downstream target anti-oxidative stress genes (126, 158). When TRAMP mice were supplemented with (γ)-tocopherol-enriched mixed tocopherol

(gTmT) or I3C in the diets, Nrf2 and Nrf2-mediated anti-oxidative stress phase II detoxifying/antioxidant enzymes were induced (126, 140, 158). I3C and DIM have been shown to be potent inducers of Nrf2-mediated anti-oxidant enzymes in TRAMP C1 cells and human hepatoma HepG2C8 cells (140, 159). In the current study, DIM enhances the expression of Nrf2 and Nrf2-target gene NQO1 proteins in TRAMP prostate tissues in vivo as compared to the controls which was undetectable (Figure 4-6).

To investigate the anti-cancer chemopreventive effect of DIM in different stages of prostate tumorigenesis, DIM was supplemented in the diet to TRAMP mice starting at 8 weeks of age (D-G1), when the LG-PIN starting to form, and 12 weeks of age (D-G2) when some of the LG-PINs progress into HG-PINs (132, 160). Interestingly, both D-G1 and D-G2 showed significantly lower percentage of genome-wide 5-MC IHC staining significantly in the IHC analysis (Figure 4-7), suggesting DIM may impact on the global CpG methylation epigenomic profiles. Focusing on specific gene, from the BGS results, DIM substantially reduced the methylation status of the first 5 CpGs of the Nrf2 promoter region (Figure 4B). The results of 5-MC (Figure 4-7) and BGS (Figure 4-8) suggests that DIM possesses the ability to reduce the methylation status of the first 5 CpGs on the Nrf2 gene promoter region may lead to increase or re-expression of Nrf2 and Nrf2-target gene NQO1 proteins *in vivo* as shown in Figure 4-6. In addition, administration of DIM at the early stage of tumorigenesis starting a 8 weeks old when low grade PIN lesions started to form achieve better anti-cancer chemopreventive effect than given later at 12 weeks old when some of the LG-PINs have progressed to HG-PINs.

To better understand the underlying in vivo epigenetic mechanisms of DIM, *in vitro* study utilized TRAMP C1 cells was conducted. Consistent with the *in vivo* BGS results, *in vitro* BGS showed that DIM reduced the methylation status of the first 5 CpGs on the Nrf2 promoter region in TRAMP C1 cells (Figure 4-10). In agreement with the BGS results, MeDIP/ChIP assay also showed that DIM reversed the CpG methylated DNA on the Nrf2 gene promoter region in TRAMP C1 cells (Figure 4-9). The demethylation of Nrf2 gene was found to be associated with the enhanced expression of Nrf2 and Nrf2-target genes (Figure 4-11) as well as proteins level (Figure 4-12). We also found that the demethylation effect of DIM is correlated with its ability to suppress the expression of DNMTs and HDACs (Figure 4-13 & 4-14). DNMT1 is one of the key maintenance DNA methyltransferases (DNMT) and the most abundance DNMT in mammalian cells (85). In human cancer cells, DNMT1 is responsible for both *de novo* and maintenance of methylation of tumor suppressor genes (161-163). Interestingly, our previous studies show that other DNA de-methylation agents curcumin and 5-aza+TSA could also decrease CpG methylation of the first 5 CpGs of the promoter of Nrf2 gene and enhanced the expression of Nrf2 and Nrf2-target genes in TRAMP C1 cells (141, 145), potentially suggest this may be a common epigenetic modification mechanism.

4.5 Summary

DIM is a multi-targeting anti-cancer chemopreventive agent as reported previously (124, 135, 140, 154-156). Among the molecular targets, DIM has been shown to strongly activate Nrf2 and induces Nrf2-mediated downstream target genes (159). Furthermore, the ability of DIM in restoring the expression of Nrf2 and its downstream genes via

epigenetic mechanism may play an important role in preventing the development and progression of prostate tumor in TRAMP mice in vivo. Since clinically, advanced and metastasized cancers in human are resistant to radiation and chemotherapy (143), and epigenetic changes arise earlier than genetic defects during prostatic carcinogenesis (138), the potential clinical use of DIM to prevent, block or delay the progression of benign tumors from becoming advanced/metastasized cancers through epigenetic modifications may be possible. In the aggregate, our results suggest that DIM as a cancer epigenetic modifying agent may contribute to the future clinical development of DIM as a cancer epigenetic modifying chemopreventive and therapeutic drug.

Table 4-1. Confirmation of genotype of the TRAMP mice

Gene	Primers
Tcrd Forward	5’- CAA ATG TTG CTT GTC TGG TG-3’
Tcrd Reverse	5’- GTC AGT CGA GTG CAC AGT TT-3’
SV1	5’- GGA CAA ACC ACA ACT ATG CAG TG-3’
SV5	5’- CAG AGC AGA ATT GTG GAG TGG-3’

Table 4-2. Murine Primers for Quantitative Real-Time PCR

Gene	Forward	Reverse
β-actin	5’-CGT TCA ATA CCC CAG CCA TG-3’	5’- GAC CCC GTC ACC AGA GTC C -3’
DNMT1	5’-CCA AGC TCC GGA CCC TGG ATG TGT-3’	5’-CGA GGC CGG TAG TAG TCA CAG TAG-3’
DNMT3a	5’-GCA CCT ATG GGC TGC TGC GAA GAC G-3’	5’-CTG CCT CCA ATC ACC AGG TCG AAT G-3’
DNMT3b	5’-GTC TGC ACA CCA GAG ACC AGA G-3’	5’-TCA GAG CCA TTC CCA TCA TCT AC-3’
Nrf2	5’-AGC AGG ACA TGG AGC AAG TT-3’	5’-TTC TTT TTC CAG CGA GGA GA-3’
NQO1	5’-AGC CCA GAT ATT GTG GCC G-3’	5’-CCT TTC AGA ATG GCT GGC AC-3’
HO-1	5’-CCC ACC AAG TTC AAA CAG CTC-3’	5’-AGG AAG GGG GTC TTA GCC TC-3’
GSTm1	5’-TTG TTC TGC CCA CGT TTC TCT AGT-3’	5’-TCT CAA ACT GGA TTC AGC AGG ACT-3’
UGT1a1	5’-GAA ATT GCT GAG GCT TTG GGC AGA-3’	5’-ATG GGA GCC AGA GTG TGT GAT GAA-3’

Table 4-3. DIM inhibit palpable tumor and metastasis in TRAMP males

	Number of animals	Incidence of palpable tumor	Incidence of lymph nodes metastasis
Control	19	6/19 [a]	5/19 [b]
DIM_8wk (D-G1)	9	1/9[a,]	0/9[b, #]
DIM_12wk (D-G2)	8	0/8[a, *]	0 /8[b, #]

[a] Numbers represent the presence of palpable tumor showed at the end of the experiment at 24 weeks of age. Fisher's exact test was used to compare the incidence of palpable tumor between the control and the DIM treated mice sacrificed at 24 weeks of age. *p* values <0.05 were considered as significant, indicated by *.

[b] Numbers represent the presence of lymph nodes metastasis showed at the end of experiment when the mice were sacrificed. Fisher's exact test was used to compare the incidence of lymph node metastasis between the control and the DIM treated mice sacrificed at 24 weeks of age. *p* values <0.05 were considered as significant, indicated by #.

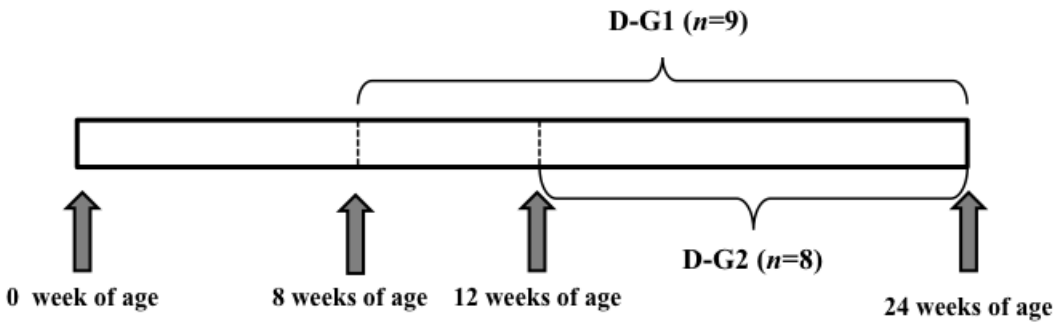

Figure 4-1 Time line, DIM supplemented diet in TRAMP mice.

D-G1= eight weeks of age TRAMP males were put on AIN-76A diet supplemented with 1% DIM and were sacrificed at 24 weeks of age; D-G2= 12 weeks old TRAMP males were put on AIN-76A with 1% DIM and were sacrificed at 24 weeks of age.

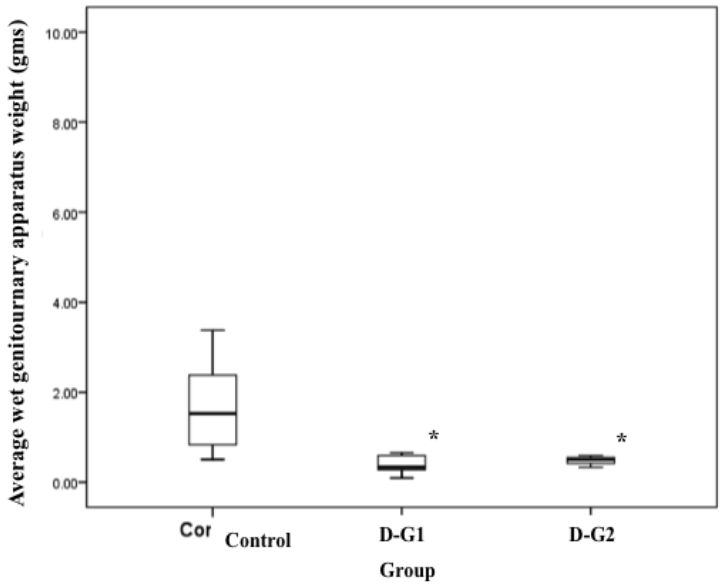

Figure 4-2 Effects of DIM on the genitourinary apparatus weights.

Effects of DIM on the genitourinary apparatus weights of animals treated from 8 weeks old and 12 weeks old. *Asterisk***.** Significantly different from the control (p<0.05) based on Mann-Whitney Test.

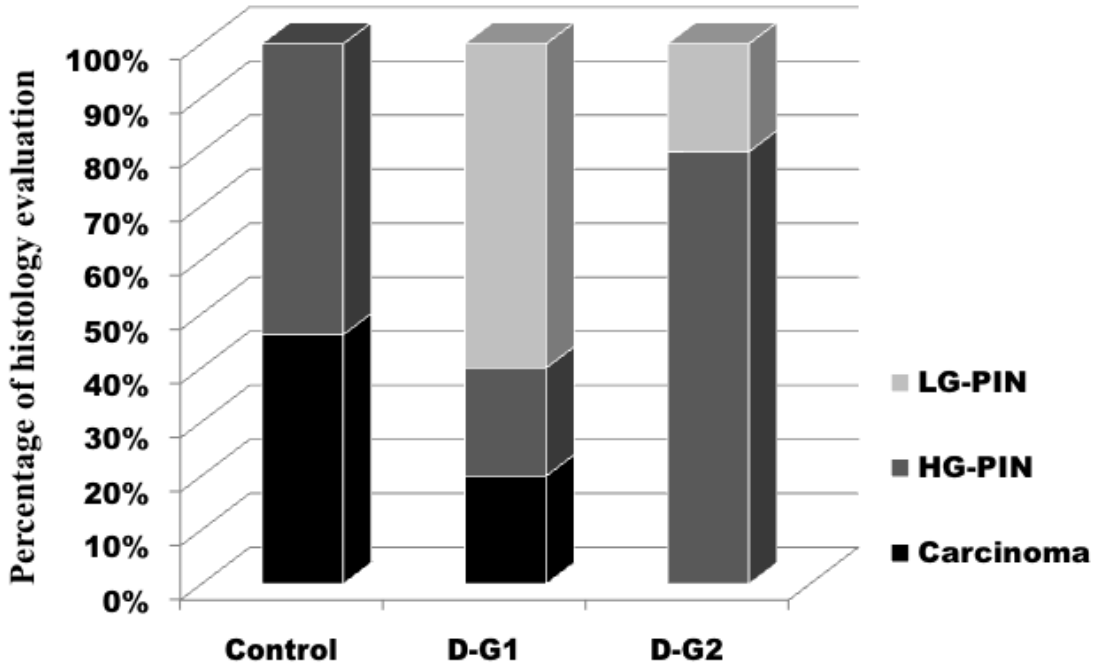

Figure 4-3 Histological evaluation of the incidence of PIN and carcinoma.

Control group, carcinoma:HG-PIN= 46%:54%; D-G1 group, carcinoma:HG-PIN:LG-PIN= 20%:20%:60%; D-G2 group, HG-PIN:LG-PIN= 80%:20%. (Please refer to Table 4-3 for further detail.)

Immunohistochemical staining of cell proliferation marker, PCNA.

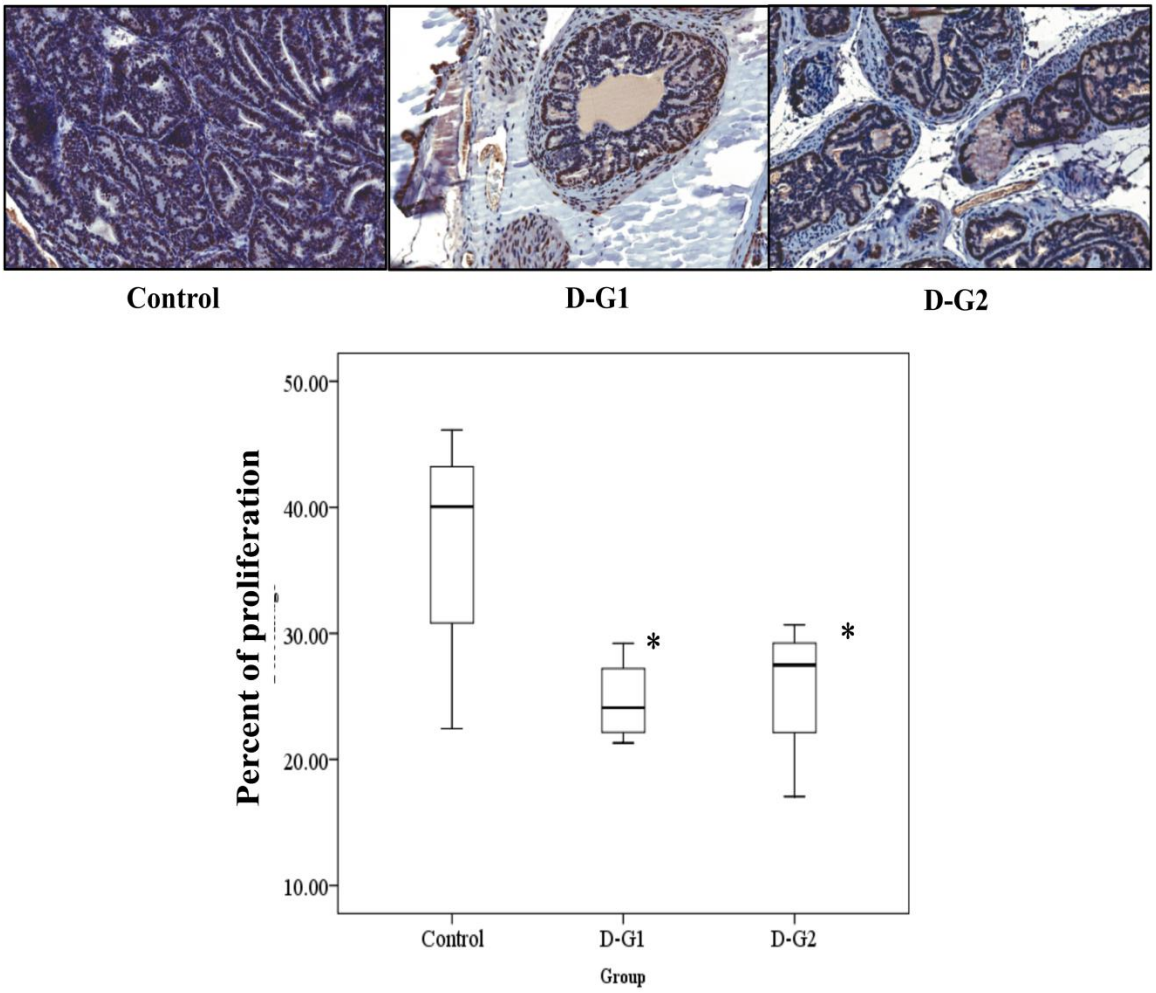

Figure 4-4 Immunohistochemical analysis of the effects of cell proliferation, PCNA.

Effects of DIM supplemented diet on TRAMP males. Representative photomicrographs (×40 magnification) of PCNA stained TRAMP prostate tissue section and percentage levels of cell proliferation. *Asterisk* Significantly different from the control (p<0.05) was based on Mann-Whitney Test.

Immunohistochemical staining of apoptotic marker, TUNEL.

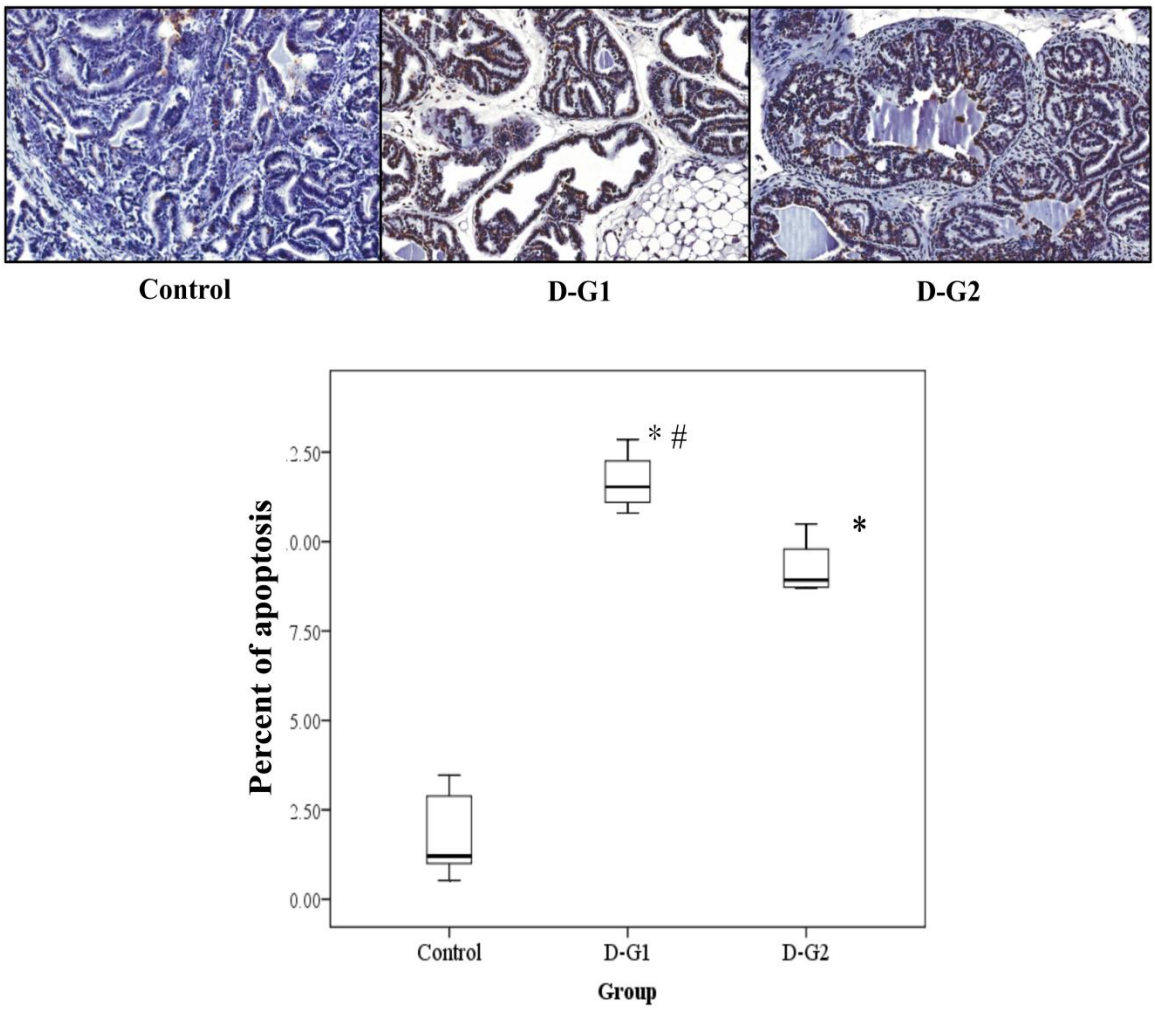

Figure 4-5 Immunohistochemical analysis of the effects of apoptosis, TUNEL.

The effects of DIM supplemented diet on TRAMP males.Representative photomicrographs (×40 magnification) of TUNEL stained TRAMP prostate tissue section and percentage levels of apoptosis. *Asterisk* Significantly different from the control (p<0.05) by Mann-Whitney Test. *Pound sign* Significantly different between D-G1 and D-G2.

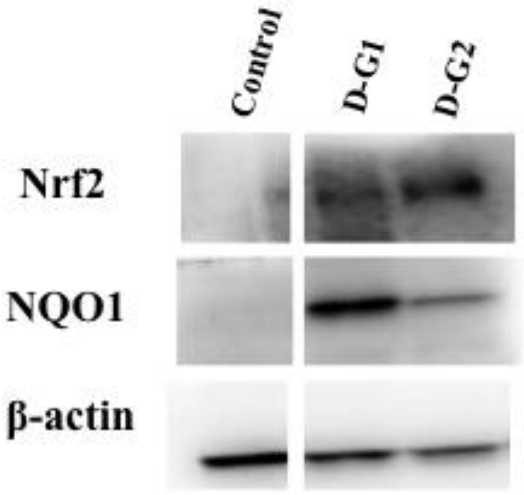

Figure 4-6 Western blots of biomarkers for Nrf2 and Nrf2-regulated NQO1.

Nrf2 and NQO1 were re-activated by DIM in D-G1 and D-G2 significantly different from the control. There was no expression of Nrf2 and NQO1 found in the control animals obviously.

Immunohistochemical staining of methylation maker, 5-methylcytosine

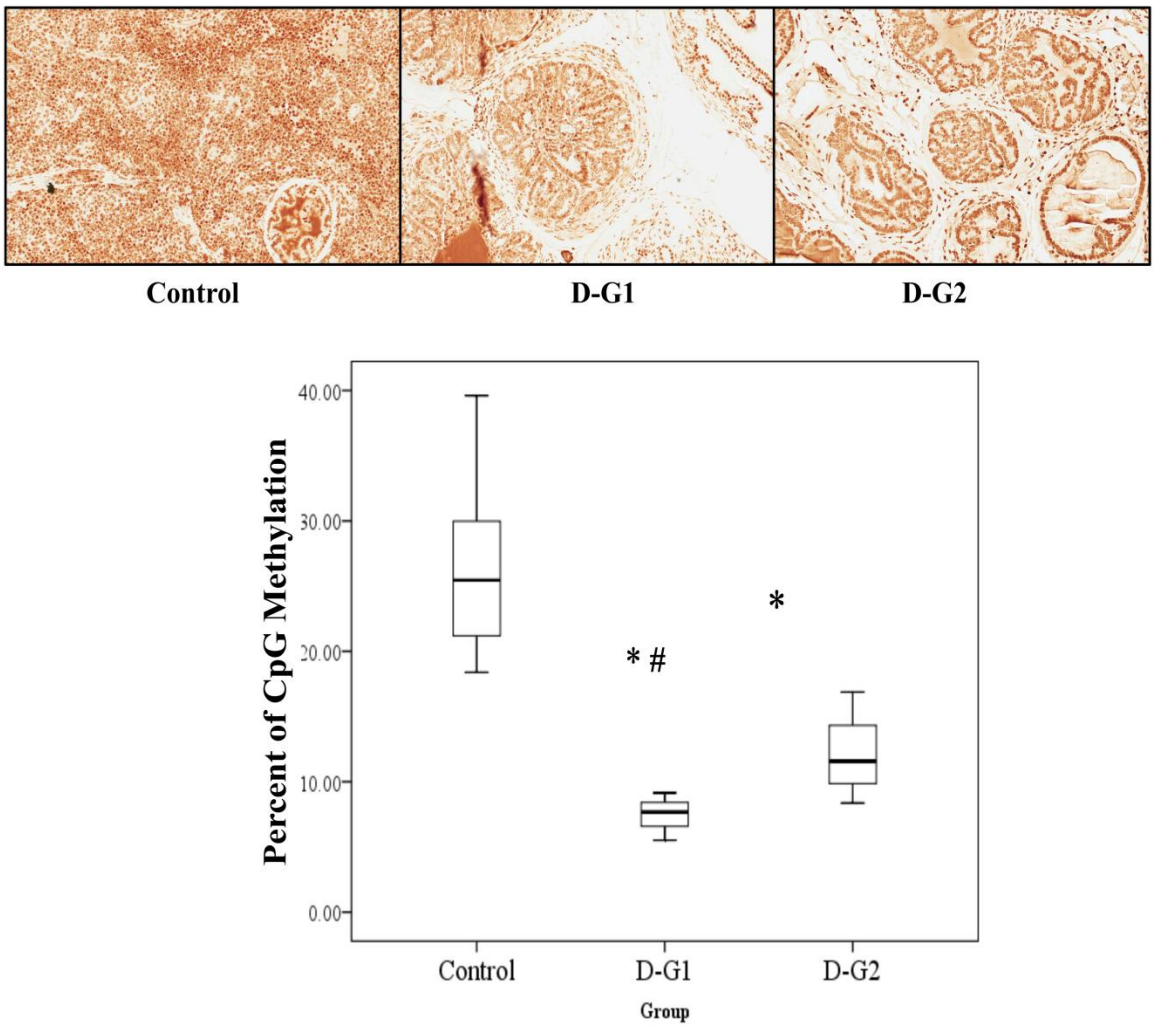

Figure 4-7 Immunohistochemical analysis on the methylation marker, 5-methylcytosin. De-methylation effects of DIM supplemented diet on TRAMP mice. Representative photomicrographs (×40 magnification) of 5-MC stained TRAMP prostate tissue section and percentage levels of methylation. *Asterisk* Significantly different from the control (p<0.05) by Mann-Whitney Test. *Pound sign* Significantly different between D-G1 and D-G2.

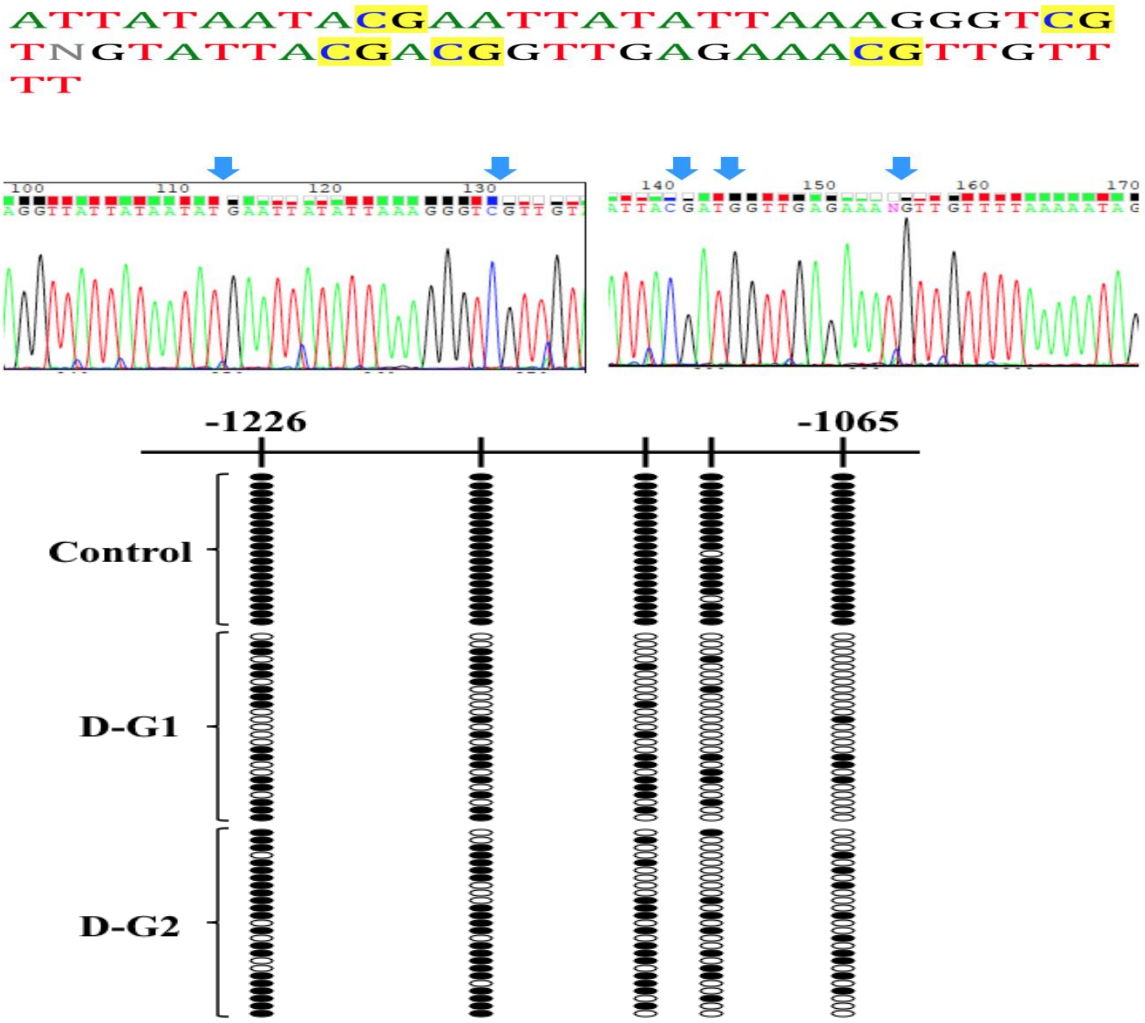

Figure 4-8 The methylation patterns of the first 5 CpGs of promoter Nrf2 gene in TRAMP prostate tissues and tumors was performed using bisulfit genomic sequencing (BGS) as described in the materials and methods section. Black dots indicate methylated CpGs and open circle indicate un-methylated CpGs. The 5 CpGs were hypermethylated in control group (98% methylation) and either D-G1 or D-G2 was found significantly to reduce the methylation of the 5 CpGs (37.6%, 54.4%, respectively, Fisher's exact test $p<0.001$). Moreover, compared with two treated groups, it was found that D-G1 was significantly lower methylation than D-G2 (Fisher's exact test $p=0.011$).

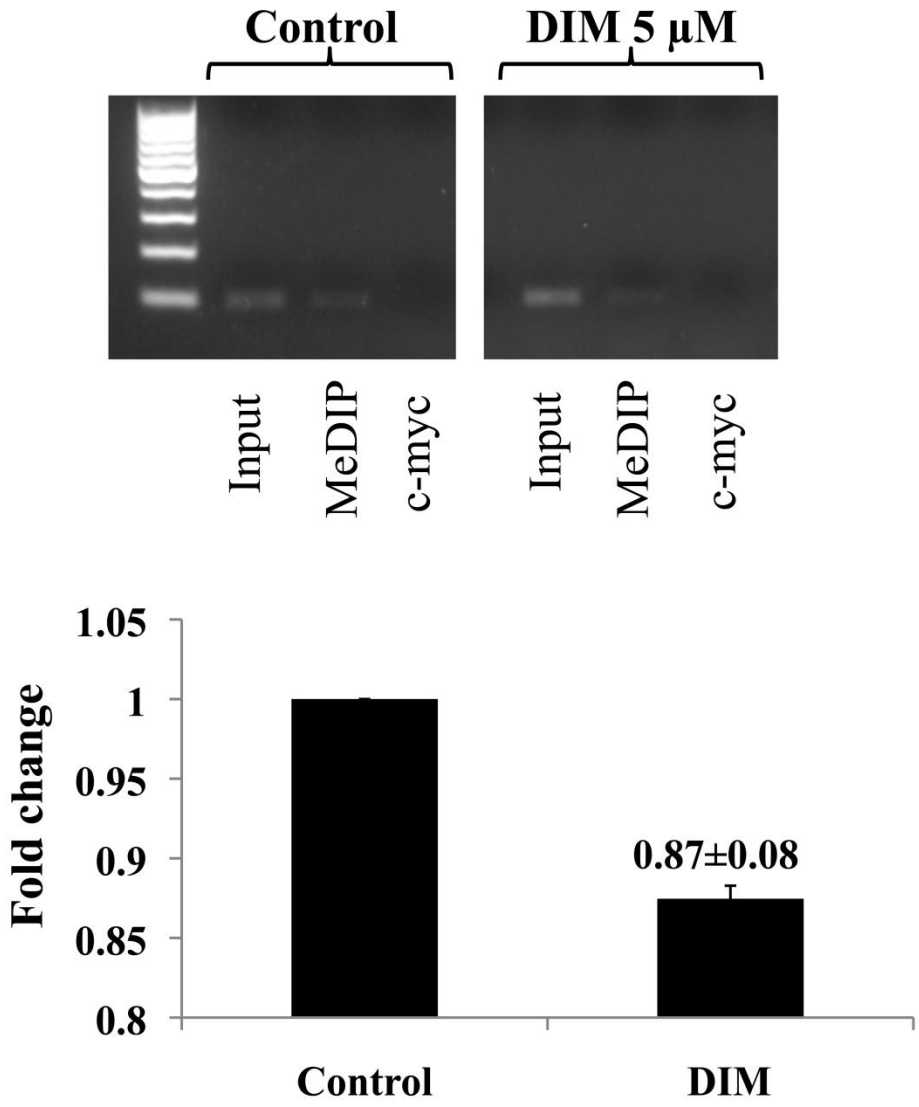

Figure 4-9 De-methylation effects of DIM treated on TRAMP C1 cells.

Methylation DNA immunoprecipation (MeDIP) analysis was performed as described in the materials and methods section. Semi-quantative PCR was performed to compare the immunoprecipatated DNA with their inputs and negative control (c-myc) (Top); the bands (MeDIP) were visualized and quantified using Gel Documentation 2000 system (Bio-Rad, Hercules, CA). Bars represent mean fold change ± SD (normalized with inputs and compared to control value) (Bottom).

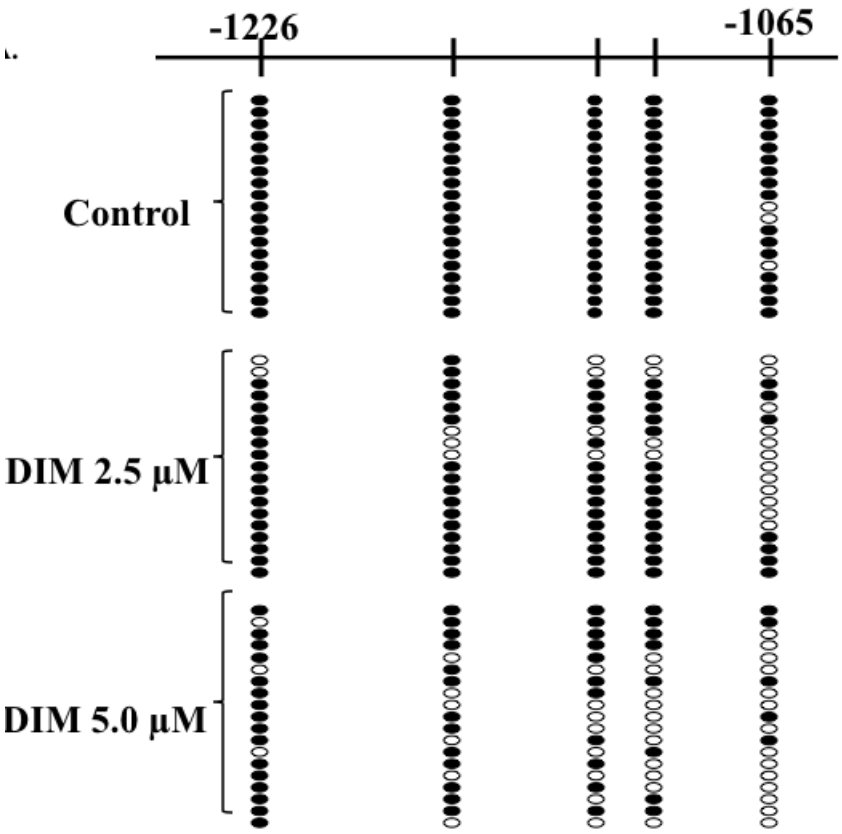

Figure 4-10 The methylation patterns of the first 5 CpGs of promoter Nrf2 gene in TRAMP C1 cells.

De-methylation effects of DIM treated on TRAMP C1 cells was performed using bisulfit genomic sequencing (BGS) as described in the materials and methods section. Black dots indicate methylated CpGs and open circle indicate un-methylated CpGs. The 5 CpGs were hypermethylated in TRAMP C1 cells which were untreated control (96.8% methylated). Cells treated with either 2.5 μM or 5 μM of DIM for 5 days, the methylation status of these 5 CpGs was reversed significantly (73.7% and 55.8% methylation, respectively, Fisher's exact test, $p<0.001$). Methylation status of TRAMP C1 cells treated with DIM 5 μM was significantly lower than DIM 2.5 μM (Fisher's exact test, $p=0.015$).

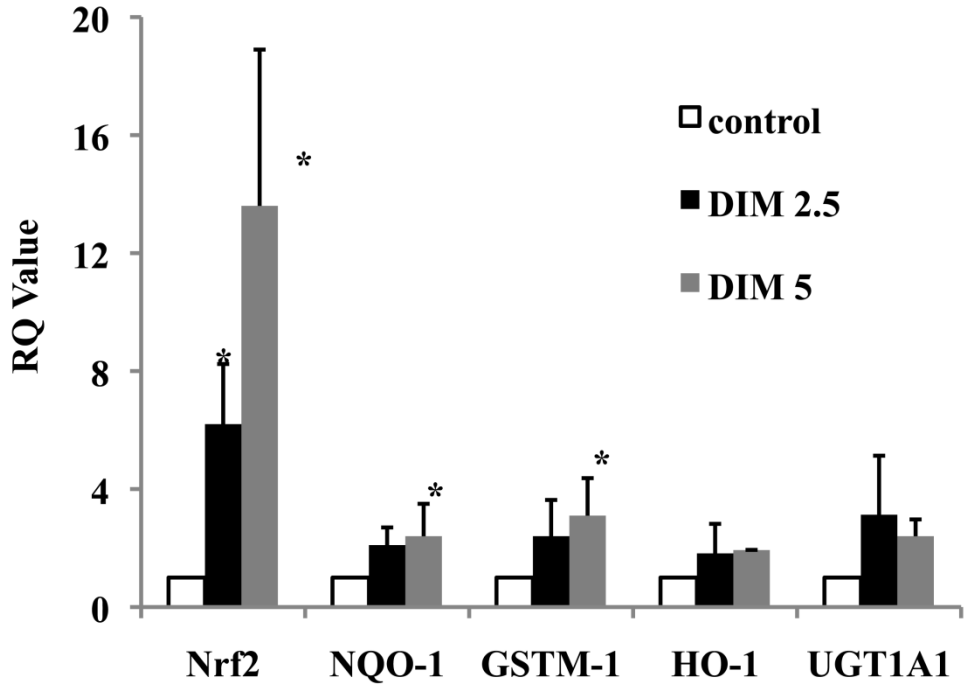

Figure 4-11 The mRNA expression levels of Nrf2 and Nrf2-mediated genes

Nrf2 and Nrf2-mediated genes were restored by DIM. *Asterisk* Significantly different from the control (p<0.05) by student's t-test.

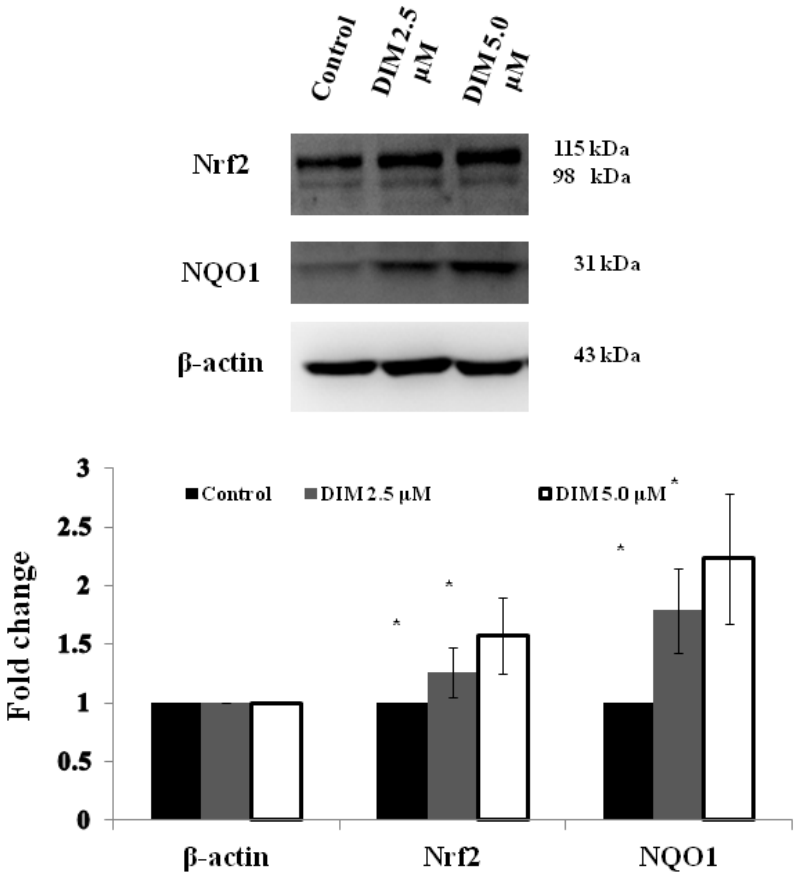

Figure 4-12 Nrf2 and Nrf2-mediated proteins were restored by DIM.

Western blots of Nrf2 and NQO1 expression in TRAMP C1 cells. *Asterisk* Significantly different from the control ($p<0.05$) by student's *t*-test.

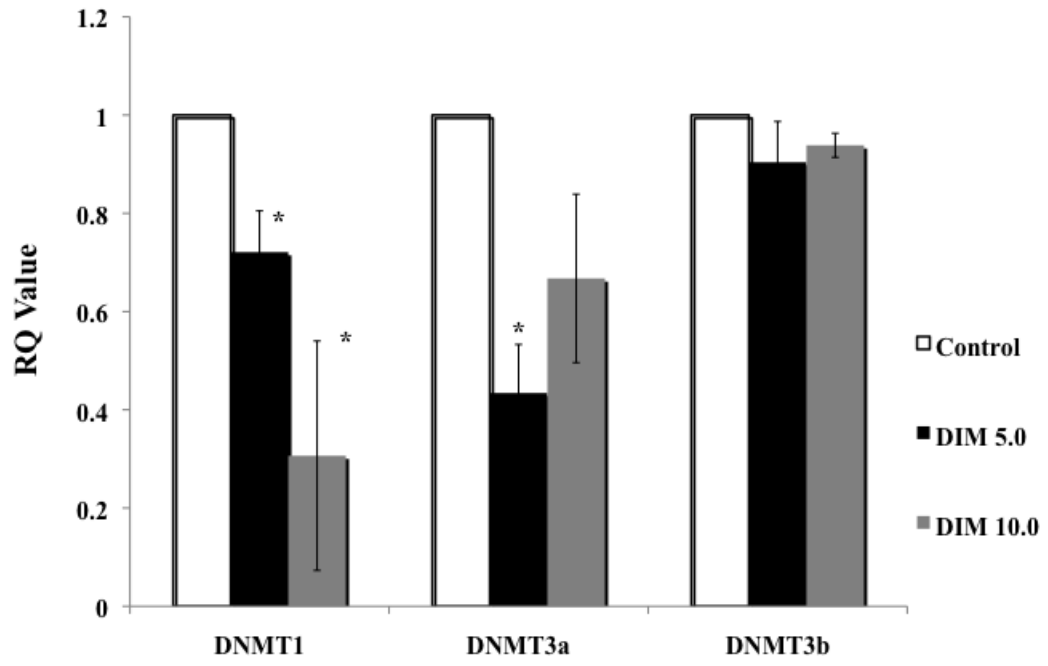

Figure 4-13 The mRNA expression levels of DNMT1, DNMT3a and DNMT3b were suppressed by DIM in TRAMP C1 cells

Asterisk Significantly different from the control ($p<0.05$) by student's *t*-test. DIM inhibited DNMT1 mRNA expression significantly by both 5 μM and 10 μM ($p<0.05$). DNMT3a was also suppressed by DIM treatments and significantly in 5 μM group ($p<0.05$). DNMT3b was also suppressed by DIM but there is no significant different.

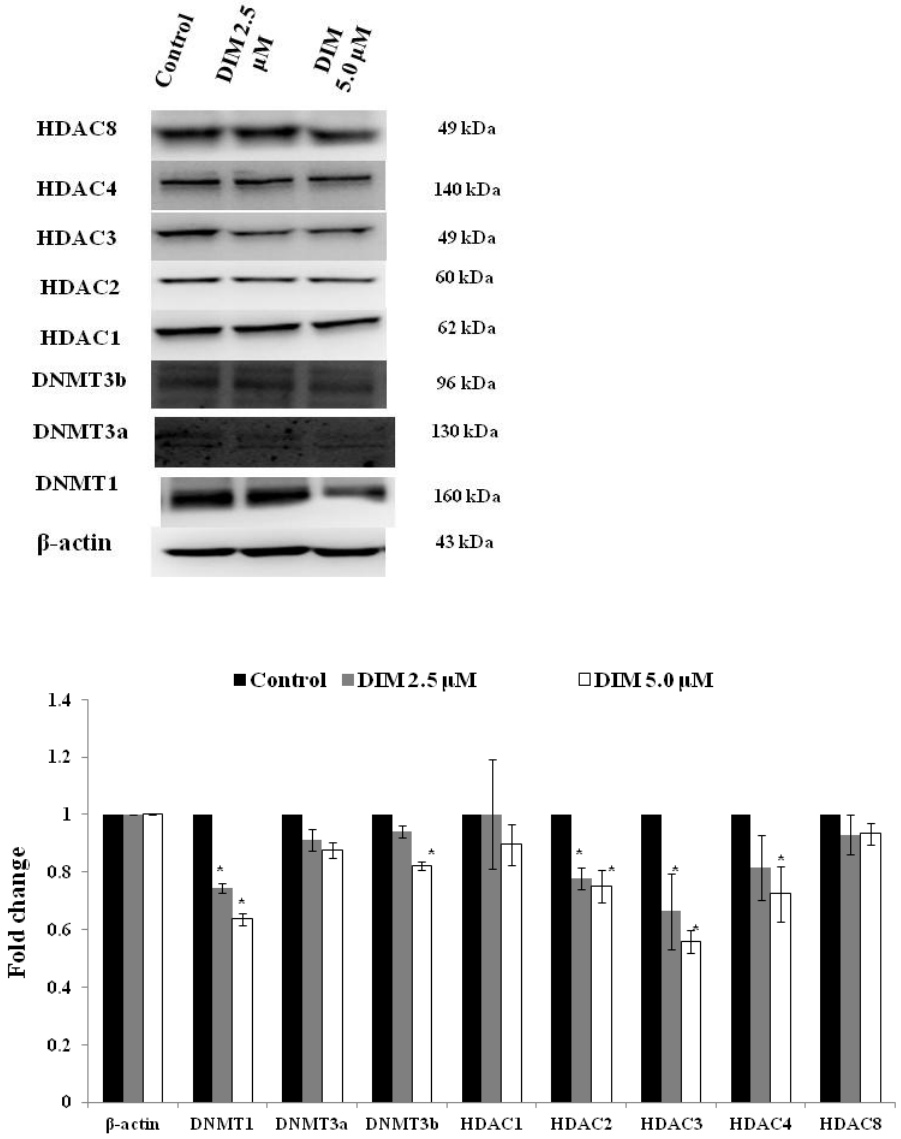

Figure 4-14 DIM suppressed DNMTs and HDACs in TRAMP C1 cells.

Western blots of the DNMTs and HDACs proteins level in TRAMP C1 cells treated with DIM. *Asterisk* Significantly different from the control ($p<0.05$) by student's *t*-test.

CHAPTER 5 Linking the Pharmacokinetics and Pharmacodynamics of Nrf2-related Genes in Rat Lymphocytes Using 3,3'-diindolylmethane [13,14,15]

5.1. Introduction

Indole-3-carbinol (I3C) and its condensation by-product, 3,3'-diindolylmethane (DIM, structures show in Figure 3-1), found abundantly in cruciferous vegetables such as broccoli, bok choy, cauliflower, cabbage and cress, have been reported to be a potent anti-cancer and cancer chemoprevention agent. Both I3C and DIM supplementation have been investigated in clinical trials for human papilloma virus related diseases such as cervical cancer and respiratory pappillomatosis as well as breast cancer and vulvar intraepithelial neoplasia (123). In addition, another study demonstrated that I3C and DIM protected human breast and prostate cancer cells against cell killing by oxidative stress induced by hydrogen peroxide (H_2O_2). In the same study, both I3C and DIM were found to induce NAD(P)H quinine oxidoreductase 1 (NQO-1) luciferase response (124).

---

[13] Work described in this chapter has been submitted to an international journal.

[14] **Key words**: pharmacokinetic-pharmacodynamic (PK-PD); 3,3'-diindolylmethane (DIM); Nrf2; lymphocyte

[15] **Abbreviations**: ARE, antioxidant response element; ACN, acetonitrile; DIM, 3,3'-diindolylmethane; DM, drug metabolizing; GST, glutathione S-transferases; HD, high dose; HPLC, high performance liquid chromatography; I3C, indole-3-carbinol; JVC, jugular vein cannulae; LD, low dose; MPA, mobile phase A; MPB, mobile phase B; NAT, *N*-acetyltransferases; NQO, NAD(P)H quinine oxidoreductase; Nrf2, nuclear factor (erythroid-derived 2)-like 2; PD, pharmacodynamic; PK, pharmacokinetic; QC, quality control; SD, Sprague-Dawley; SULT, sulfotransferases; UGT, UDP-glucuronosyl-transferases

It is believed that one of the underlying mechanisms behind the chemopreventive activities of phytochemicals such as I3C and DIM is induction of detoxifying enzymes. Phase II drug metabolism (DM) enzymes primarily catalyze conjugation reactions to facilitate the excretion and elimination of their substrates, which can be cytotoxic agents or carcinogens (6). The phase II DMEs include sulfotransferases (SULT), UDP-glucuronosyltransferases (UGT), NAD(P)H quinone oxidoreductase (NQO), glutathione S-transferases (GST), and *N*-acetyltransferases (NAT). Compared to the phase I DMEs, the phase II DMEs are more prone to have protective effects against carcinogens and to prevent carcinogenesis. Reactive metabolites are detoxified by phase II DMEs via conjugation leading to increase hydrophilicity and thus facilitate the excretion into the bile or urine (6, 7).

The protective effects of phase II DMEs can be induced through the exposure of xenobiotics. One major class of the inducers of phase II DMEs are the electrophiles capable of enhancing the binding of a transcription factor, nuclear factor (erythroid-derived 2)-like 2 (Nrf2), to the antioxidant response element (ARE) in the promoter region of many phase II DME genes in the action of cell protection and cancer chemoprevention. Nrf2 plays an important role to mediate phase II detoxifying/ antioxidant enzymes expression. Under normal conditions, Nrf2 appears to be associated with actin-binding Keap 1 that forms Nrf2-Keap1 complex preventing Nrf2 from entering into the nuclear and promoting its proteasomal degradation. Typically, the half-life of Nrf2 in un-stimulated mammalian cells is 15-45 min. Upon treatments of the cells with oxidants such as H_2O_2, oxidative stress or cancer chemopreventive compounds,

conformational changes occur due to oxidation of thiol sensitive amino acids present in the Nrf2-Keap 1 complex and would drive the dissociation of Nrf2 from Keap 1, thereby allowing the translocation of Nrf2 into the nucleus, Nrf2 binds to ARE of ARE-target genes and leads to enhanced phase II detoxifying/ antioxidant enzymes expression (76, 77). Modulation of the phase II DME genes by phytochemicals can enhance elimination of reactive species and is beneficial in chemoprevention.

Several preclinical and clinical studies have been conducted with DIM on the drug metabolism, bioavailability, and pharmacokinetics by oral administration. We have previously reported the *in vivo* and *in vitro* studies of DIM on the phase II gene expression in different models (140). However, no study has involved the simultaneous study of the pharmacokinetics (PK) and pharmacodynamics (PD) of DIM, especially in the lymphocytes. In additional, there is no report linking plasma concentration of DIM and lymphocyte phase II gene expression which can be a potentially cancer prevention biomarker for clinical studies for phytochemicals and other cancer chemopreventive agents. In this study, we report the PK profiles in rat plasma and the PD profiles of phase II DM/ antioxidant gene expression in rat lymphocytes following intravenous (i.v.) administration of 10 mg/kg and 20 mg/kg of DIM.

5.2. Material and Methods

5.2.1 Chemicals and supplies

3,3’-diindolylmethane (DIM), 4-methoxyindole (99%, IS, internal standard), ethanol (99%), diisopropyl ether (98%), ammonium acetate (99%, HPLC/LC-MS grade),

formic acid (98%, UPLC/LC-MS grade) were purchased from Sigma-Aldrich (St. Louis, MO). Acetonitrile (ACN) and pure water (HPLC/GC/MS grade) were purchased from Honeywell Burdick & Jackson (Muskegon, MI). De-ionized water was obtained from a MiliQ system (Milipore, Bedford, MA). Heparin Sodium Injection, USP (1000U/mL) and Sodium Chloride Injection, USP (0.9%) were obtained from Baxter Healthcare Corporation (Deerfield, IL) and Hospira Inc. (Lake Forest, IL), respectively. Ficoll-Paque^{TM} PREMIUM 1.084 was purchased from GE Healthcare (Piscataway, NJ).

5.2.2 Experiment design of animal study

Male Sprague-Dawley (SD) rats with jugular vein cannulae (JVC) and weighing 250-300 g were purchased from Hilltop Laboratories (Scottsdale, PA). The animals were maintained in the Laboratory Animal Service facility at Rutgers University. Housing and care of the animals was performed in accordance with the guidelines established by the University's Animal Research Committee consistent with the NIH Guidelines for the Care and Use of Laboratory Animals. SD rats were allowed free access to food and water during a three day acclimatization period (12-hour dark-light cycles) after which they were fed AIN-76A diets (Research Diets Inc., New Brunswick, NJ) free of antioxidant and acclimatized to the laboratory conditions to commencing the studies. On the day of study, the cannulae was exteriorized and connected to polyethylene tubes (Instech Laboratories, PA). Heparinized saline (50U/mL) was used to flush the cannulae and tubes. The drug, DIM (suspended in the vehicle) 20 mg/kg, (high dose (HD), total n=8), and 10 mg/kg, (low dose (LD), total n=6) and the vehicle (composition of cremaphor/Tween-80/ PEG 400/ ethanol/ water (2:1:1:1:5) control (total n=5), were

administered via intravenous (i.v.) jugular vein cannulae. Blood samples (0.3mL) were withdrawn at regular time intervals at 0, 5, 10, 15, 30 minutes, and 1, 2, 4, 8, 12, 24, and 48 hour and transferred to heparinized vials, followed by replacement with an equal volume of saline. All blood samples were immediately centrifuged at 2500 rpm at 4˚C to obtain plasma samples (supernatants) and stored at -80˚C until analysis. Due to the small amount of mononuclear cells in the blood and the limited amount of blood withdrawn at each time point from rats, the blood cell samples (n=2 or 3 from each group) were pooled together at the same time point and added 4X volume of Hank's Balanced Salt Solution (HBSS, Invitrogen, Grand Island, NY). The separation of mononuclear cells was performed using Ficoll-Paque^{TM} PREMIUM 1.084 density gradient medium and following manufacture's instruction. The cell pellets were dissolved in Trizol reagent (Invitrogen, Grand Island, NY) and frozen at -80˚C until analysis. (Figure 1)

5.2.3 Instrumentation and chromatographic conditions

Plasma-drug concentrations analysis was performed using a Thermo Surveyor high performance liquid chromatography (HPLC) system (Thermo Fisher Scientific Inc., San Jose, CA) equipped with a Surveyor quaternary pump with build-in degasser, a Surveyor auto-sampler with cooling system, and a Surveyor PDA detector. The method was validated following the Food and Drug Administraion (FDA)'s Guidance for Industry for Bioanalytical Method Validation. Xcalibur 1.3 software (Thermo Fisher Scientific Inc., San Jose, CA) was used for data acquisition and processing. Chromatographic separations were archived using a Phenomenex Luna C18(2), 3µm 3.0x150 mm column (Phenomenex, Torrance, CA) along with a SecurityGuard column

(Phenomenex, Torrance, CA). The analysis method used an aqueous mobile phase A (MPA) composed of 20 mM formic acid and 20 mM ammonium acetate and an organic mobile phase B (MPB) composed of acetonitrile (ACN). A needle wash solution (3.0 mL) composed of methanol and water (70:30) was used successively between injections to clean injection port. The column oven temperature was set at 40˚C and the autosampler temperature was set to 4˚C. The injection volume was 100 µL. The gradient was set to 60:40 (MPA:MPB) for the first 4 min and gradually changed to 20:80 (MPA:MPB) at 7 min and kept at the same ratio until 17 min and then back to initial equilibration status at 18 min and for two more min at 600 µL/min flow rate. Peak quantification was achieved using PDA data extracted at 270 nm.

5.2.4 Preparation of standard and quality control (QC) samples

Primary stock solutions, DIM (1mg/mL) and IS (0.4mg/mL), were prepared in DMSO and stored at -80˚C. Working solutions were prepared by serial dilution in ACN:Water (50:50 v/v) with concentrations of 20, 10, 5, 2.5, 1.25, 0.625, 0.3125, 0.15625, 0.078, 0.039, 0.0195 µg/mL for the standard curve. Calibration curve samples (20, 10, 5, 2.5, 1.25, 0.625, 0.3125, 0.15625, 0.078, 0.039, 0.0195 µg/mL) and QC samples (20, 2.5, 0.15625 µg/mL) were prepared fresh by spiking 100 µL of plasma in addition to 10 µL of IS (0.08 mg/mL).

5.2.5 Plasma sample extraction procedure

Aliquots of 100 µL of blank plasma, spiked plasma, or pharmacokinetic samples were vortexed for 2 min and allowed to equilibrate 10 min at room temperature. The

plasma samples were extracted by adding 200 µL of extraction solution (diisopropyl ether: ethanol=90:10, v/v) and followed by vortex mixing of samples for 2 min and centrifugation at 10,000 rpm for 2 min at room temperature. The organic layer (supernatant) was removed into a clean microcentrifuge-tube. The extraction procedure was repeated again and the organic layers were combined. The samples were evaporated to dryness under a stream of pure nitrogen (Air Gas Corp., Piscataway, NJ), and reconstituted in 200 µL of ACN:water=50:50 (v/v) and centrifuged at 17,500xg at 18-20 ˚C for 5 min. The supernatant was collected for HPLC analysis. On analysis of pharmacokinetic samples, if DIM concentration was beyond the upper limit of quantification (20 µg/mL), the samples were diluted within the calibration range. The extracted plasma samples compared to the ratios of sample solutions prepared at equivalent concentration resulted in excellent recovery of 97.7±0.98%.

5.2.6 Mononuclear cells mRNA and qRT-PCR for pharmacodynamic measurements

HBSS diluted blood cells were layered carefully on Ficoll-Paque^{TM} PREMIUM 1.084 and centrifuged at 400xg (IEC Model CL centrifuge, International Equipment Co., Needham Heights, MA) for 30 min. at 18-20 ˚C. Mononuclear cells layer was carefully removed and mixed with HBSS. Mix solutions were centrifuged again at 400xg for 15 min. at 18-20 ˚C. Supernatant was removed and fresh HBSS was added to wash the cells again. Trizol reagent (Invitrogen, Grand Island, NY) was added after removing the supernatant and frozen at -80˚C until analysis. Total RNA extracted from mononuclear cells were reversed transcribed. The primers, Nrf2, NQO1, GSTp1, UGT1a1, Keap1 and control GAPDH for qPCR are listed in Table 5-1 (Integrated DNA Technologies,

Coralville, IA, U.S.A.). The qPCR reactions were carried out with 1 µl cDNA product, 50 nM of each primer, and Power SYBR Green master mix (Applied Biosystems, Foster City, CA, U.S.A.) in 10 µl reactions. The reactions were performed using an ABI Prism 7900HT sequence detection system; specificity of amplification was verified by first-derivative melting curve analysis using the ABI software (SDS 2.3, Applied Biosystems, Foster City, CA, U.S.A.). Relative quantification of gene expression profile was calculated using a ΔΔCt method (RQ manager, Applied Biosystems, Foster City, CA, U.S.A.) as we have performed previously (38). The results are presented as mean ±SD.

5.2.7 Pharmacokinetic/Phamrmacodynamic Modeling

The time-course of the DIM plasma concentration was fitted according to the following system of differential equations and the resulting PK profile was input into the PD model below:

$$\frac{dA_c(t)}{dt} = k_{pc} \cdot A_p - (k_{cp} + k_{10}) \cdot A_c; A_c(t = 0) = dose \quad \text{……Eq. 1}$$

$$\frac{dA_p(t)}{dt} = -k_{pc} \cdot A_p + k_{cp} \cdot A_c; A_p(t = 0) = 0 \quad \text{……Eq. 2}$$

where k_{pc}, k_{cp} represent the inter-compartment rate constants between the central (c) and peripheral (p) compartments; k_{10}, elimination rate constant; A_c and A_p, amount of drug at central and peripheral compartments, respectively.

The pharmacodynamic response in this study is presented by Phase II/ antioxidant/ detoxifying genes mRNA expression levels (R) in the mononuclear cells in

the blood and the indirect stimulatory (k_{in}) response model is performed to describe the response-time profile as

$$\frac{dR}{dt} = k_{in} \cdot E(t) - k_{out} \cdot R \ldots\ldots \text{Eq. 3}$$

where the effect function was given by

$$E(t) = 1 + \frac{E_{max} \cdot C_c(t)}{EC_{50} + C_c(t)} \ldots\ldots \text{Eq. 4}$$

for all mRNA in the study. The initial condition is defined as E(0)=1. All pharmacokinetic and pharmacodynamic parameters were estimated by nonlinear regression analysis using the maximum likelihood estimator in GastroPlus™ version 8.0.

5.2.8 Evaluation of Pharmacodynamic parameters and confidence intervals by bootstrap methods

We applied a bootstrap in conjunction with least square methods (164) to calibrate the values estimated by GastroPlus™ version 8.0. This method offers a robust estimation of the parameter values as well as associated confidence intervals as previously demonstrated in the context of indirect response modeling (165).

5.3. Results

5.3.1 Assay validation of pharmacokinetic analysis

5.3.1.1 Specificity and Selectivity. Retention times for IS and DIM were approximately 4.79 and 8.21 min respectively (Figure 5-2). Figure 5-2 shows representative chromatogram of extracted plasma spiked with IS, DIM. Neither endogenous matrix

plasma peaks nor any in vivo metabolites of DIM were found to interfere with any of the compounds evaluated. Furthermore, the chromatograms of the vehicles were equal to of blank plasma.

5.3.1.2 Sensitivity. In this study, 100 μL of plasma was used for extracted, reconstituted to 200 μL, and 100 μL as the HPLC injection volume. The upper limit of quantification was 20 μg/mL and the lower limit of quantification was 20 ng/mL for DIM.

5.3.1.3 Linearity. Plasma calibration curve for DIM was linear over the concentration range of 20 ng/mL- 20 μg/mL. The calibration curve was $y=0.00273359+0.385301x$ and correlation coefficients was 0.9951.

5.3.1.4 Recovery. The comparison of the ratios of DIM/IS obtained from the extracted quality control plasma samples to the ratios of sample solutions prepared at equivalent concentrations results in excellent mean recovery of 97.7±0.98 % for DIM.

5.3.2 Pharmacokinetics of DIM

DIM plasma concentration-time profiles are displayed in Figure 5-3. The two-compartment PK estimated parameters are listed in Table 5-2. The pharmacokinetics parameters appear that the two compartmental PK model fitted well for the plasma concentration versus time of both low dose and high dose administered groups. However, there is not linear correlation of PK parameters between high dose and low dose groups. The software generated two-compartment PK parameters of DIM were then used to fit the DIM PK-PD data.

5.3.3 Pharmacokinetic-Pharmacodynamic correlation

The mRNA expression of the selected phase II antioxidant/ detoxifying genes was quantitated by qRT-PCR. Indirect response model III generated by Jusko was used in this study (166) (Figure 5-4). The pharmacokinetic-pharmacodynamic analysis results were fitted using GastroPlus^{TM} version 8.0. The fold changes of the mRNA expression from lymphocytes versus time for Nrf2, NQO1, GSTP1 and UGT1a1 were shown in Figures 5-5 and 5-6. The profiles show that Nrf2 and its related genes were induced in the lymphocytes by DIM plasma concentrations after DIM administration and then decrease with DIM elimination. The estimated pharmacodynamic parameters are shown in Table 5-3. The EC_{50} values range from 1.305 (HD) and 0.211 (LD) for GSTP1 (most sensitive) to 6.448 (HD) and 0.944 (LD) for UGT1a1 (least sensitive) and E_{max} ranges from 70.245 (HD) and 6.448 (LD) for UGT1a1 to 1210.153 (HD) and 19.602 (LD) for GSTP1. Although the relationships of EC_{50} and E_{max} between HD and LD were not linear, the estimated parameters showed the higher induction in HD than in LD.

5.4 Discussion

DIM is a well-known anti-cancer agents via different mechanisms. Our and other previous studies also showed that DIM possesses the ability to suppress the oxidative stress and to induce the phase II antioxidant/detoxifying enzymes *in vivo* and *in vitro* (124, 140). Different formulations of DIM were administered orally and were shown linear or non-linear pharmacokinetic behaviors in human and mouse model (148, 167, 168). In this study, we administered the 20 mg/kg and 10 mg/kg intravenously in rats and established the PK-PD correlation of DIM-induced phase II DM/antioxidant/detoxifying

gene mRNA expression in rat lymphocytes. The results show that induction of phase II genes (NQO1, GSTP1, UGT1a1) by DIM was changed significantly. However, Nrf2 mRNA expression was not as much as other phase II genes.

In this current study, the PK parameters show different behavior in high dose and low dose. Low dose group can be fitted in the two-compartment simulation linear PK model very well. However, high dose group can not be fitted in the linear PK model but non-linear PK mode. The different PK parameters between high dose and low dose groups are in the distribution phase. This difference may due to the saturation of the transporters, receptors, protein binding or enzymes carrying the drug in and out the organs and cells. The further investigation may need to be done for more clear understandings.

The Nrf2-mediated genes, NQO1, GSTP1, UGT1a1, were selected based on our current understanding of Nrf2 signaling pathway. NQO1, induced by many phytochemicals, subsequently shows the ability to protect against the toxic and carcinogenic effects *in vivo*. Our previous studies showed that DIM induced NQO1 strongly *in vivo* and *in vitro* (124, 140). In our current study, DIM induced NQO1 mRNA expression in rat lymphocytes by about six folds in low dose group and fifteen folds in high dose group after i.v. administration. DIM also increased GSTP1 and UGT1a1 mRNA expression in both high dose group and low dose group. The maximum effect time of these genes were around one to four hours after i.v. injection. The fast response could be potentially achieved via fast-acting transcription factors such as Nrf2, which maximum effect time was 0.5-1 hour. The primary mRNA expression occurr in the

timeframe of hours (169). Although the high dose pharmacokinetic behaviors appeared as non-linear pharmacokinetic model, the mRNA response showed likelihood dose-dependent manner. The 24-hour and 48-hour data were collected, but we did not detect the mRNA expression change in these times.

5.5 Summary

In summary, we conducted pharmacokinetic and pharmacodynamic assessment after i.v. administration of DIM in rats. In this study, the plasma concentrations of DIM and the levels of Nrf2 and its mediated mRNA expression were linked by applying the indirect response models. DIM induced Nrf2 and Nrf2-target phase II genes, NQO1, GSTP1 and UGT1a1, mRNA expression in rat lymphocytes after i.v. administration, suggesting that these mRNA expressions in lymphocytes may be as potential biomarkers. The preclinical study approach presented in this study may provide a framework for future clinical studies in evaluating drug candidates on the PK-PD correlation. Our study may lead to a better understanding of DIM PK-PD modeling and simulation in clinical studies.

Table 5-1. Rat Primers for Quantitative Real-Time PCR

Gene	Forward	Reverse
GAPDH	3’- ACA TGC CGC CTG GAG AAA CCT-5’	3’- GCC CAG GAT GCC CTT TAG TGG-5’
Nrf2	3’- ATG CCT TCC TCT GCT GCC ATT AGT-5’	3’- TCA GTG AAA TGC CGG AGT CAG AGT-5’
NQO1	3’- AGG CTG GTT TGA GAG AGT GCT TGT-5’	3’- ATG CCA CTC TGA ATT GGC CAG AGA-5’
GSTP1	3’- GCT GCC TTG GTG GAT ATG GTG AAT-5’	3’- ACC CAC AAT GAA AGC TTT GCC TCC-5’
UGT1a1	3’- GAA ATT GCT GAG GCT TTG GGCAGA-5’	3’- AAT ACC ATG GGA ACC GGA GTG TGT-5’

Table 5-2A Two-compartment simulation linear model in rat plasma using GastroPlus™.

PK parameter	High Dose (20 mg/kg)			Low Dose (10 mg/kg)		
	Value	Unit	CV%	Value	Unit	CV%
CL	0.503	L/h	7.64	1.085	L/h	7.67
Vc	0.124	L	29.1	0.316	L	22.5
CL2	0.496	L/h	19.11	0.536	L/h	22.78
V2	0.27	L	11.54	0.38	L	16.38
A	37.54	ug/mL		7.381	ug/mL	
B	5.268	ug/mL		0.962	ug/mL	
Alpha	9.075	1/h		5.694	1/h	
Beta	0.821	1/h		0.851	1/h	
K10	4.057	1/h	30.13	3.316	1/h	69.44
Kcp	4.002	1/h	34.85	1.739	1/h	106.79
Kpc	1.837	1/h	22.32	1.496	1/h	96.66
t 1/2	0.844	h	0	0.793	h	0
AUC	10.84	ug-h/mL		2.598	ug-h/mL	
AUMC	8.104	ug-h^2/mL		1.547	ug-h^2/mL	
MRT	0.748	h		0.595	h	
K(z)	0.762	1/h		0.783	1/h	
Vss	0.366	L		0.603	L	

AUC, area under the curve; CL, distribution phase clearance; CL2, elimination phase clearance; Vc, volume of distribution of the central compartment; V2, volume of distribution of the peripheral compartment; A, B, Alpha, Beta are two compartment PK parameters as defined in bi-exponential decline model, $C=Ae^{-\alpha t}+Be^{-\beta t}$; t1/2, terminal half life.

Table 5-2B Two-compartment simulation non-linear model in rat plasma using GastroPlus™.

PK	High Dose 20 mg/kg			Low Dose 10 mg/kg		
parameter	Value	Unit	CV	Value	Unit	CV
Vc	0.129	L	28.75%	0.323	L	36.50%
CL2	0.582	L/h	18.16%	1.398	L/h	133.77%
V2	0.317	L	11.03%	1.392	L	547.90%
Vmax	40.96	mg/h	4.78%	1.51	mg/h	850.95%
Km	70.32	ug/mL	1.43%	0.322	ug/mL	1783.11%

Table 5-3 Pharmacodynamic analysis of phase II genes mRNA expression driven by DIM using Class III Indirect Model for Nrf2, NQO1, GSTP1 and UGT1a1.

	Parameter	Dose	Fitted Value	CV%
NQO1	Emax	10 mg/kg	60.75	0
	EC50	10 mg/kg	0.571	0.01
	Kin	10 mg/kg	0.123	0.027
	Kout	10 mg/kg	0.239	0.041
GSTp1	Emax	10 mg/kg	19.402	0.002
	EC50	10 mg/kg 10 mg/kg	0.184 0.571	0.339
	Kin	10 mg/kg	0.688	0.062
	Kout	10 mg/kg	0.654	0.006
UGT1a1	Emax	10 mg/kg	6.314	0.005
	EC50	10 mg/kg	0.784	0.022
	Kin	10 mg/kg	2.112	0.017
	Kout	10 mg/kg	1.512	0.014

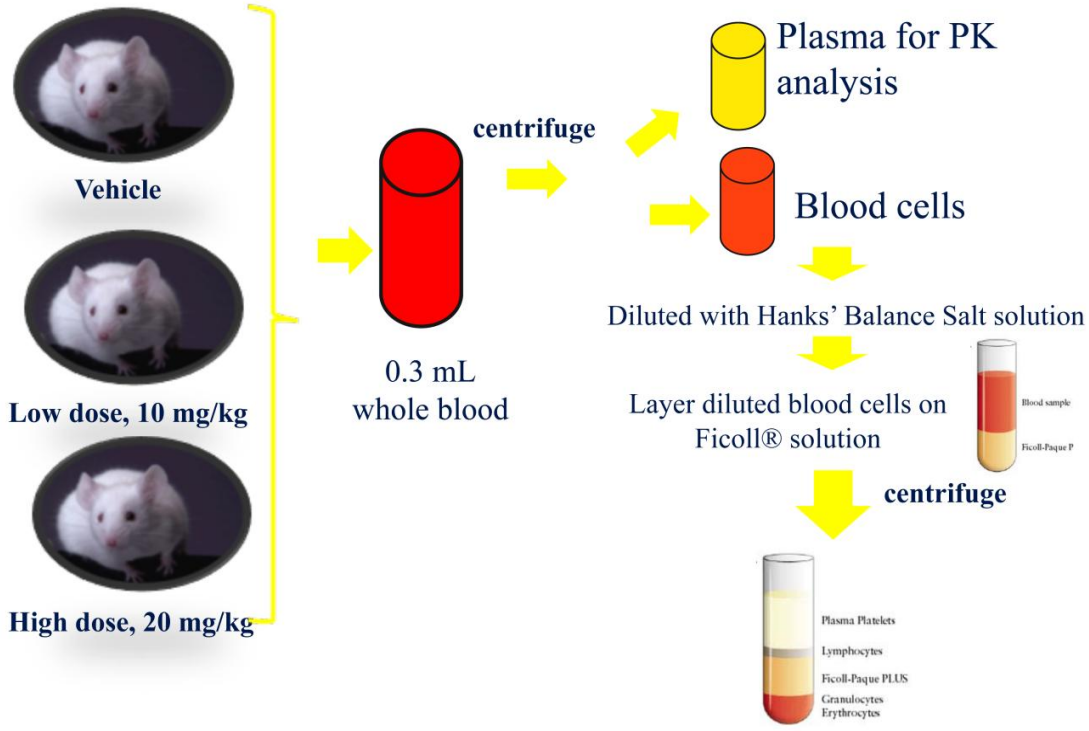

Figure 5-1 Pharmacokinetic and Pharmacodynamic study approaches

Three groups of Sprague-Dawley JVC rats, each group of three rats were dosed with DIM 10 or 20 mg/kg or vehicle. The experiments were repeated 3 times. Collect ~ 0.3 mL of blood samples at 0, 3, 5, 15, 30, 60 min., 2, 4, 8, 12, 24 or 48 hours. Plasma samples from each rat were reserve for PK study. Combination of the blood samples at each time point for each group of rats were reserve for PD study

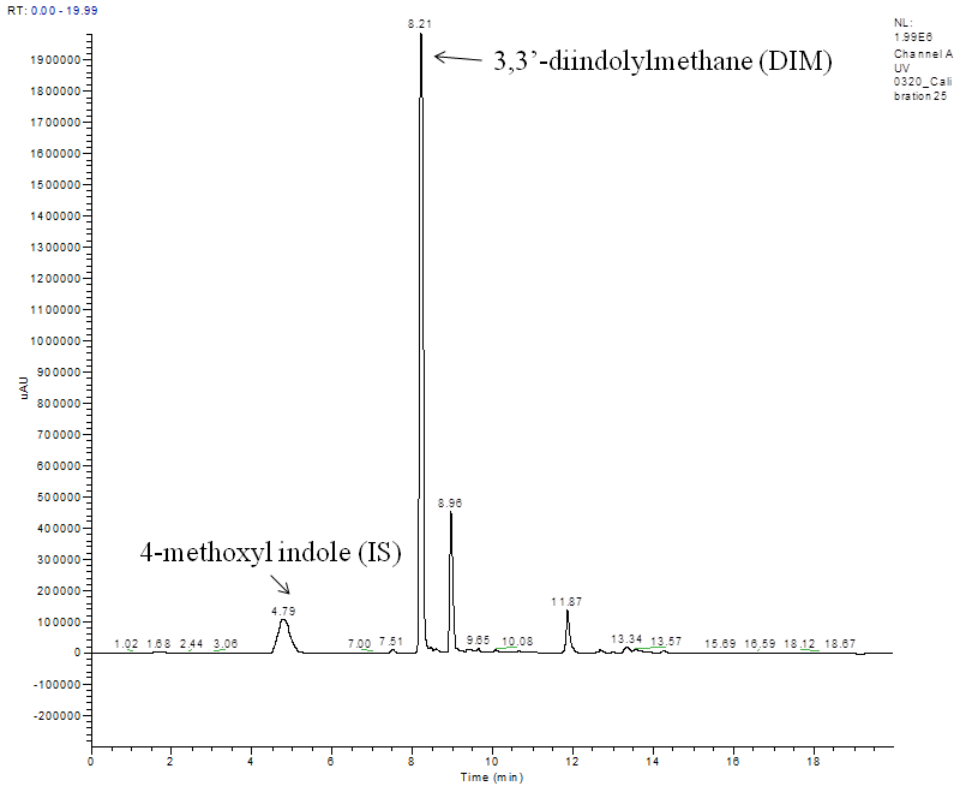

Figure 5-2 Chromatogram of blank rat plasma spiked with DIM and IS

Retention times of DIM and IS were approximately 8.21 and 4.79 min, respectively. Neither endogenous matrix plasma peaks nor any in vivo metabolites of DIM were found to interfere with any of the compounds evaluated.

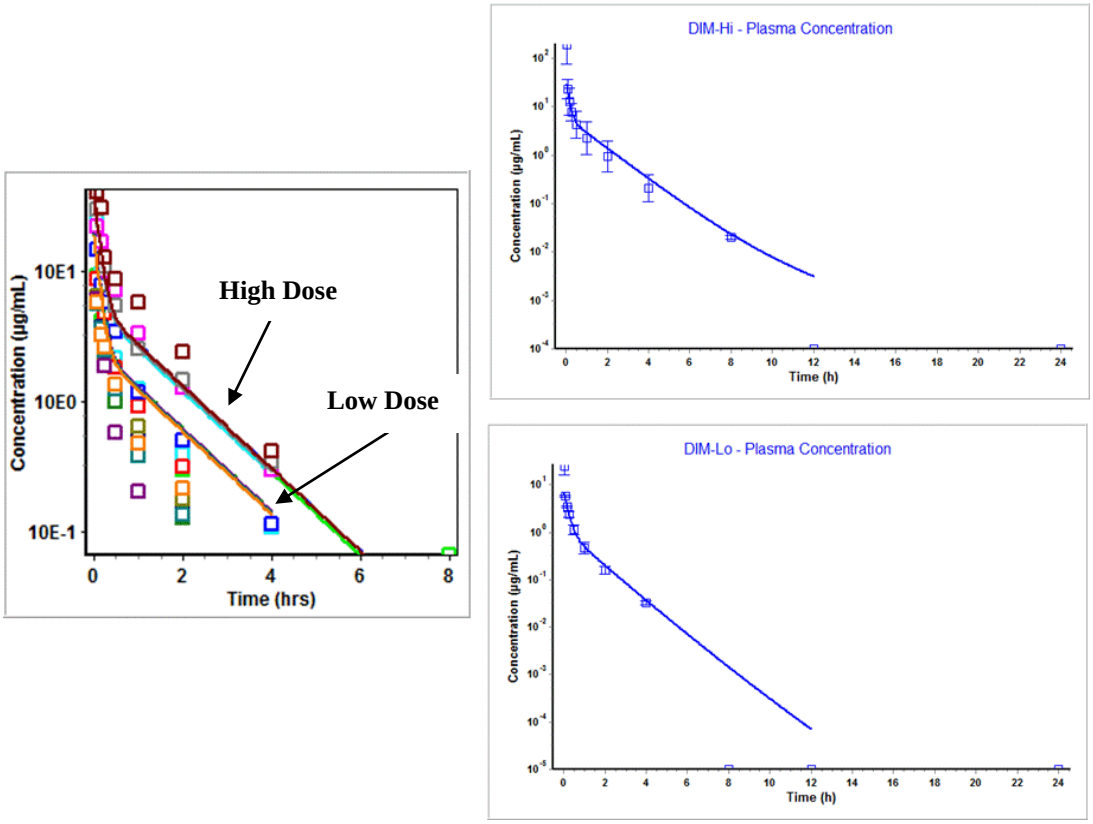

Figure 5-3 Mean pharmacokinetic profiles.

Two-compartment pharmacokinetic model estimate both high and low doses pharmacokinetic profiles (Left). DIM 20 mg/kg (high dose) administration to Sprague Dawley rats profile (right top) and DIM 10 mg/kg (low dose) administration profile (right bottom).

Figure 4

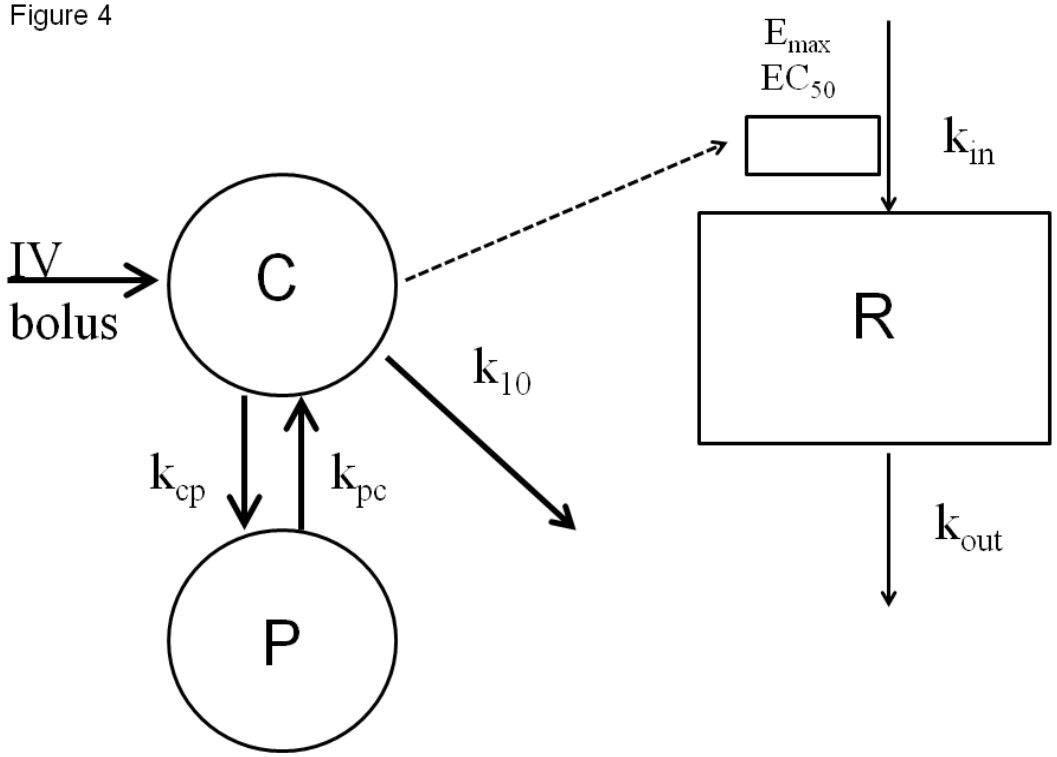

Figure 5-4 Pharmacokinetic-Pharmacodynamic modeling of indirect response model.

The model was first described as Indirect Response Model III by Dayneka, et al 1993. C, represents as central compartment; P, represents as peripheral compartment; R, response of mRNA expression level change over that at initial (t=0).

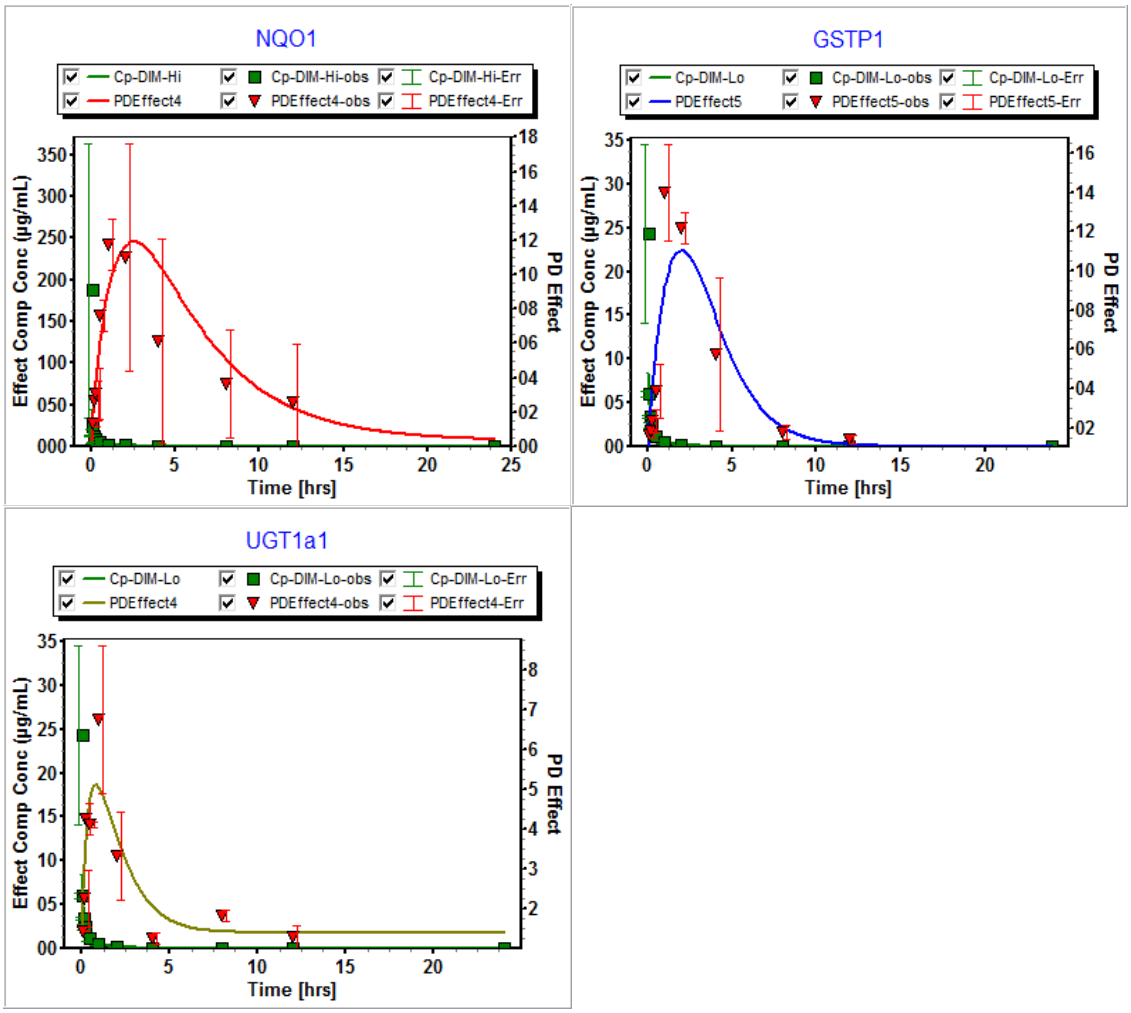

Figure 5-5 Pharmacokinetic-Pharmacodynamic profiles of mRNA expression in DIM 10 mg/kg administration group.

The mRNA expression change in lymphocytes with time in folds for Nrf2, NQO1, GSTP1, and UGT1a1. Lines represent model predicted values. Observed data are presented in mean±CV%.

Reference:

1. Shen G, Jeong WS, Hu R, Kong AN. Regulation of Nrf2, NF-kappaB, and AP-1 signaling pathways by chemopreventive agents. Antioxid Redox Signal. 2005;7(11-12):1648-63. Epub 2005/12/17.
2. Surh YJ. Cancer chemoprevention with dietary phytochemicals. Nat Rev Cancer. 2003;3(10):768-80. Epub 2003/10/23.
3. Bird A. DNA methylation patterns and epigenetic memory. Genes Dev. 2002;16(1):6-21. Epub 2002/01/10.
4. Mandlekar S, Hong JL, Kong AN. Modulation of metabolic enzymes by dietary phytochemicals: a review of mechanisms underlying beneficial versus unfavorable effects. Curr Drug Metab. 2006;7(6):661-75. Epub 2006/08/22.
5. Pool-Zobel B, Veeriah S, Bohmer FD. Modulation of xenobiotic metabolising enzymes by anticarcinogens -- focus on glutathione S-transferases and their role as targets of dietary chemoprevention in colorectal carcinogenesis. Mutat Res. 2005;591(1-2):74-92. Epub 2005/08/09.
6. Xu C, Li CY, Kong AN. Induction of phase I, II and III drug metabolism/transport by xenobiotics. Arch Pharm Res. 2005;28(3):249-68. Epub 2005/04/19.
7. Jana S, Mandlekar S. Role of phase II drug metabolizing enzymes in cancer chemoprevention. Curr Drug Metab. 2009;10(6):595-616. Epub 2009/08/26.
8. Jeong WS, Jun M, Kong AN. Nrf2: a potential molecular target for cancer chemoprevention by natural compounds. Antioxid Redox Signal. 2006;8(1-2):99-106. Epub 2006/02/21.
9. Goldberg AD, Allis CD, Bernstein E. Epigenetics: a landscape takes shape. Cell. 2007;128(4):635-8. Epub 2007/02/27.
10. Gomez A, Ingelman-Sundberg M. Pharmacoepigenetics: its role in interindividual differences in drug response. Clin Pharmacol Ther. 2009;85(4):426-30. Epub 2009/02/27.
11. Esteller M. Epigenetics in cancer. N Engl J Med. 2008;358(11):1148-59. Epub 2008/03/14.
12. Baker EK, El-Osta A. MDR1, chemotherapy and chromatin remodeling. Cancer Biol Ther. 2004;3(9):819-24. Epub 2004/08/25.
13. Baker EK, Johnstone RW, Zalcberg JR, El-Osta A. Epigenetic changes to the MDR1 locus in response to chemotherapeutic drugs. Oncogene. 2005;24(54):8061-75. Epub 2005/08/11.
14. Sharma G, Mirza S, Parshad R, Srivastava A, Datta Gupta S, Pandya P, et al. CpG hypomethylation of MDR1 gene in tumor and serum of invasive ductal breast carcinoma patients. Clin Biochem. 2010;43(4-5):373-9. Epub 2009/11/03.
15. To KK, Zhan Z, Bates SE. Aberrant promoter methylation of the ABCG2 gene in renal carcinoma. Mol Cell Biol. 2006;26(22):8572-85. Epub 2006/09/07.

16. Bram EE, Stark M, Raz S, Assaraf YG. Chemotherapeutic drug-induced ABCG2 promoter demethylation as a novel mechanism of acquired multidrug resistance. Neoplasia. 2009;11(12):1359-70. Epub 2009/12/19.
17. Robey RW, To KK, Polgar O, Dohse M, Fetsch P, Dean M, et al. ABCG2: a perspective. Adv Drug Deliv Rev. 2009;61(1):3-13. Epub 2009/01/13.
18. Kacevska M, Ivanov M, Ingelman-Sundberg M. Perspectives on epigenetics and its relevance to adverse drug reactions. Clin Pharmacol Ther. 2011;89(6):902-7. Epub 2011/04/22.
19. Rieder MJ, Livingston RJ, Stanaway IB, Nickerson DA. The environmental genome project: reference polymorphisms for drug metabolism genes and genome-wide association studies. Drug Metab Rev. 2008;40(2):241-61. Epub 2008/05/09.
20. Efferth T, Volm M. Pharmacogenetics for individualized cancer chemotherapy. Pharmacol Ther. 2005;107(2):155-76. Epub 2005/05/14.
21. Brinkmann U, Eichelbaum M. Polymorphisms in the ABC drug transporter gene MDR1. Pharmacogenomics J. 2001;1(1):59-64. Epub 2002/03/27.
22. Brinkmann U, Roots I, Eichelbaum M. Pharmacogenetics of the human drug-transporter gene MDR1: impact of polymorphisms on pharmacotherapy. Drug Discov Today. 2001;6(16):835-9. Epub 2001/08/10.
23. Bolt HM, Thier R. Relevance of the deletion polymorphisms of the glutathione S-transferases GSTT1 and GSTM1 in pharmacology and toxicology. Curr Drug Metab. 2006;7(6):613-28. Epub 2006/08/22.
24. Lee SA, Fowke JH, Lu W, Ye C, Zheng Y, Cai Q, et al. Cruciferous vegetables, the GSTP1 Ile105Val genetic polymorphism, and breast cancer risk. Am J Clin Nutr. 2008;87(3):753-60. Epub 2008/03/11.
25. Cheung KL, Khor TO, Huang MT, Kong AN. Differential in vivo mechanism of chemoprevention of tumor formation in azoxymethane/dextran sodium sulfate mice by PEITC and DBM. Carcinogenesis.31(5):880-5. Epub 2009/12/05.
26. White DL, Li D, Nurgalieva Z, El-Serag HB. Genetic variants of glutathione S-transferase as possible risk factors for hepatocellular carcinoma: a HuGE systematic review and meta-analysis. Am J Epidemiol. 2008;167(4):377-89. Epub 2007/12/11.
27. Moaven O, Raziee HR, Sima HR, Ganji A, Malekzadeh R, A'Rabi A, et al. Interactions between Glutathione-S-Transferase M1, T1 and P1 polymorphisms and smoking, and increased susceptibility to esophageal squamous cell carcinoma. Cancer Epidemiol.34(3):285-90. Epub 2010/04/23.
28. Hanene C, Jihene L, Jamel A, Kamel H, Agnes H. Association of GST genes polymorphisms with asthma in Tunisian children. Mediators Inflamm. 2007;2007:19564. Epub 2007/05/15.
29. Guha N, Chang JS, Chokkalingam AP, Wiemels JL, Smith MT, Buffler PA. NQO1 polymorphisms and de novo childhood leukemia: a HuGE review and meta-analysis. Am J Epidemiol. 2008;168(11):1221-32. Epub 2008/10/24.
30. Reddy AJ, Christie JD, Aplenc R, Fuchs B, Lanken PN, Kleeberger SR. Association of human NAD(P)H:quinone oxidoreductase 1 (NQO1) polymorphism with development of acute lung injury. J Cell Mol Med. 2009;13(8B):1784-91. Epub 2008/11/20.

31. Guillemette C, Levesque E, Harvey M, Bellemare J, Menard V. UGT genomic diversity: beyond gene duplication. Drug Metab Rev.42(1):22-42. Epub 2009/10/28.
32. Font A, Sanchez JM, Taron M, Martinez-Balibrea E, Sanchez JJ, Manzano JL, et al. Weekly regimen of irinotecan/docetaxel in previously treated non-small cell lung cancer patients and correlation with uridine diphosphate glucuronosyltransferase 1A1 (UGT1A1) polymorphism. Invest New Drugs. 2003;21(4):435-43. Epub 2003/10/31.
33. Gupta E, Lestingi TM, Mick R, Ramirez J, Vokes EE, Ratain MJ. Metabolic fate of irinotecan in humans: correlation of glucuronidation with diarrhea. Cancer Res. 1994;54(14):3723-5. Epub 1994/07/15.
34. Shen G, Kong AN. Nrf2 plays an important role in coordinated regulation of Phase II drug metabolism enzymes and Phase III drug transporters. Biopharm Drug Dispos. 2009;30(7):345-55. Epub 2009/09/03.
35. Khor TO, Huang MT, Kwon KH, Chan JY, Reddy BS, Kong AN. Nrf2-deficient mice have an increased susceptibility to dextran sulfate sodium-induced colitis. Cancer Res. 2006;66(24):11580-4. Epub 2006/12/21.
36. Chanas SA, Jiang Q, McMahon M, McWalter GK, McLellan LI, Elcombe CR, et al. Loss of the Nrf2 transcription factor causes a marked reduction in constitutive and inducible expression of the glutathione S-transferase Gsta1, Gsta2, Gstm1, Gstm2, Gstm3 and Gstm4 genes in the livers of male and female mice. Biochem J. 2002;365(Pt 2):405-16. Epub 2002/05/07.
37. Thimmulappa RK, Mai KH, Srisuma S, Kensler TW, Yamamoto M, Biswal S. Identification of Nrf2-regulated genes induced by the chemopreventive agent sulforaphane by oligonucleotide microarray. Cancer Res. 2002;62(18):5196-203. Epub 2002/09/18.
38. Barve A, Khor TO, Nair S, Lin W, Yu S, Jain MR, et al. Pharmacogenomic profile of soy isoflavone concentrate in the prostate of Nrf2 deficient and wild-type mice. J Pharm Sci. 2008;97(10):4528-45. Epub 2008/02/01.
39. Nair S, Xu C, Shen G, Hebbar V, Gopalakrishnan A, Hu R, et al. Pharmacogenomics of phenolic antioxidant butylated hydroxyanisole (BHA) in the small intestine and liver of Nrf2 knockout and C57BL/6J mice. Pharm Res. 2006;23(11):2621-37. Epub 2006/09/14.
40. Shen G, Xu C, Hu R, Jain MR, Gopalkrishnan A, Nair S, et al. Modulation of nuclear factor E2-related factor 2-mediated gene expression in mice liver and small intestine by cancer chemopreventive agent curcumin. Mol Cancer Ther. 2006;5(1):39-51. Epub 2006/01/25.
41. Thimmulappa RK, Rangasamy T, Alam J, Biswal S. Dibenzoylmethane activates Nrf2-dependent detoxification pathway and inhibits benzo(a)pyrene induced DNA adducts in lungs. Med Chem. 2008;4(5):473-81. Epub 2008/09/11.
42. Wu TY, Khor TO, Saw CL, Loh SC, Chen AI, Lim SS, et al. Anti-inflammatory/Anti-oxidative Stress Activities and Differential Regulation of Nrf2-Mediated Genes by Non-Polar Fractions of Tea Chrysanthemum zawadskii and Licorice Glycyrrhiza uralensis. AAPS J. 2011;13(1):1-13. Epub 2010/10/23.
43. Shu L, Cheung KL, Khor TO, Chen C, Kong AN. Phytochemicals: cancer chemoprevention and suppression of tumor onset and metastasis. Cancer Metastasis Rev.29(3):483-502. Epub 2010/08/28.

44. Khor TO, Yu S, Kong AN. Dietary cancer chemopreventive agents - targeting inflammation and Nrf2 signaling pathway. Planta Med. 2008;74(13):1540-7. Epub 2008/10/22.
45. Kwon KH, Barve A, Yu S, Huang MT, Kong AN. Cancer chemoprevention by phytochemicals: potential molecular targets, biomarkers and animal models. Acta Pharmacol Sin. 2007;28(9):1409-21. Epub 2007/08/29.
46. Shen G, Xu C, Hu R, Jain MR, Nair S, Lin W, et al. Comparison of (-)-epigallocatechin-3-gallate elicited liver and small intestine gene expression profiles between C57BL/6J mice and C57BL/6J/Nrf2 (-/-) mice. Pharm Res. 2005;22(11):1805-20. Epub 2005/09/01.
47. Nair S, Li W, Kong AN. Natural dietary anti-cancer chemopreventive compounds: redox-mediated differential signaling mechanisms in cytoprotection of normal cells versus cytotoxicity in tumor cells. Acta Pharmacol Sin. 2007;28(4):459-72. Epub 2007/03/23.
48. Khor TO, Yu S, Barve A, Hao X, Hong JL, Lin W, et al. Dietary feeding of dibenzoylmethane inhibits prostate cancer in transgenic adenocarcinoma of the mouse prostate model. Cancer Res. 2009;69(17):7096-102. Epub 2009/08/27.
49. Keum YS, Jeong WS, Kong AN. Chemopreventive functions of isothiocyanates. Drug News Perspect. 2005;18(7):445-51. Epub 2005/12/20.
50. Lin W, Wu RT, Wu T, Khor TO, Wang H, Kong AN. Sulforaphane suppressed LPS-induced inflammation in mouse peritoneal macrophages through Nrf2 dependent pathway. Biochem Pharmacol. 2008;76(8):967-73. Epub 2008/08/30.
51. Hu R, Xu C, Shen G, Jain MR, Khor TO, Gopalkrishnan A, et al. Identification of Nrf2-regulated genes induced by chemopreventive isothiocyanate PEITC by oligonucleotide microarray. Life Sci. 2006;79(20):1944-55. Epub 2006/07/11.
52. Jeong WS, Keum YS, Chen C, Jain MR, Shen G, Kim JH, et al. Differential expression and stability of endogenous nuclear factor E2-related factor 2 (Nrf2) by natural chemopreventive compounds in HepG2 human hepatoma cells. J Biochem Mol Biol. 2005;38(2):167-76. Epub 2005/04/14.
53. Nair S, Barve A, Khor TO, Shen GX, Lin W, Chan JY, et al. Regulation of Nrf2- and AP-1-mediated gene expression by epigallocatechin-3-gallate and sulforaphane in prostate of Nrf2-knockout or C57BL/6J mice and PC-3 AP-1 human prostate cancer cells. Acta Pharmacol Sin.31(9):1223-40. Epub 2010/08/24.
54. Chen C, Shen G, Hebbar V, Hu R, Owuor ED, Kong AN. Epigallocatechin-3-gallate-induced stress signals in HT-29 human colon adenocarcinoma cells. Carcinogenesis. 2003;24(8):1369-78. Epub 2003/06/24.
55. Jeong WS, Kim IW, Hu R, Kong AN. Modulation of AP-1 by natural chemopreventive compounds in human colon HT-29 cancer cell line. Pharm Res. 2004;21(4):649-60. Epub 2004/05/14.
56. Keum YS, Khor TO, Lin W, Shen G, Kwon KH, Barve A, et al. Pharmacokinetics and pharmacodynamics of broccoli sprouts on the suppression of prostate cancer in transgenic adenocarcinoma of mouse prostate (TRAMP) mice: implication of induction of Nrf2, HO-1 and apoptosis and the suppression of Akt-dependent kinase pathway. Pharm Res. 2009;26(10):2324-31. Epub 2009/08/12.

57. Lii CK, Liu KL, Cheng YP, Lin AH, Chen HW, Tsai CW. Sulforaphane and alpha-lipoic acid upregulate the expression of the pi class of glutathione S-transferase through c-jun and Nrf2 activation. J Nutr.140(5):885-92. Epub 2010/03/20.
58. Danilov CA, Chandrasekaran K, Racz J, Soane L, Zielke C, Fiskum G. Sulforaphane protects astrocytes against oxidative stress and delayed death caused by oxygen and glucose deprivation. Glia. 2009;57(6):645-56. Epub 2008/10/24.
59. Yeh CT, Chiu HF, Yen GC. Protective effect of sulforaphane on indomethacin-induced cytotoxicity via heme oxygenase-1 expression in human intestinal Int 407 cells. Mol Nutr Food Res. 2009;53(9):1166-76. Epub 2009/08/05.
60. Xu C, Huang MT, Shen G, Yuan X, Lin W, Khor TO, et al. Inhibition of 7,12-dimethylbenz(a)anthracene-induced skin tumorigenesis in C57BL/6 mice by sulforaphane is mediated by nuclear factor E2-related factor 2. Cancer Res. 2006;66(16):8293-6. Epub 2006/08/17.
61. Nishinaka T, Ichijo Y, Ito M, Kimura M, Katsuyama M, Iwata K, et al. Curcumin activates human glutathione S-transferase P1 expression through antioxidant response element. Toxicol Lett. 2007;170(3):238-47. Epub 2007/04/24.
62. Shen SQ, Zhang Y, Xiang JJ, Xiong CL. Protective effect of curcumin against liver warm ischemia/reperfusion injury in rat model is associated with regulation of heat shock protein and antioxidant enzymes. World J Gastroenterol. 2007;13(13):1953-61. Epub 2007/04/28.
63. Sharma V, Nehru B, Munshi A, Jyothy A. Antioxidant potential of curcumin against oxidative insult induced by pentylenetetrazol in epileptic rats. Methods Find Exp Clin Pharmacol.32(4):227-32. Epub 2010/05/29.
64. Barve A, Khor TO, Hao X, Keum YS, Yang CS, Reddy B, et al. Murine prostate cancer inhibition by dietary phytochemicals--curcumin and phenyethylisothiocyanate. Pharm Res. 2008;25(9):2181-9. Epub 2008/04/26.
65. Jeong WS, Kim IW, Hu R, Kong AN. Modulatory properties of various natural chemopreventive agents on the activation of NF-kappaB signaling pathway. Pharm Res. 2004;21(4):661-70. Epub 2004/05/14.
66. Kim JH, Xu C, Keum YS, Reddy B, Conney A, Kong AN. Inhibition of EGFR signaling in human prostate cancer PC-3 cells by combination treatment with beta-phenylethyl isothiocyanate and curcumin. Carcinogenesis. 2006;27(3):475-82. Epub 2005/11/22.
67. Sharma S, Kelly TK, Jones PA. Epigenetics in cancer. Carcinogenesis. 2010;31(1):27-36. Epub 2009/09/16.
68. Baylin SB, Herman JG, Graff JR, Vertino PM, Issa JP. Alterations in DNA methylation: a fundamental aspect of neoplasia. Adv Cancer Res. 1998;72:141-96. Epub 1997/10/24.
69. Belanger AS, Tojcic J, Harvey M, Guillemette C. Regulation of UGT1A1 and HNF1 transcription factor gene expression by DNA methylation in colon cancer cells. BMC Mol Biol.11:9. Epub 2010/01/26.
70. Yu S, Khor TO, Cheung KL, Li W, Wu TY, Huang Y, et al. Nrf2 expression is regulated by epigenetic mechanisms in prostate cancer of TRAMP mice. PLoS One.5(1):e8579. Epub 2010/01/12.

71. Dashwood RH, Ho E. Dietary histone deacetylase inhibitors: from cells to mice to man. Semin Cancer Biol. 2007;17(5):363-9. Epub 2007/06/09.
72. Li Y, Tollefsbol TO. Impact on DNA methylation in cancer prevention and therapy by bioactive dietary components. Curr Med Chem. 2010;17(20):2141-51. Epub 2010/04/29.
73. Huang J, Plass C, Gerhauser C. Cancer Chemoprevention by Targeting the Epigenome. Current drug targets. 2010. Epub 2010/12/17.
74. Kim JY, Park SJ, Yun KJ, Cho YW, Park HJ, Lee KT. Isoliquiritigenin isolated from the roots of Glycyrrhiza uralensis inhibits LPS-induced iNOS and COX-2 expression via the attenuation of NF-kappaB in RAW 264.7 macrophages. Eur J Pharmacol. 2008;584(1):175-84. Epub 2008/02/26.
75. Clevers H. At the crossroads of inflammation and cancer. Cell. 2004;118(6):671-4. Epub 2004/09/17.
76. Villeneuve NF, Lau A, Zhang DD. Regulation of the Nrf2-Keap1 Antioxidant Response by the Ubiquitin Proteasome System: An Insight into Cullin-Ring Ubiquitin Ligases. Antioxid Redox Signal. 2010. Epub 2010/05/22.
77. Hayes JD, McMahon M, Chowdhry S, Dinkova-Kostova AT. Cancer Chemoprevention Mechanisms Mediated Through the Keap1-Nrf2 Pathway. Antioxid Redox Signal. 2010. Epub 2010/05/08.
78. Kwak MK, Wakabayashi N, Kensler TW. Chemoprevention through the Keap1-Nrf2 signaling pathway by phase 2 enzyme inducers. Mutat Res. 2004;555(1-2):133-48. Epub 2004/10/13.
79. Kim SN, Kim MH, Min YK, Kim SH. Licochalcone A inhibits the formation and bone resorptive activity of osteoclasts. Cell Biol Int. 2008;32(9):1064-72. Epub 2008/06/10.
80. Lee CK, Son SH, Park KK, Park JH, Lim SS, Kim SH, et al. Licochalcone A inhibits the growth of colon carcinoma and attenuates cisplatin-induced toxicity without a loss of chemotherapeutic efficacy in mice. Basic Clin Pharmacol Toxicol. 2008;103(1):48-54. Epub 2008/05/20.
81. Fu Y, Hsieh TC, Guo J, Kunicki J, Lee MY, Darzynkiewicz Z, et al. Licochalcone-A, a novel flavonoid isolated from licorice root (Glycyrrhiza glabra), causes G2 and late-G1 arrests in androgen-independent PC-3 prostate cancer cells. Biochem Biophys Res Commun. 2004;322(1):263-70. Epub 2004/08/18.
82. Kim YW, Zhao RJ, Park SJ, Lee JR, Cho IJ, Yang CH, et al. Anti-inflammatory effects of liquiritigenin as a consequence of the inhibition of NF-kappaB-dependent iNOS and proinflammatory cytokines production. Br J Pharmacol. 2008;154(1):165-73. Epub 2008/03/12.
83. Takei M, Kobayashi M, Herndon DN, Pollard RB, Suzuki F. Glycyrrhizin inhibits the manifestations of anti-inflammatory responses that appear in association with systemic inflammatory response syndrome (SIRS)-like reactions. Cytokine. 2006;35(5-6):295-301. Epub 2006/11/23.
84. Shunying Z, Yang Y, Huaidong Y, Yue Y, Guolin Z. Chemical composition and antimicrobial activity of the essential oils of Chrysanthemum indicum. J Ethnopharmacol. 2005;96(1-2):151-8. Epub 2004/12/14.

85. Kho MR, Baker DJ, Laayoun A, Smith SS. Stalling of human DNA (cytosine-5) methyltransferase at single-strand conformers from a site of dynamic mutation. Journal of molecular biology. 1998;275(1):67-79. Epub 1998/02/06.
86. Matsuda H, Morikawa T, Toguchida I, Harima S, Yoshikawa M. Medicinal flowers. VI. Absolute stereostructures of two new flavanone glycosides and a phenylbutanoid glycoside from the flowers of Chrysanthemum indicum L.: their inhibitory activities for rat lens aldose reductase. Chem Pharm Bull (Tokyo). 2002;50(7):972-5. Epub 2002/07/20.
87. Yoshikawa M, Morikawa T, Toguchida I, Harima S, Matsuda H. Medicinal flowers. II. Inhibitors of nitric oxide production and absolute stereostructures of five new germacrane-type sesquiterpenes, kikkanols D, D monoacetate, E, F, and F monoacetate from the flowers of Chrysanthemum indicum L. Chem Pharm Bull (Tokyo). 2000;48(5):651-6. Epub 2000/05/24.
88. Cheng W, Li J, You T, Hu C. Anti-inflammatory and immunomodulatory activities of the extracts from the inflorescence of Chrysanthemum indicum Linne. J Ethnopharmacol. 2005;101(1-3):334-7. Epub 2005/07/21.
89. Yu R, Mandlekar S, Lei W, Fahl WE, Tan TH, Kong AN. p38 mitogen-activated protein kinase negatively regulates the induction of phase II drug-metabolizing enzymes that detoxify carcinogens. J Biol Chem. 2000;275(4):2322-7. Epub 2000/01/25.
90. Chen C, Yu R, Owuor ED, Kong AN. Activation of antioxidant-response element (ARE), mitogen-activated protein kinases (MAPKs) and caspases by major green tea polyphenol components during cell survival and death. Arch Pharm Res. 2000;23(6):605-12. Epub 2001/01/13.
91. Prawan A, Keum YS, Khor TO, Yu S, Nair S, Li W, et al. Structural influence of isothiocyanates on the antioxidant response element (ARE)-mediated heme oxygenase-1 (HO-1) expression. Pharm Res. 2008;25(4):836-44. Epub 2007/07/28.
92. Prawan A, Saw CL, Khor TO, Keum YS, Yu S, Hu L, et al. Anti-NF-kappaB and anti-inflammatory activities of synthetic isothiocyanates: effect of chemical structures and cellular signaling. Chem Biol Interact. 2009;179(2-3):202-11. Epub 2009/01/23.
93. Nair S, Hebbar V, Shen G, Gopalakrishnan A, Khor TO, Yu S, et al. Synergistic effects of a combination of dietary factors sulforaphane and (-) epigallocatechin-3-gallate in HT-29 AP-1 human colon carcinoma cells. Pharm Res. 2008;25(2):387-99. Epub 2007/07/28.
94. Nair S, Barve A, Khor TO, Shen GX, Lin W, Chan JY, et al. Regulation of Nrf2- and AP-1-mediated gene expression by epigallocatechin-3-gallate and sulforaphane in prostate of Nrf2-knockout or C57BL/6J mice and PC-3 AP-1 human prostate cancer cells. Acta Pharmacol Sin. 2010;31(9):1223-40. Epub 2010/08/24.
95. Li C, Wong WH. Model-based analysis of oligonucleotide arrays: expression index computation and outlier detection. Proc Natl Acad Sci U S A. 2001;98(1):31-6. Epub 2001/01/03.
96. Li C, Hung Wong W. Model-based analysis of oligonucleotide arrays: model validation, design issues and standard error application. Genome Biol. 2001;2(8):RESEARCH0032. Epub 2001/09/05.
97. Prawan A, Buranrat B, Kukongviriyapan U, Sripa B, Kukongviriyapan V. Inflammatory cytokines suppress NAD(P)H:quinone oxidoreductase-1 and induce

oxidative stress in cholangiocarcinoma cells. J Cancer Res Clin Oncol. 2009;135(4):515-22. Epub 2008/09/30.
98. Saw CL, Huang Y, Kong AN. Synergistic anti-inflammatory effects of low doses of curcumin in combination with polyunsaturated fatty acids: docosahexaenoic acid or eicosapentaenoic acid. Biochem Pharmacol.79(3):421-30. Epub 2009/09/12.
99. Saw CL, Olivo M, Chin WW, Soo KC, Heng PW. Transport of hypericin across chick chorioallantoic membrane and photodynamic therapy vasculature assessment. Biol Pharm Bull. 2005;28(6):1054-60. Epub 2005/06/03.
100. Wakabayashi N, Slocum SL, Skoko JJ, Shin S, Kensler TW. When NRF2 talks, who's listening? Antioxid Redox Signal. 2010;13(11):1649-63. Epub 2010/04/07.
101. Oliveira-Marques V, Marinho HS, Cyrne L, Antunes F. Role of hydrogen peroxide in NF-kappaB activation: from inducer to modulator. Antioxid Redox Signal. 2009;11(9):2223-43. Epub 2009/06/06.
102. Li W, Khor TO, Xu C, Shen G, Jeong WS, Yu S, et al. Activation of Nrf2-antioxidant signaling attenuates NFkappaB-inflammatory response and elicits apoptosis. Biochem Pharmacol. 2008;76(11):1485-9. Epub 2008/08/13.
103. Khor TO, Keum YS, Lin W, Kim JH, Hu R, Shen G, et al. Combined inhibitory effects of curcumin and phenethyl isothiocyanate on the growth of human PC-3 prostate xenografts in immunodeficient mice. Cancer Res. 2006;66(2):613-21. Epub 2006/01/21.
104. Shen G, Khor TO, Hu R, Yu S, Nair S, Ho CT, et al. Chemoprevention of familial adenomatous polyposis by natural dietary compounds sulforaphane and dibenzoylmethane alone and in combination in ApcMin/+ mouse. Cancer Res. 2007;67(20):9937-44. Epub 2007/10/19.
105. Li W, Kong AN. Molecular mechanisms of Nrf2-mediated antioxidant response. Mol Carcinog. 2009;48(2):91-104. Epub 2008/07/12.
106. Lin W, Shen G, Yuan X, Jain MR, Yu S, Zhang A, et al. Regulation of Nrf2 transactivation domain activity by p160 RAC3/SRC3 and other nuclear co-regulators. J Biochem Mol Biol. 2006;39(3):304-10. Epub 2006/06/08.
107. Wang T, Jiang H, Ji Y, Xu J. [Anti-oxidation effect of water extract of Flos chrysanthemi on heart and brain in vivo and in vitro]. Zhong Yao Cai. 2001;24(2):122-4. Epub 2001/06/14.
108. Jemal A, Siegel R, Xu J, Ward E. Cancer statistics, 2010. CA Cancer J Clin. 2010;60(5):277-300. Epub 2010/07/09.
109. Safe S, Papineni S, Chintharlapalli S. Cancer chemotherapy with indole-3-carbinol, bis(3'-indolyl)methane and synthetic analogs. Cancer Lett. 2008;269(2):326-38. Epub 2008/05/27.
110. Abate-Shen C, Shen MM. Molecular genetics of prostate cancer. Genes Dev. 2000;14(19):2410-34. Epub 2000/10/06.
111. Carter BS, Carter HB, Isaacs JT. Epidemiologic evidence regarding predisposing factors to prostate cancer. Prostate. 1990;16(3):187-97. Epub 1990/01/01.
112. Sarkar FH, Li Y. Indole-3-carbinol and prostate cancer. J Nutr. 2004;134(12 Suppl):3493S-8S. Epub 2004/12/01.
113. Bradlow HL, Michnovicz J, Telang NT, Osborne MP. Effects of dietary indole-3-carbinol on estradiol metabolism and spontaneous mammary tumors in mice. Carcinogenesis. 1991;12(9):1571-4. Epub 1991/09/01.

114. Grubbs CJ, Steele VE, Casebolt T, Juliana MM, Eto I, Whitaker LM, et al. Chemoprevention of chemically-induced mammary carcinogenesis by indole-3-carbinol. Anticancer Res. 1995;15(3):709-16. Epub 1995/05/01.
115. Jin L, Qi M, Chen DZ, Anderson A, Yang GY, Arbeit JM, et al. Indole-3-carbinol prevents cervical cancer in human papilloma virus type 16 (HPV16) transgenic mice. Cancer Res. 1999;59(16):3991-7. Epub 1999/08/27.
116. Kojima T, Tanaka T, Mori H. Chemoprevention of spontaneous endometrial cancer in female Donryu rats by dietary indole-3-carbinol. Cancer Res. 1994;54(6):1446-9. Epub 1994/03/15.
117. Oganesian A, Hendricks JD, Williams DE. Long term dietary indole-3-carbinol inhibits diethylnitrosamine-initiated hepatocarcinogenesis in the infant mouse model. Cancer Lett. 1997;118(1):87-94. Epub 1997/10/06.
118. Yu Z, Mahadevan B, Lohr CV, Fischer KA, Louderback MA, Krueger SK, et al. Indole-3-carbinol in the maternal diet provides chemoprotection for the fetus against transplacental carcinogenesis by the polycyclic aromatic hydrocarbon dibenzo[a,l]pyrene. Carcinogenesis. 2006;27(10):2116-23. Epub 2006/05/18.
119. Weng JR, Tsai CH, Kulp SK, Chen CS. Indole-3-carbinol as a chemopreventive and anti-cancer agent. Cancer Lett. 2008;262(2):153-63. Epub 2008/03/04.
120. Higdon JV, Delage B, Williams DE, Dashwood RH. Cruciferous vegetables and human cancer risk: epidemiologic evidence and mechanistic basis. Pharmacol Res. 2007;55(3):224-36. Epub 2007/02/24.
121. Kim YS, Milner JA. Targets for indole-3-carbinol in cancer prevention. J Nutr Biochem. 2005;16(2):65-73. Epub 2005/02/01.
122. Tsai JT, Liu HC, Chen YH. Suppression of inflammatory mediators by cruciferous vegetable-derived indole-3-carbinol and phenylethyl isothiocyanate in lipopolysaccharide-activated macrophages. Mediators Inflamm.2010:293642. Epub 2010/04/24.
123. Minich DM, Bland JS. A review of the clinical efficacy and safety of cruciferous vegetable phytochemicals. Nutr Rev. 2007;65(6 Pt 1):259-67. Epub 2007/07/04.
124. Fan S, Meng Q, Saha T, Sarkar FH, Rosen EM. Low concentrations of diindolylmethane, a metabolite of indole-3-carbinol, protect against oxidative stress in a BRCA1-dependent manner. Cancer Res. 2009;69(15):6083-91. Epub 2009/07/23.
125. Pathak SK, Sharma RA, Steward WP, Mellon JK, Griffiths TR, Gescher AJ. Oxidative stress and cyclooxygenase activity in prostate carcinogenesis: targets for chemopreventive strategies. Eur J Cancer. 2005;41(1):61-70. Epub 2004/12/25.
126. Barve A, Khor TO, Nair S, Reuhl K, Suh N, Reddy B, et al. Gamma-tocopherol-enriched mixed tocopherol diet inhibits prostate carcinogenesis in TRAMP mice. Int J Cancer. 2009;124(7):1693-9. Epub 2008/12/31.
127. Frohlich DA, McCabe MT, Arnold RS, Day ML. The role of Nrf2 in increased reactive oxygen species and DNA damage in prostate tumorigenesis. Oncogene. 2008;27(31):4353-62. Epub 2008/04/01.
128. Hu R, Saw CL, Yu R, Kong AN. Regulation of NF-E2-related factor 2 signaling for cancer chemoprevention: antioxidant coupled with antiinflammatory. Antioxid Redox Signal. 2010;13(11):1679-98. Epub 2010/05/22.

129. Foster BA, Gingrich JR, Kwon ED, Madias C, Greenberg NM. Characterization of prostatic epithelial cell lines derived from transgenic adenocarcinoma of the mouse prostate (TRAMP) model. Cancer Res. 1997;57(16):3325-30. Epub 1997/08/15.
130. Souli E, Machluf M, Morgenstern A, Sabo E, Yannai S. Indole-3-carbinol (I3C) exhibits inhibitory and preventive effects on prostate tumors in mice. Food Chem Toxicol. 2008;46(3):863-70. Epub 2007/12/08.
131. Kassie F, Matise I, Negia M, Upadhyaya P, Hecht SS. Dose-dependent inhibition of tobacco smoke carcinogen-induced lung tumorigenesis in A/J mice by indole-3-carbinol. Cancer Prev Res (Phila Pa). 2008;1(7):568-76. Epub 2009/01/14.
132. Park JH, Walls JE, Galvez JJ, Kim M, Abate-Shen C, Shen MM, et al. Prostatic intraepithelial neoplasia in genetically engineered mice. Am J Pathol. 2002;161(2):727-35. Epub 2002/08/07.
133. Nachshon-Kedmi M, Yannai S, Haj A, Fares FA. Indole-3-carbinol and 3,3'-diindolylmethane induce apoptosis in human prostate cancer cells. Food Chem Toxicol. 2003;41(6):745-52. Epub 2003/05/10.
134. Hsu JC, Dev A, Wing A, Brew CT, Bjeldanes LF, Firestone GL. Indole-3-carbinol mediated cell cycle arrest of LNCaP human prostate cancer cells requires the induced production of activated p53 tumor suppressor protein. Biochem Pharmacol. 2006;72(12):1714-23. Epub 2006/09/15.
135. Cho HJ, Park SY, Kim EJ, Kim JK, Park JH. 3,3'-Diindolylmethane inhibits prostate cancer development in the transgenic adenocarcinoma mouse prostate model. Mol Carcinog. 2011;50(2):100-12. Epub 2011/01/14.
136. Brait M, Sidransky D. Cancer epigenetics: above and beyond. Toxicol Mech Methods. 2011;21(4):275-88. Epub 2011/04/19.
137. Huang J, Plass C, Gerhauser C. Cancer chemoprevention by targeting the epigenome. Current drug targets. 2011;12(13):1925-56. Epub 2010/12/17.
138. Nelson WG, De Marzo AM, Yegnasubramanian S. Epigenetic alterations in human prostate cancers. Endocrinology. 2009;150(9):3991-4002. Epub 2009/06/13.
139. Hayes JD, McMahon M, Chowdhry S, Dinkova-Kostova AT. Cancer chemoprevention mechanisms mediated through the Keap1-Nrf2 pathway. Antioxid Redox Signal. 2010;13(11):1713-48. Epub 2010/05/08.
140. Wu TY, Saw CL, Khor TO, Pung D, Boyanapalli SS, Kong AN. In vivo pharmacodynamics of indole-3-carbinol in the inhibition of prostate cancer in transgenic adenocarcinoma of mouse prostate (TRAMP) mice: Involvement of Nrf2 and cell cycle/apoptosis signaling pathways. Mol Carcinog. 2011. Epub 2011/08/13.
141. Yu S, Khor TO, Cheung KL, Li W, Wu TY, Huang Y, et al. Nrf2 expression is regulated by epigenetic mechanisms in prostate cancer of TRAMP mice. PLoS One. 2010;5(1):e8579. Epub 2010/01/12.
142. Huang Y, Khor TO, Shu L, Saw CL, Wu TY, Suh N, et al. A gamma-Tocopherol-Rich Mixture of Tocopherols Maintains Nrf2 Expression in Prostate Tumors of TRAMP Mice via Epigenetic Inhibition of CpG Methylation. J Nutr. 2012. Epub 2012/03/30.
143. Ren J, Singh BN, Huang Q, Li Z, Gao Y, Mishra P, et al. DNA hypermethylation as a chemotherapy target. Cell Signal. 2011;23(7):1082-93. Epub 2011/02/25.
144. Sporn MB, Suh N. Chemoprevention: an essential approach to controlling cancer. Nat Rev Cancer. 2002;2(7):537-43. Epub 2002/07/03.

145. Khor TO, Huang Y, Wu TY, Shu L, Lee J, Kong AN. Pharmacodynamics of curcumin as DNA hypomethylation agent in restoring the expression of Nrf2 via promoter CpGs demethylation. Biochem Pharmacol. 2011;82(9):1073-8. Epub 2011/07/27.
146. Shu L, Khor TO, Lee JH, Boyanapalli SS, Huang Y, Wu TY, et al. Epigenetic CpG Demethylation of the Promoter and Reactivation of the Expression of Neurog1 by Curcumin in Prostate LNCaP Cells. AAPS J. 2011. Epub 2011/09/23.
147. Banerjee S, Kong D, Wang Z, Bao B, Hillman GG, Sarkar FH. Attenuation of multi-targeted proliferation-linked signaling by 3,3'-diindolylmethane (DIM): from bench to clinic. Mutat Res. 2011;728(1-2):47-66. Epub 2011/06/28.
148. Anderton MJ, Manson MM, Verschoyle R, Gescher A, Steward WP, Williams ML, et al. Physiological modeling of formulated and crystalline 3,3'-diindolylmethane pharmacokinetics following oral administration in mice. Drug Metab Dispos. 2004;32(6):632-8. Epub 2004/05/25.
149. Xue L, Pestka JJ, Li M, Firestone GL, Bjeldanes LF. 3,3'-Diindolylmethane stimulates murine immune function in vitro and in vivo. J Nutr Biochem. 2008;19(5):336-44. Epub 2007/08/21.
150. Weber M, Davies JJ, Wittig D, Oakeley EJ, Haase M, Lam WL, et al. Chromosome-wide and promoter-specific analyses identify sites of differential DNA methylation in normal and transformed human cells. Nat Genet. 2005;37(8):853-62. Epub 2005/07/12.
151. Cheung HH, Lee TL, Davis AJ, Taft DH, Rennert OM, Chan WY. Genome-wide DNA methylation profiling reveals novel epigenetically regulated genes and non-coding RNAs in human testicular cancer. Br J Cancer. 2010;102(2):419-27. Epub 2010/01/07.
152. Taberlay PC, Jones PA. DNA methylation and cancer. Prog Drug Res. 2011;67:1-23. Epub 2010/12/15.
153. Chen ZX, Riggs AD. DNA methylation and demethylation in mammals. J Biol Chem. 2011;286(21):18347-53. Epub 2011/04/02.
154. Kim EJ, Shin M, Park H, Hong JE, Shin HK, Kim J, et al. Oral administration of 3,3'-diindolylmethane inhibits lung metastasis of 4T1 murine mammary carcinoma cells in BALB/c mice. J Nutr. 2009;139(12):2373-9. Epub 2009/10/30.
155. Kim YH, Kwon HS, Kim DH, Shin EK, Kang YH, Park JH, et al. 3,3'-diindolylmethane attenuates colonic inflammation and tumorigenesis in mice. Inflamm Bowel Dis. 2009;15(8):1164-73. Epub 2009/04/01.
156. Chinnakannu K, Chen D, Li Y, Wang Z, Dou QP, Reddy GP, et al. Cell cycle-dependent effects of 3,3'-diindolylmethane on proliferation and apoptosis of prostate cancer cells. J Cell Physiol. 2009;219(1):94-9. Epub 2008/12/09.
157. Fang M, Chen D, Yang CS. Dietary polyphenols may affect DNA methylation. J Nutr. 2007;137(1 Suppl):223S-8S. Epub 2006/12/22.
158. Barve A, Khor TO, Reuhl K, Reddy B, Newmark H, Kong AN. Mixed tocotrienols inhibit prostate carcinogenesis in TRAMP mice. Nutr Cancer. 2010;62(6):789-94. Epub 2010/07/28.
159. Saw CL, Cintron M, Wu TY, Guo Y, Huang Y, Jeong WS, et al. Pharmacodynamics of dietary phytochemical indoles I3C and DIM: Induction of Nrf2-

mediated phase II drug metabolizing and antioxidant genes and synergism with isothiocyanates. Biopharm Drug Dispos. 2011;32(5):289-300. Epub 2011/06/10.
160. Gingrich JR, Barrios RJ, Morton RA, Boyce BF, DeMayo FJ, Finegold MJ, et al. Metastatic prostate cancer in a transgenic mouse. Cancer Res. 1996;56(18):4096-102. Epub 1996/09/15.
161. Smith SS, Kaplan BE, Sowers LC, Newman EM. Mechanism of human methyl-directed DNA methyltransferase and the fidelity of cytosine methylation. Proc Natl Acad Sci U S A. 1992;89(10):4744-8. Epub 1992/05/15.
162. Jair KW, Bachman KE, Suzuki H, Ting AH, Rhee I, Yen RW, et al. De novo CpG island methylation in human cancer cells. Cancer Res. 2006;66(2):682-92. Epub 2006/01/21.
163. Shukla V, Coumoul X, Lahusen T, Wang RH, Xu X, Vassilopoulos A, et al. BRCA1 affects global DNA methylation through regulation of DNMT1. Cell Res. 2010;20(11):1201-15. Epub 2010/09/08.
164. Lee KY, Chrysikopoulos CV. Dissolution of a well-defined trichloroethylene pool in saturated porous media: experimental results and model simulations. Water research. 2002;36(15):3911-8. Epub 2002/10/09.
165. Yang Q, Berthiaume F, Androulakis IP. A quantitative model of thermal injury-induced acute inflammation. Mathematical biosciences. 2011;229(2):135-48. Epub 2010/08/17.
166. Dayneka NL, Garg V, Jusko WJ. Comparison of four basic models of indirect pharmacodynamic responses. Journal of pharmacokinetics and biopharmaceutics. 1993;21(4):457-78. Epub 1993/08/01.
167. Patel AR, Spencer SD, Chougule MB, Safe S, Singh M. Pharmacokinetic evaluation and In Vitro-In Vivo Correlation (IVIVC) of novel methylene-substituted 3,3' diindolylmethane (DIM). European journal of pharmaceutical sciences : official journal of the European Federation for Pharmaceutical Sciences. 2012;46(1-2):8-16. Epub 2012/02/22.
168. Anderton MJ, Jukes R, Lamb JH, Manson MM, Gescher A, Steward WP, et al. Liquid chromatographic assay for the simultaneous determination of indole-3-carbinol and its acid condensation products in plasma. Journal of chromatography B, Analytical technologies in the biomedical and life sciences. 2003;787(2):281-91. Epub 2003/03/26.
169. Mager DE, Jusko WJ. Development of translational pharmacokinetic-pharmacodynamic models. Clin Pharmacol Ther. 2008;83(6):909-12. Epub 2008/04/05.

Curriculum vitae

TIEN-YUAN WU

EDUCATION

2012 Ph.D., Pharmaceutical Science, Rutgers University, New Jersey, U.S.A.

2003 B.S. in Pharmacy, Taipei Medical University, Taipei City, TAIWAN

RESEARCH AND PROFESSIONAL EXPERIENCE

Sep 2007- June 2012

Graduate Student in Pharmaceutical Science, Rutgers, The State University of New Jersey, NJ, U.S.A.

June 2011- August 2011

Summer intern, Translational Science, DMPK-Clinical PK/PD, Novartis Institute for Biomedical Research, East Hanover, NJ, U.S.A.

May 2006- July 2007

Registered Pharmacist II, Buddhist Tzu-Chi General Hospital, Taipei Branch, New Taipei City, TAIWAN

May 2005- Apr 2006

Registered Pharmacist, China Medical University Hospital, Taichung City, TAIWAN

Feb 2003- May 2003

Internship of Pharmacist, Cathay Medical Center, Taipei City, TAIWAN,

Sep 2001- June 2003 (Junior- Senior)

Pharmacy research student, Clinical Pharmacy laboratory, School of Pharmacy, Taipei Medical University, Taipei City, TAIWAN